FABRICATION, MECHANICAL AND PHYSICAL PROPERTIES CHARACTERIZATION OF SISAL FIBER REINFORCED EPOXY COMPOSITES FOR AUTOMOTIVE PARTS.

Araya Abera Betelie

Supervisors: - Anthony N. Sinclair (Professor)

Daniel T. Redda (Associate Professor)

A Dissertation Submitted to

School of Mechanical and Industrial Engineering

Presented in Fulfillment of the Requirements for the Degree of Doctor of Philosophy (PhD) in Mechanical Engineering

(Mechanical Design)

Addis Ababa Institute of Technology (AAiT)

Addis Ababa University

Addis Ababa, Ethiopia

September 2021

Addis Ababa University (AAU)

Addis Ababa Institute of Technology (AAiT)

School of Mechanical and Industrial Engineering (SMIE)

Mechanical Design Chair

Fabrication, Mechanical and Physical properties Characterization of Sisal Fiber reinforced Epoxy Composites for Automotive parts.

Araya Abera Betlie

Approved by Board of Examiners

_____	_____	_____
Dean, SMiE	Signature	Date
_____	_____	_____
Mechanical Design Chair	Signature	Date
_____	_____	_____
External Examiner	Signature	Date
_____	_____	_____
External Examiner	Signature	Date
_____	_____	_____
Post Graduate Director	Signature	Date

AUTHORS' DECLARATION

I, hereby declare that this dissertation entitles '***Fabrication, Mechanical and Physical properties Characterization of Sisal Fiber reinforced Epoxy Composites for automotive parts'*** was own research work. It has not been submitted in whole or part to another university for a degree award.

Araya Abera Betelie

We, hereby declare that this dissertation entitles ***'Fabrication, Mechanical and Physical properties Characterization of Sisal Fiber reinforced Epoxy Composites for Automotive parts'*** was conducted under our supervision. We have confirmed that it has not been submitted in whole or part to another university for any degree award.

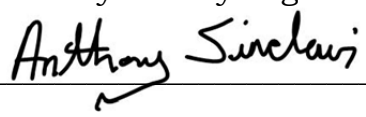

September , 2021

Anthony N. Sinclair (Professor) **Date**

Septembe1, 2021

Daniel T. Redda (Associate Professor) **Date**

ABSTRACT

The demand for natural fibers to replace synthetic fibers in composites manufacturing has grown as a result of the high energy consumption and pollution created in the production and usage of synthetic fibers. Natural fibers have several advantages over synthetic fibers, including low cost, biodegradability, and nontoxicity. In this study, as received Sisal fibers (SF) and those whose surface were chemically modified using 10 wt.% NaOH for 3 h at 60oC and compression molded to produce epoxy matrix composites containing 15, 25, 30, 35, and 40 wt.% of SFs. The composites' morphological, thermal, tensile, flexural, impact physical, and structural characteristics were studied before and after treatment. Scanning electron microscopy (SEM), thermography analysis (TGA), dynamic mechanical analysis (DMA), and Fourier transform infrared spectroscopy (FTIRS) are some of the techniques used. The impact of different fiber loadings and chemical treatments on the mechanical, physical, and thermal characteristics of sisal fiber reinforced Epoxy composites were studied. Mechanical properties of the composites were investigated using InstronTM machine. The effect of chemical modification on water uptake of the composites was also studied.

Surface chemical treatment of the SFs by soaking in 10 wt.% NaOH for 3 h at 60oC resulted in 20% increase in the cellulose content of the fiber. In the treated SFs, FTIR spectroscopy revealed a decrease and removal of certain non-cellulosic components. Although the treated fibers increased, their tensile strength and water absorption capacity decreased as compared to non-treated fibers. The use of sisal fiber in reinforcing epoxy for both treated and untreated led to increase in tensile modulus, tensile strength, flexural strength, flexural modulus and crystallization temperature of the composite when compared to less fiber loading. The rate of water absorption for composites containing treated fibers is lower than that for composites containing untreated fiber. Results also showed that increasing fiber content decreased the tensile

strength and flexural strength after 30wt. percentage fiber loading is reached and the impact strength increase with increase of fiber loading. After characterization of the physical and mechanical properties of sisal fiber reinforced epoxy composite, we have seen good agreement with the literature reviewed materials so that this composite can also be used for substitute of materials for automotive parts application. After all we have developed lowvelocity drop weight impactor and we have seen the results which we found from our test machine agreed with the other machines which has similar features.

ACKNOWLEDGEMENT

I would like to convey my heartfelt thanks and deep appreciation to Professor Anthony N. Sinclair, my academic supervisor, for his invaluable advice, support, patience, and enthusiastic encouragement during the duration of my project, which enabled me to achieve a significant life goal.

I am also grateful to Dr. Daniel Tilahun Reda, my supervisor, for his invaluable advice, support, and ideas during this research project.

I want to express my gratitude to Professor Mark Kortschot and Professor Mohini for their encouragement, lab space, and support during my time as a PhD guest student at the University of Toronto.

I would like to appreciate the efforts of Mrs Sindy and Mr crestian for their supports during my stay in doing Experiments at university of Toronto.

To my friends at SMIE, your contribution and moral supports towards the completion of this thesis cannot be quantified. Thanks all. Finally, I am very grateful to my wife Samrawit Beyin, my brothers, and sister who has been source of help, inspiration and guide, I am grateful to have you. God bless you all

DEDICATION

I dedicate my Thesis first for God who strengthen me and give me life to complete it, To My Mather, my Father, my brothers, my only sister, my wife, and my kids, you mean so much more to me.

CONTENTS

LISTS OF FIGURES

LISTS OF TABLES

LIST OF ABBREVIATIONS

ASTM	American society for Testing and Materials
DMA	Dynamic Mechanical Analysis
FTIR	Fourier Transform Infrared spectroscopy
GPa	Giga Pascal
h	Hours
mg	Milligram
MPa	Mega Pascal
ml	Millimeter
NaOH	Sodium hydroxide
µm	Micrometer
OH	Hydroxide
Pa	Pascal
SF	Sisal Fibers
SFREC	Sisal Fiber epoxy composites
S	Second
TGA	Thermo-gravimetric analysis
Wt%	Weight Percentage
oC	Celsius
J/m	Jule per meter
DSC	Differential Scanning Calorimetry
HIU	High-intensity ultrasound
HDPE	High-density polyethylene
NFRPMC	polymer matrix reinforced with natural fiber
MHz	Megahertz
kHz	kilohertz
kJ/Mol	Kilojoule /mole
NF	Natural fiber
PP	polypropylene
TPS	Thermoplastic starch

UN	untreated sisal fiber
T	treated
W/v	weight per volume
Mm	millimeter
SEM	scanning electron microscope
mm/min	millimeter per minute
kN/min	kilo newton per minute
E’	storage modulus
E”	loss modulus
K_{IC}	critical stress intensity factor
G_{IC}	critical strain energy release rate,
DMB	Dry matter basis
kV	Kilovolt

CHAPTER 1. INTRODUCTION

1.1 Background

The use of natural fiber-reinforced composite polymer materials is increasing as they benefit from green technology, industrial applications, and basic research. These materials are reusable, fully or partially recyclable, and biodegradable, making them environmentally friendly. Natural fibers are harvested from plants and there is no need for complicated processing methods to prepare them; this results in the composites being inexpensive. Thus, the synthesis, characterization, design, and production of composite reinforced natural fiber materials are now becoming active areas of research that can be related to these advantages. Plants such as flax, cotton, hemp, jute, sisal, kenaf, pineapple, ramie, bamboo, banana, etc., as well as wood, used since ancient times as a source of lingo cellulosic fibers, are often added as composite reinforcement. Because of their availability, renewability, low density, comparatively low price and satisfactory mechanical properties, they are a desirable, natural alternative to glass, cement and man-made fibers used for the manufacture of composites.

The idea of using bio-based materials in vehicle parts was first considered by the founder of the Ford Motor Company in early 1930s. The Ford Motor Company then conducted an aggressive analysis of the widespread use of natural fibers in vehicles, resulting in the unveiling of the Ford Model T in 1941[1]. This had a body consisting mainly of composites of soy resin-reinforced cotton, sisal, and wheat straw; the Ford Model T had a weight of two thirds that of a standard car, with an engine running on hemp oil fuel.

The requirement for energy saving in the automotive industry has risen dramatically over the years. One of the options to reduce energy consumption is weight reduction. A major development in material technology was introduced with polymeric based composite materials, which offer high stiffness, low weight, absence of corrosion, and the ability to be produce in complex shapes with high specific strength and high impact

energy absorption. Substitution of polymeric based composite material in automotive components was successfully implemented for fuel and weight reduction by various auto makers [1].

Fiber reinforced composite materials have been widely used in various vehicle structures because of their high specific strength, modulus and high damping capability. If composite materials are applied to vehicles, it is expected that not only the weight of the vehicle is decreased but also that noise and vibration are reduced. In addition, composites have a very high resistance to fatigue and corrosion [2][3][4].

Then, beginning with executive class vehicles, aluminum-intensive body designs were used and later extended to other car types. Now, plastics primarily occupy the interior of the car, their outward use being mainly limited to non-load-bearing elements, while some revolutionary plastic technologies, such as engine sub-frames, frontal bumpers, and subsystems have recently been introduced on some vehicle parts to reduce the vehicle weight and improve occupant and pedestrian safety, [5].

Weight redaction has become the key priority of car producers in order to save natural resources including oil. Weight reduction can be accomplished mainly by the use of quality materials, optimization of design and enhanced development processes[6]. Owing to the growing need for lightweight vehicles and the increased mechanical efficiency of materials in automobile applications, various types of composites, plastics and lightweight metals, are being added to main and secondary structural components of vehicles. Many primary and secondary components, such as dashboard, windshield, pavement, front & back bumper, passenger safety cell, and occasionally, A-pillar and B-pillar, already contain applications of composite materials in the automotive industry[6].

Even though several factors influence the entire product development process to realize a lightweight vehicle, from the point of view of vehicle structural design, the main governing criteria for material selection are stiffness and strength properties that will determine the overall performance of the vehicle during static and dynamic loading conditions[7], [8].

In this study, the fabrication of composite with different fiber/matrix ratio and mechanical property characterization of the sisal fiber reinforced epoxy composite are the key issues to development of alternative materials for the automotive industry.

1.3. Problem Statement

In recent years, a significant trend has emerged in the automotive industry to improve fuel efficiency by making automotive parts with reduced weight. The automotive assembly industries are becoming increasingly significantly in Ethiopia which is a key location for the African market. There are currently several automotive assembly lines for lightweight cars here in Ethiopia. Bishoftu Automotive is government-owned and has the largest assembly line which integrates assembling of different types of automobiles, buses, and trucks. This includes assembly of Addis Ababa lightweight city buses by Bishoftu Automotive and Locomotive Industry, which is part of the Metal and Engineering Corporation (METEC) based in Bishoftu, Ethiopia.

The parts to be assembled are not manufactured in Ethiopia, bur are imported from other car manufacturing plants abroad. Among these, China is the main supplier. Some parts for various applications in the aircraft and automotive sectors are manufactured in Ethiopia by Dejen Aviation Industry (DAVI) but the supply chain for these industries are not organized in such a way that they can help as a substitute for the imported parts. DAVI is highly dependent on imported synthetic fibers for the fabrication of lightweight automotive body parts; however, these synthetic fibers are not the only option for automotive applications. In recent years, research on natural fiber-based composites is being conducted all over the world. Ethiopia has a lot of natural resources for fiber production including sisal fiber.

Thus, this paper tries to promote the use of natural fiber reinforced polymer composite here in Ethiopia. Sisal fiber reinforced thermoset polymer composite has seen rapid development for application in the automotive industry. Therefore, by conducting further research on this topic, we can

contribute to the Ethiopia automotive industry by using locally available resources, while also contributing to the global automotive industry.

1.4. Objective of the Study

The primary objective of this study is to create and classify epoxy polymer composites reinforced with sisal fiber for automotive use. The following particular goals are listed below to realize this aim.

1.4.1. The specific objectives:

1. To identify and select good chemical treatments to produce better surface properties for sisal fibers and ;
2. To characterized mechanical and Physical properties at different fiber and matrix ratios of the sisal fiber epoxy composite, and determining a good fiber to matrix ratio;
3. To identify the orientation and fiber length of fiber that provides a better mechanical property characteristics.
4. To compare the fabricated sisal fiber reinforced epoxy composite material properties against those of currently used materials for automotive applications, and determine appropriate areas of application for the new product.
5. To develop and low velocity impact testing machine used to determine the impact resistance of sisal reinforced epoxy composites.

The contributions from this research work to the existing knowledge of natural fiber composite materials may be listed as follows:

- The effects of chemical treatments on the water absorption, and other physical, chemical, and mechanical behavior of sisal fiber in particular, and on composite materials in general, and
- The establish the optimal spatial distribution and concentration of fibers for specific applications in the automotive industry.

1.5 Scope of the Study

This study aims to explore the best possible use of epoxy composites reinforced with sisal fiber for automotive parts production. Mechanical properties such as tensile strength, flexural strength, impact strength, dynamic mechanical analysis (DMA), water absorption, and storage modulus and weight loss will be measured experimentally, based on the chosen mechanical components for automotive applications.

1.6 Limitation of the Study

This study tries to characterize the physical and mechanical properties of sisal fiber reinforced epoxy composites for selected applications, but with specific limitations.

First, since research on the use of sisal fiber-reinforced composite is an on-going effort, there are only a limited number of published papers available that provide detailed date relevant to automotive parts application.

Second, since there is no well-established and standard testing facility, which is crucial for the fabrication and characterization of composite materials. A testing facility will therefore be developed to meet the specific needs of this project.

Third, due to the shortage of test equipment and facilities, this thesis focused only on the specific properties as listed in the objectives and scope of the study.

1.7 Organization of the Thesis

This report focuses on the fabrication and property characterization of sisal fiber reinforced epoxy composites, specifically tensile strength, flexural stiffness, impact properties dynamic mechanical properties, thermo gravimetric analysis, fracture toughness and water absorption. There are five chapters.

Chapter 1: An introduction to natural fiber-reinforced composite materials, background, and statement of the problem, objectives, scope, and project limitations are provided in this chapter.

Chapter 2: A review of recent and important scientific papers on natural fiber composite materials, ranging from the chemical and mechanical properties of polymer forms, fiber types, and composites is provided.

Chapter 3: In this chapter the materials and methods used for the preparation of test specimens and property measurements (physical and mechanical properties), and characterization techniques are presented.

Chapter 4: Results on the fabrication, treatment, and characterization of composite material are provided. In addition, based on the flexural, tensile, impact, and other property analysis results, application areas for sisal reinforced composite materials are discussed.

Chapter 5: The results of the research work are outlined and proposals for future work are listed. The field of application where sisal reinforced epoxy composite can be used in the automotive sector is also explored in this chapter.

CHAPTER 2: LITERATURE REVIEW

This chapter reviews the types, synthesis, and properties of composite materials, with a particular focus on natural fiber-based composites. Recent literature was reviewed to understand the different classifications of natural fibers, the techniques used in the manufacturing of natural fiber reinforced polymer matrix composites, the treatment used for the surface modification of fibers, mechanical properties of sisal fiber-reinforced polymer composites,

and their application in the automotive industry. Finally, summarizing the gaps and the findings of the researchers will conclude the chapter.

2.1 Composite materials

The term "composite material" is derived from "composition material" which refers to material with different physical and chemical properties consisting of two or more constituent materials. The primary objective of combining the constituent materials in a composite is to produce superior and special materials that while maintaining their identity in the new component, incorporate the desired properties of all the constituents, specifically to achieve new materials with higher performance, low cost and green technology while maintaining their authenticity in the new product[9], [10].

2.1.1 Classification of Composite materials

2.1.1.1 Reinforcement Classification

Some researchers have classified composte materials based on their reinforcement mechanism, as shown in figure 2.1.

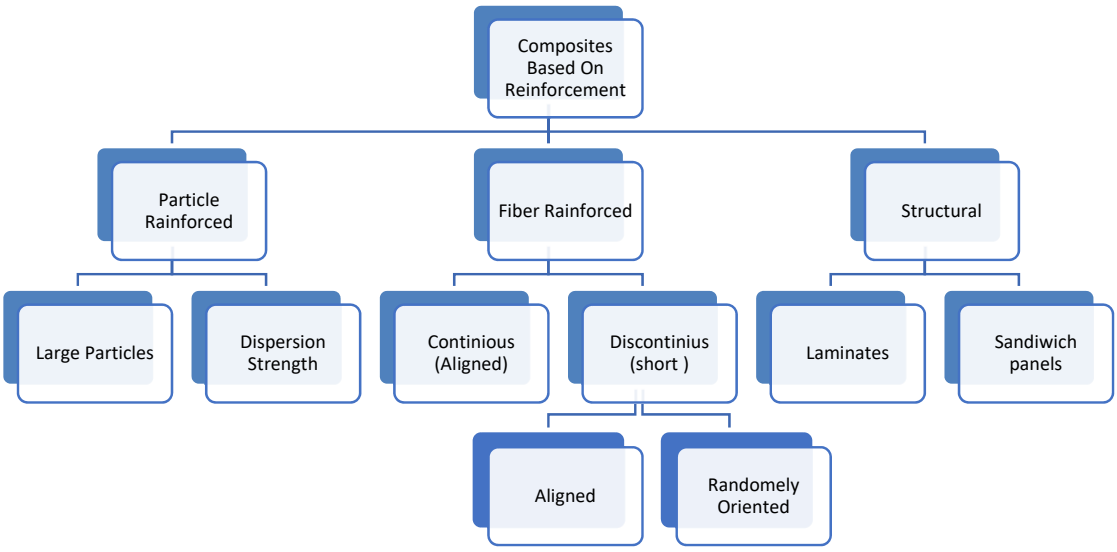

Figure 2-1 Composite materials classification based on reinforcement mechanism [11]

2.1.1.2. Matrix Type Classification

Depending on the type of matrix material, composites can be classified as metal, polymer, or ceramic matrix composites. A metal or polymer matrix can be reinforced by fibers, whiskers, or particles to increase its strength or/and stiffness. For ceramic matrix composite materials, the reinforcing element is added to improve fracture toughness[10]. Since the applied load on the matrix is transmitted to the embedded fiber through the matrix fiber interface, the fracture resistance of the composite is usually determined by the fiber toughness [11].

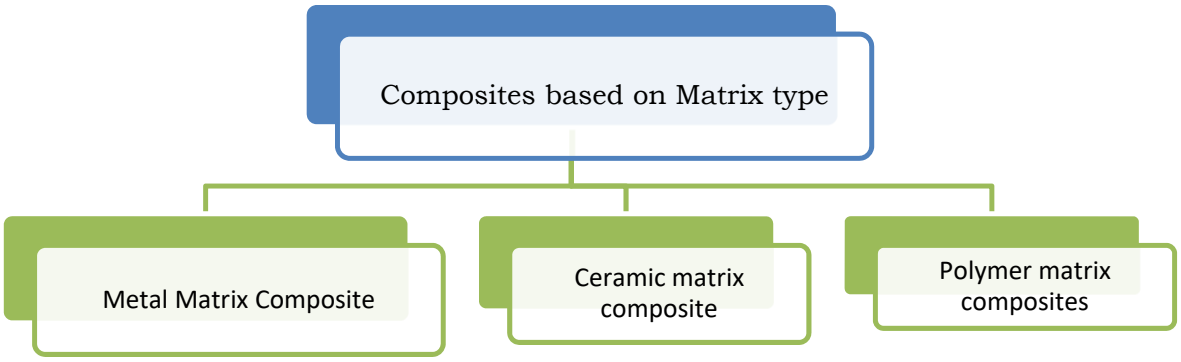

Figure 2-2 Composites Based on Matrix Type [10][13]

The matrix is a key element in the preparation of composite materials. As shown in figure 2.2, there are different types of matrix used in composite development. Polymer-based matrix has replaced other types and is used in several fields of application due to its low weight, high strength, easy processing, productivity, and low cost[12]. The matrix provides many functions for the composites, such as keeping the fiber in proper position, resistance against adverse environmental conditions (chemicals and moisture), transfer of stress between fibers, and protecting the fiber's surface from mechanical degradation such as abrasion [12]. Moreover, most matrix materials for composites are polymeric because of their easy process ability, good surface quality, resistance to corrosion, and lower weight than metallic and ceramic materials.

A polymer consists of long-chain molecules that have covalent bonds connecting one or more repeating units of atoms. Often known as plastic, a polymer substance consists of large polymer molecules with identical chemical composition. Polymers are graded in two main groups: thermoplastics and thermosets. Specific molecules are not chemically bound together in thermoplastic polymers. Instead, weak secondary bonds such as hydrogen bonds and Vander Waals bonds bind them together. A thermoplastic polymer can be softened and redesigned by the application of heat.

In contrast, thermoset molecules are chemically linked together by cross-links, having a rigid 3D network structure. A thermoset polymer cannot be melted through application of heat [13].Mechanical properties of polymers are given in Table 2.1.

Table 2-1 Mechanical Properties of Polymers by different researchers

Polymer	Type of polymer	Density (g/cm^3)	Tensile strength (MPa)	Tensile Modulus (MPa)	Flexural Strength (MPa)	Flexural Modulus (GPa)	Impact Strength (J/m)	Reference
Epoxies	Thermosetting	1.23	55-130	2.7-4.1	110-150	3--4		[14]
Phenolic			50-60	4-7.0	80-135	2-4.0		[14]
Polyesters			34-105	2.1-3.5	70-110	2-4.0		[14]
Vinyl esters			73-81	3-3.5	130-140	3		[14]
Polylactide		1.24	56.3	3.6				[15]
polyester		1.2	61	4				[15]
Polyvinyl Chloride (PVC)	Thermoplastic	1.35	48	3.3			32	[16]
Polystyrene			46	2.9			17	[16]
Polypropylene (PP)		0.899-0.92	26-41.4	0.95-1.776	55.2	0.83-1.73	21.4-267	[16]
Low density Polyethylene (LDPE)		0.91	4-78.6	0.055-0.38			>854	[16]
High density Polyethylene (HDPE)		0.925	14.5-38	0.413-1.490		0.41-1.07	26.7	[16]

Among the mentioned mechanical properties of thermoplastic and thermoset polymers, epoxy shows the highest tensile and flexural strength as

compared to other polymer matrices, as shown in Table 2.1. In addition, The Flexural modulus for epoxy is higher than for the other polymer matrices.

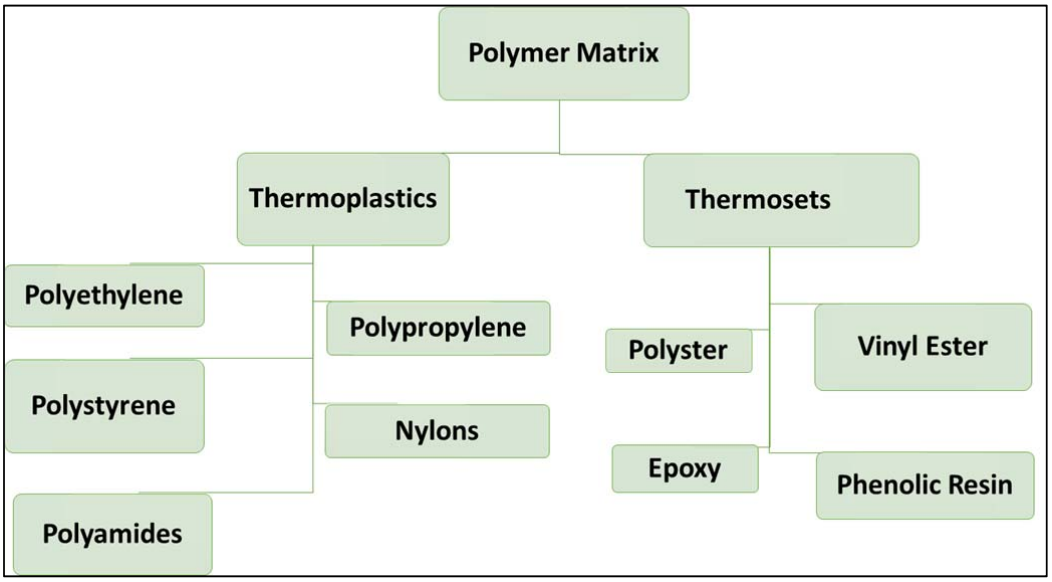

Figure 2-3 Various Polymer Matrices [17]

2.3 Fibers

Fiber is a thin thread of either natural or synthetic material that is generally characterized by a circular cross-section. Its length is many times greater than its diameter, having an aspect ratio greater than 100, and can be either continuous or discontinuous[17][18]. The main purposes of fiber in composites are to enhance both strength and stiffness[5]. Figure 2.4 illustrates the classification of fibers.

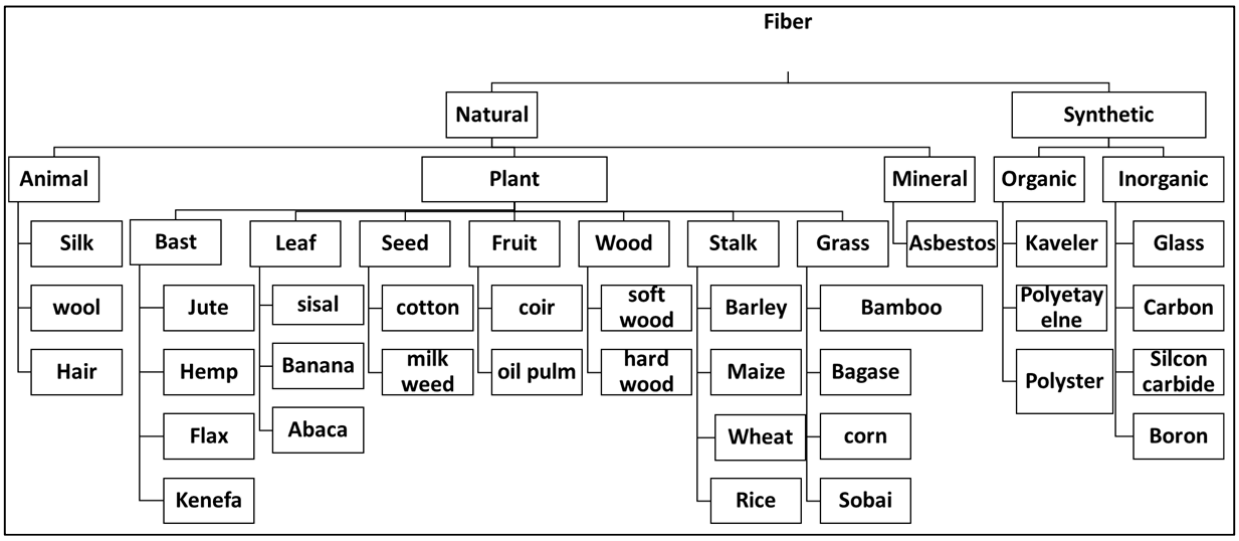

Figure 2-4 Classification of Fiber [5]

Fibers used for the manufacturing of composite materials are typically categorized into two types: natural and synthetic. Natural fibers are usually non-toxic and harmless compared to synthetic fibers and are composed of plant, mineral, and/or animal matter. Bamboo, cotton, sugarcane bagasse, flax, abaca sisal, and banana are examples of plant fibers used for composite manufacture, while examples of animal fiber include fur, skin and hair [1].

2.3.1 Synthetic Fiber (SF)

Artificial synthetic fibers include carbon, aramid, and glass. They have been used as reinforcement for polymer and metal matrices, producing high-performance material for applications such as pipes, tanks, sporting goods, bridges, boat hulls, automotive components, and aircraft secondary structures [10]. Synthetic fiber-reinforced composites have superior mechanical properties, but also have some drawbacks that include high cost, poor recyclability, and non-biodegradability[19].

2.3.2 Natural Fibers (NF)

Natural fibers are gaining increasing attention, as an alternative to synthetic fibers because of their advantages such as renewability, abundant availability, and environmental compatibility. Natural fibers are classified based on their source as animal (wool and silk), mineral (asbestos), and

plant, as shown in figure 2.4. The use of natural fiber as reinforcement materials in polymer matrix composites provides positive environmental benefits in terms of sustainability[1][15]. The properties of these composites depend mainly on the properties of the fiber, properties of the polymer, and bond strength of the fiber-matrix interface[16]. In recent years, natural fiber reinforced polymer composites have been used in automotive parts, aerospace components, and construction industries.

2.4 Chemical Composition of Natural Plant Fiber

The main elements of natural fibers (NF) are cellulose, hemicellulose lignin, wax, and pectin. From the above listed elements of natural fiber structure, cellulose hemicellulose and lignin are the basic components of NF, which have the greatest effect on its mechanical properties [18]. Most natural fiber has cellulose as the major component of its composition[18]. Cellulose is highly crystalline, with a slightly amorphous region [15][1][19]. Hemicellulose consists of branched, short chains groups of polysaccharides with a lower degree of polymerization than cellulose [1], [15], [19], [20]. Due to the branched structured nature, most hemicellulose is highly amorphous; hence, hemicellulose mechanical properties are inferior to those with cellulose [12]. Most natural fiber change their dimensions during growth since hemicellulose swells due to water absorbed [20]. Lignin has a complex 3-dimensional polymer structure and is amorphous [20]. Both hemicellulose and lignin acts as glue, which hold the cell wall of each individual fiber in a fiber bundle together[18][14].

Table 2.2: -

Table 2-2 Chemical Constituents of Plant Fiber[21].

Fiber	Cellulose (wt.%)	Lignin (wt.%)	Hemicellulose (Wt.%)	Pectin (wt.%)	Wax (wt.%)	Moisture content (wt.%)
Sisal	62-78	8--11	10---14.2	10	2	11
Jute	61-71.5	12.13	13.6--20.4	0.4	0.5	12.6

Hemp	70.2-74.4	3.7--5.7	17.9-22.4	0.9	0.8	10
Kenaf	31-39	15-19	21.5			
flax	71	2.2	18.6-20.6	2.3	1.7	10
Ramie	67.8-76.2	0.6-0.7	13-16	0.3	0.3	10
cotton	82.6		5.7		0.6	
coir	36-43	41-45	10--20	3--4		8
Banana	63-67.6	5	19			8.7
Bamboo	26-43	21-31	30			
Oil palm	65		29			
Pineapple	81		12.7			
Wheat straw	38-45	12-20	15-31			
Rice husk	35-45	20	19-25		14-17	
Rice Straw	41-57	8-19	33		8-38	

Climatic conditions, age and processing method are the three basic factors which influence mechanical properties and chemical composition of most plant fiber [20]. The variation of properties occurs from plant to plant and within different parts of the same plant. Cellulose is the basic element of fibers; higher content of cellulose promotes better mechanical properties[21]. The structural arrangements of the plant fiber cell wall features the lignin material in the secondary cell wall, bonded together with cellulose and hemicellulose, which is used to cement the material. The cellulose is bound by pectin that holds all the fiber structure together. Both Lignin and pectin are amorphous in their arrangement compared with cellulose

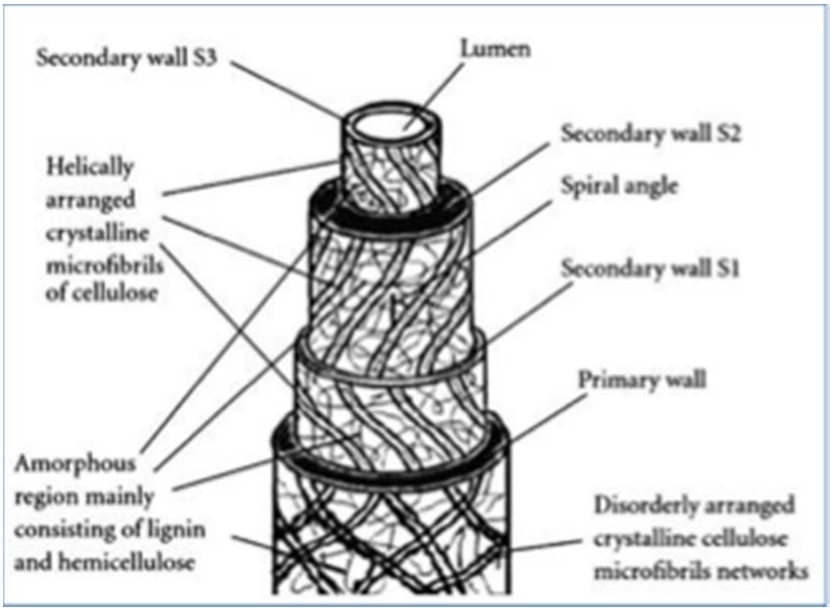

Figure 2-5 Plant Cell Wall Constituents and Structural Arrangement [16]

2.5 Characterization of Natural Fiber

2.5.1 Mechanical and Physical Properties

Most natural fibers have inferior mechanical properties compared with synthetic fiber. Some of the mechanical properties of natural fiber compared with E-glass and carbon fiber are shown in the Table2.3.

Table 2-3 Mechanical Properties of Some Natural and Synthetic Fibers.

Fiber	Density (g/cm^3)	Tensile Strength (MPa)	Elastic Modulus (GPa)	Elongation at break (%)	Reference
Sisal	1.45	349-635	9.4-22	2-3.5	[14]
Jute	1.46	200-450	20-55	2.0-3.0	[14][22]
Hemp	1.47	690	70	2.0-4.0	[22],24
Kenaf	1.2	785	40	1.9	[23],[24], [25]
Flax	1.5	345-1035	27.6	1.1-2.5	[22]
Banana	1.3	529-914	7.7-32	1-3.0	[21],[26]
Pineapple	1.52	170-1627	6.2	1.6	[21],[25]
E-Glass	2.55	3400	11-Mar	4.5-4.9	[22]
Carbon	1.4	4000	230-240	1.4-1.8	[22]

2.5.2. Water Absorption

Natural fibers are highly hydrophilic and penetrable to water. Water uptake in these fibers depends greatly on morphology and chemical structure [20][27]. From the chemical composition of bio fibers, hemicellulose is the constituent that is primarily responsibility for water absorption[20]. However, some literature reported lignin also has some effect on the water absorption capacity of NF [28]. The penetration of water into the fiber occurs through the micropores present on the fiber surface [29][30].

2.5.3. Thermal Conductivity

Thermal Conductivity describes a material's ability to transport heat from high to low-temperature regions [31]. The thermal conductivity of natural fiber reinforced polymer composites is poor, such that it is a good insulator. Various methods have been employed in measuring the thermal conductivity of natural fiber, such as transient line source, transient plane source, laser flash and steady-state heat transfer [32],[33],[34][35].

2.5.3.1 Thermal Analysis of Natural fibers

The thermal stability of fiber is an important factor in the processing of NFRC. Since natural fibers are lingo-cellulosic and consist mainly of lignin, hemicellulose, and cellulose, their cell walls undergo decomposition with increasing processing temperature [36]. Different researchers with the aid of scanning Calorimetry (DSC) and thermo gravimetric analysis (TGA) [45-49] studied the thermal stability of natural fiber[37][38][39].

2.6 Chemical Treatment of Natural Fibers

The major challenge in manufacturing natural fiber composites is poor interfacial adhesion and poor compatibility between the hydrophilic fiber and the hydrophobic matrix. The inhomogeneity of mixing the natural fiber and polymer is a basic problem for the inconsistency of properties. The difference between the chemical structure of fiber and the matrix leads the bonding strength to be challenging. A weak fiber-matrix bond leads to failed

stress transfer throughout the fiber-matrix interface. Therefore, chemical treatment for the fiber helps to improve bonding between fiber and polymers and increases the performance of the composites. The most commonly used chemical treatment used for treating the fibers to improve the surface chemistry of the fiber are, sodium hydroxide(NaOH), silane, sulphuric acid, benzoylation, permanganate, and peroxide treatments. Surface treatments of the fiber helps to improve the water absorption property of the fiber and facilitate compatibility of the fiber with the polymer matrix [40], [41].

2.6.1. Sodium Hydroxide (NaOH)

This treatment is the most common and effective method used for improving the interfacial compatibility between the fiber and the matrix. The water uptake of treated fiber with this method has shown reduced. The significant modification done by alkaline treatment is the disruption of hydrogen bonding in the network structure, thereby increasing surface roughness. This treatment removes a huge amount of lignin, wax, and oils covering the external surface of the fiber cell wall, depolymerizes cellulose, and exposes the short length crystallites[42].

Fiber cell-OH +NaOH------ Fiber cell –O- Na + H_2O [42]

NaOH treatment effectiveness depends on the concentration of the solution, its temperature, and duration of treatment. Jacob et al. [43] studied the effect of NaOH solution concentration (0.5, 1, 2, 4, and 10%) for treatment of sisal fiber-reinforced composites and found that maximum tensile strength resulted from a 4% NaOH treatment which is performed at room temperature. M.Rokbi et al. [44] studied the effect of NaOH concentration on the sisal fiber surface modification and reported that 5% NaOH treated sisal fiber-reinforced polyester composite had better tensile strength than 10% NaOH treated composites. M. A. Sawpan et al. [45] Investigated the effect of various chemical treatments. Gassan et al. [46] tried to indicate the effect of alkali treatment on the mechanical properties of jute-epoxy composites. The treatment is done with varying concentrations of NaOH (up to 28 wt.%)

for a maximum time of 30 minutes at a temperature of 20_0C followed by washing the fibers in distilled water mixed with 2 wt.% sulfuric acids, then washing again with pure distilled water before drying. They found NaOH treatment improved the tensile strength and modulus of elasticity by 120% and 150% respectively [46][47].

M.waikambo et al. [48] studied the effect of alkalization on natural fiber for jute, hemp, and sisal fiber; they tried to see the effects on thermal properties, degree of crystallinity, and surface morphology. The treatment removes pectin, waxy substances, and essential oils from the fiber surface. Additionally, chemical treatment breaks fiber bundles into microfibrils and increases the roughness of the fiber surface. The increase in roughness improves both mechanical interlocking at the fiber-matrix interface and improved wetting characteristics by allowing the resin to deposited in the porous structure of the fiber [48].

2.6.2. Silane Treatment

Silane treatment is done by soaking the fibers in a weak solution of a silane diluted in a water/alcohol or water/ketone mixture. Due to the presence of water in the solution, saline breaks down into silanol and alcohol during the reaction. The silane reacts with the OH groups of the cellulose in natural fibers, creating stable covalent bonds on the fiber surface[48]. The use of silane helps the fiber to improve cross-linking in the interface region and increases the fiber surface area which helps to create stronger bonding between the fiber and matrix[49].

$$CH_2\,CHSi(OH_3) + \text{Fiber} - OH \rightarrow CH_2\,CHSi(OH)_2O - \text{Fiber} + H_2O$$

Rong et al. [50]soaked sisal fiber in a solution of 2% amino silane in 95% alcohol for 5 min at a pH value of 4.5–5.5 followed by 30 min air-drying for hydrolyzing the coupling agent. Mughal et al.[51] Investigated the effect of alkali and silane treatments on the adhesion characteristics of sisal fiber epoxy composites. They reported that the compression strength is improved but flexural strength and stiffness are unchanged.

From the literature reviewed, we can conclude that chemical treatment of

fiber produces enhanced adhesion between hydrophilic natural fiber and hydrophobic polymers. This indirectly influences positively the mechanical, thermal, and tribological properties of the resulting composites.

2.6.4. High intensity ultrasound (HIU) treatment

High-intensity ultrasound (HIU) treatment has achieved increasing acceptance in recent years due to its effectiveness in removing amorphous materials from the surface of natural fibers. Furthermore, HIU treatment improves the separation of cellulose Nano fibers from their bundles, increasing the surface area of the fibers and improving interfacial adhesion between the fibers and the matrix[52]. Ultrasound is produced by a transducer that transforms electrical energy into high frequency sound waves in the range of 20 kHz to 10 MHz. Ultrasound transducers can generate cavitation by creating high-energy tiny air bubbles in a solution[53]. The energy released by cavitation breakdown is roughly equivalent to the energy released by hydrogen bonds (10-100 kJ/mol). As a result of the HIU treatment, the hydrogen bonds between cellulose and amorphous materials dissolve, allowing amorphous materials to be removed from the surface of natural fibers[52].

2.7 Manufacturing process for natural fiber-reinforced composites

The technologies used to process polymer matrix composites are extrusion, compression, rotational, and injection molding techniques. Processing of NF reinforced polymer composites is based on mixing of short NFs and polymer matrix followed by subsequent molding [54]. Thermoplastics offer many advantages over thermosets. Thermoplastics offer design flexibility and ease of molding complex parts. The two common methods for processing NF-reinforced polymer composites are injection molding and compression molding. Both are usually preceded by extrusion molding to attain a uniform dispersion of fibers in the melted polymer[55].

2.8 Characterization of Natural Fiber-reinforced polymer composite

The key properties of the composite polymer matrix reinforced with natural fiber (NFRPMC) depend primarily on the properties of the two constituents and their interfacial compatibility. The degree of adhesion between the components has a direct effect on the stress transfer and load distribution efficiency at the interface [58].

2.8.1 Mechanical Properties

The mechanical properties of NFRPMC depend on different factors such as volume fraction of the fiber, fiber-matrix adhesion, stress transfer at the interface, and the orientation of the fiber[56]. Since the fiber has much higher strength and stiffness compared with the matrix, the tensile property of polymer matrix composites depends on the interfacial strength achieved between the fiber and the matrix[57]. El-Shekeil et al. [58] studied the influence of kenaf fiber on the tensile and flexural properties of polyurethane thermoplastics using ASTM D-638[59] and ASTM 790 [60] standards respectively. Low fiber content has been reported to result in low tensile strength. This is due to the inefficient transition of load across the interface from the matrix to the fibers. With 30 wt. % fiber loading, the maximum strength of kenaf fiber reinforced polyurethane composite (i.e. 33.5 MPa) was achieved. There is a drop in the tensile strength of the composite with a higher fiber ratio of 40 to 50-wt %. Increasing fiber percentage leads to heavy agglomeration and inadequate stress transfer. In their report, they also noted an increase in Young's modulus. They observed that as the fiber ratio in the composite increase is increased, there is a consistent increase in both the flexural strength and modulus. Li et al.[61] Considered the effect of flax fiber on the mechanical properties of high-density polyethylene (HDPE) [64]. They found that flax fiber-reinforced HDPE containing the highest flexural strength and modulus with 30 wt.% fiber ratio, which were 51% and 128% respectively over that of pure HDPE. Also, they reported the tensile strength of 30 wt. % fibers has an improvement of 17 % as compared with pure HDPE.

2.8.2. Thermal Properties

Different researchers studied the thermal properties of NFRPC using TGA (Thermogravimetric analysis) and Scanning Calorimetry (DSC). Tajvidi and Takemura[62] studied the effect of kenaf fibers addition on the thermal degradation of polypropylene (PP) using DSC from room temperature to 200^{o}C at a heating rate of 20^{o}C/min. Approximately 10 mg of the ground composite was heated in an aluminum pan, while an empty pan of the same material was used as the reference. They observed a slight reduction in the melting and an increase in crystallization temperature. It is reported that kenaf fibers act as a nucleating agent, thereby increasing the crystallization temperature of the composites.

2.8.3 Water Absorption

Water absorption is the main challenge in NFRPC. It has a direct effect on the breakdown of the fiber-matrix interface resulting in swelling of the fiber, loss in load transfer between matrix and fiber, and a reduction in the strength and stiffness of the composites[63]. Maya et al. evaluated the water absorption characteristics of sisal and oil palm composites treated with varying concentrations of sodium hydroxide (NaOH) [64]. They reported that the composites containing fibers treated with 0.5% NaOH showed the highest water uptake, while those treated with 4% NaOH samples exhibited the minimum water uptake. It was observed that as the concentration of NaOH increases, the adhesion between the fiber and the matrix increases, and the uptake of water decreases. They also observed that the hydrophilic character of natural fiber is responsible for water uptake in the composites, and as the volume percent of fibers increases, there was a corresponding increase in the rate of water absorption[64]. They also reported a two-stage water saturation level, which was due to prolonged exposure of the swollen samples in water [30].

2.9 Application of Natural Fiber-reinforced polymer composites

In many engineering areas, the applications of natural fiber reinforced polymer composites are expanding rapidly. As seen in Fig 2.6, these composites are used in numerous industrial and structural settings, such as aircraft, automobiles, athletic products, maritime applications, infrastructure, electronics, furniture, and building industries[65].

Natural fiber-reinforced polymer matrix composites are used in the production of various parts of an automobile [66]. The manufacturing process for making parts to be used in industrial applications requires good finishes, which can be achieved with compression molding. Examples of compression-molded automotive parts using natural fiber-reinforced polymer matrix composites include bumper covers, roof frames, door frames, door panels, engine valve covers, dashboards, and truck car mats [67], [68].

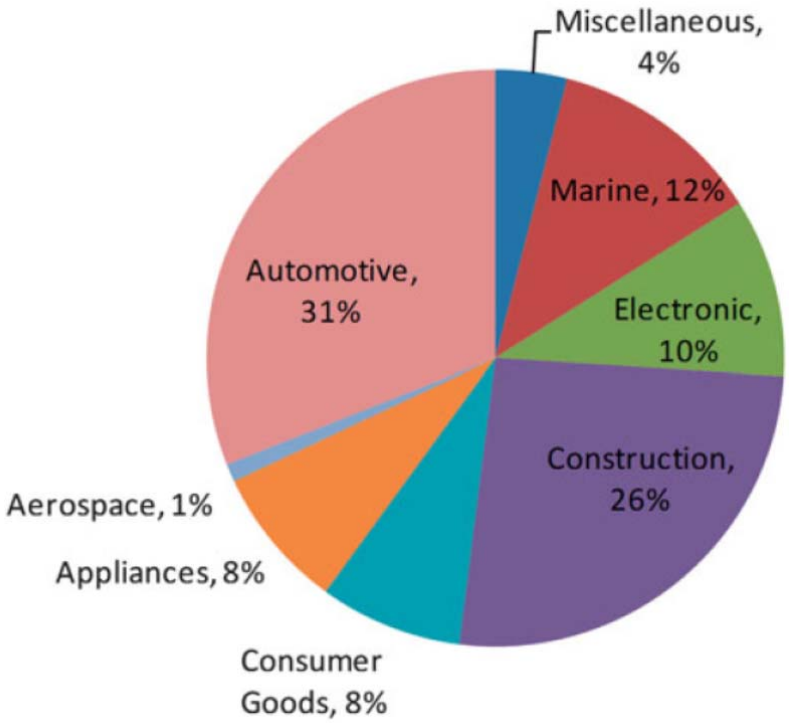

Figure 2-6 Natural fiber-reinforced Polymer Composites Applications in Different Industries [69]

2.10. Factor affecting Natural Fiber Reinforced Polymer Composites

To determine engineering characteristics of fibre reinforced polymer composites, appropriate fiber and processing techniques must be chosen. Several parameters, including fibre dispersion, orientation, aspect ratio, volume, and essential characteristics of the fibres, must be considered when using natural fibres as reinforcing materials.

2.10.1 Dispersion of Fibres

Fiber dispersion is one of the most important variables influencing the mechanical characteristics of fiber reinforced polymer composites, particularly short fiber reinforced composites. The inadequate dispersion of fibres across composites causes a substantial decrease in tensile and impact characteristics, according to the literature. Fiber agglomeration occurs in composites due to poor fibre dispersion, resulting in stress concentration areas and mechanical failure. The incompatibility of natural fibers (hydrophilic nature) with polymer matrices (hydrophobic nature) is the primary cause of poor fibre dispersion. Natural fibres and polymer matrices can be made more compatible by applying an appropriate surface treatment to either natural fibres or polymer matrices.

Mixing time during composite processing is another key factor that contributes to poor dispersion. A longer mixing period allows the fibres to disperse more evenly over the polymer matrix[69].

2.10.2. Fiber Orientation

Fibre orientation, also known as fiber direction, is a crucial element to consider when using fibre-reinforced composites for certain technical purposes. It is well known that unidirectional long fibre reinforced polymer composites have better mechanical characteristics than short randomly oriented fibre composites. It is also quite difficult to determine fiber orientation in short fibre reinforced composites. The influence of fibre length and fiber orientation distribution on the tensile strength of short fibre reinforced polymer composites was investigated by[70]. They discovered that

as the fibre orientation coefficient was raised, the composites' strength rose.

2.10.3. Aspect Ratio

The length-to-width ratio of fibers is known as the aspect ratio. It's a crucial element that has a direct impact on the mechanical characteristics of fiber reinforced polymer composites. The chemical composition and particle size of oak and pine wood particle reinforced PP composites was investigated by[71]. The aspect ratio of pine fibre wood was found to be greater than oak fibre; this improves interfacial adhesion between the fibre and matrix in fibre-reinforced composites.

2.10.4. Fiber Loading

Fiber volume fraction affects the mechanical and thermal properties of fiber reinforced composites. It has been well documented that when the volume percentage of natural fibres in polymer composites is low, the material properties of the composites decrease. This is because it produced gaps between the fibre and the matrix materials at low fibre concentration, which resulted in mechanical failure. The influence of fiber loading on the mechanical characteristics of thermoplastic starch (TPS) bio-composites reinforced with newspaper fiber was investigated by[72]. When 15 weight percent newspaper fibres were added to pure TPS resin, the tensile strength improved by 150 percent. However, when more fiber components were added, the tensile strength began to decline.

2.11 Sisal plant:

In the modern age of science different types of natural fiber are being explored for making biodegradable polymer composites[73][74]. There are more than one thousand types of fiber available worldwide and most of them are studied by different researchers[74]. Among these fibers, sisal fiber is one of the best reinforcement materials for polymer composites due to its higher cellulose content (78%), good tensile strength (>600MPa), and

availability[75]. Sisal or sisal hemp fiber is one of the families of Agavesisalana. It is an agave plant native to Central and South America and is now present in other countries such as Brazil, Tanzania, China, Ethiopia, Angola, South Africa, and Morocco because of its ability to thrive under a variety of ecological and climate conditions[76]. One sisal plant can produce 200-250 leaves in which 15 kg of fibers are extracted in a year [76].

Figure 2-7 Picture of the Sisal Plant

Figure 2.8 shows a picture of a sisal plant. Fibers are extracted from the leaves using different techniques. Water retting is a biodegradation process that separates the fibers from the leaf by breaking the chemical bonds. After extraction, the fibers are washed. It is a very slow process that may take 20 days for a single cycle of extraction of fiber. The process is unhygienic and produces a poor quality of fibers.

Boiling the leaves of the sisal followed by beating the leaves to get the fibers, and then cleaning using water and then drying in sunlight for a couple of days to get dried fibers is advisable for large-scale extraction of fibers. Inserting the sisal fibers into a decorticator machine powered by electric or diesel motors and pulling out the raw materials can mechanize this method.

This process is preferred because it is eco-friendly, hygienic, and fast compared with the other two processes.

Sisal fiber consists of 60-78% of cellulose, 10-14% of hemicellulose, 8-11% of lignin, and about 1.2 % of Pectin [77]. Mechanical fibers are easily extracted from the wall of the sisal leaf during the retting process. Ribbon fibers are extracted from the tissues in the median line of the sisal leaf; these fibers are long compared to mechanical fibers and they are easily split longitudinally from the leaf during the mechanical extraction process. Xylem fibers are irregular fibers from the very thin cell wall and have low strength and are easily broken during processing Figure2.8 these fibers are extracted from the vascular bundles of the sisal leaf [71]. The structure of sisal fiber cell wall is a form of composite structure[78].

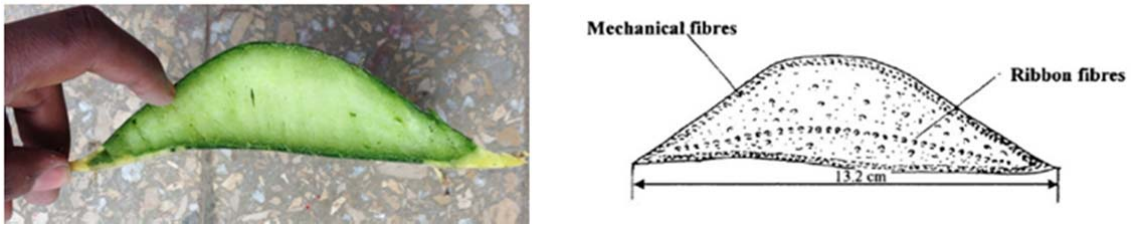

Figure 2-8 (a) Photograph Of A Sisal Plant; (b) The Cross-Section Of A Sisal Leaf [79]

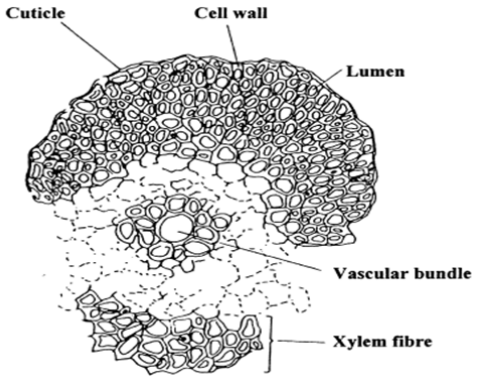

Figure 2-9 Cross-sectional View of Sisal Leaf Ribbon Bundles [71]

The mechanical and physical properties of sisal fibers are compared with other natural fibers in Table 2.3. Sisal fibers are one of the most widely used natural fibers for the development of natural fiber-reinforced composites. Joseph et al. (1996) [79] studied the mechanical properties and fracture toughness behavior of sisal fiber reinforced composites. They found the tensile strength of sisal fiber-reinforced LDPE composites increased by 66% as compared with raw LDPE. Joseph et al. (2003) [80] studied the thermal and crystallization properties of fiber reinforced polypropylene composites. Compared to pure polypropylene resin, thermal stability and crystallinity improved by 14_0c and 23 percent, respectively. The interfacial adhesion between the fiber and the polypropylene is the cause for its increase in thermal stability and crystallinity.

Oksman et al. (2000) [76] studied unidirectional sisal reinforced epoxy composite manufactured using the resin transfer molding method. It was found that the stiffness of the composite was 20 GPa, which was more than the stiffness of pure epoxy resin of 3.2GPa. The tensile strength was also higher at 210MPa compared with the pure epoxy resin value of 80MPa.

Rong Et.al (2002)[81] tried to study the impact performance of sisal and epoxy composite by modifying the sisal fiber using alkali, acetylation, and silane coupling agents, and heat treatment of fibers before combining with an epoxy resin matrix. In this study, a tensiometer, and dynamic mechanic analysis were applied to the surface to find the interfacial interactions of the composite. How the interaction mechanism influences the impact properties was also studied.

In previous years, the primary use of sisal was to make ropes and twines, with application only to these industries. Due to its good mechanical properties, sisal was also converted to yarn, string, bags floor mats, wall coverings, and handicrafts; today's paper industry also uses this plant as a substitute source of cellulose pulp. Currently, its application has extended to the automotive and building industries in the form of sisal reinforced composites. (Anandjiwal and John, 2010; Mussig, 2010). Sisal has also become a potential candidate to replace asbestos in roofing materials[82].

Among various natural fibers extracted from plant leaves, sisal fibers possess a higher percentage of cellulose components, which are the responsible factor for increasing tensile properties; also, they are less prone to water absorption. Among the various plant fibers, sisal fiber makes a major contribution in the construction industry for several reasons, i.e. abundant availability, low cost, good thermal and acoustic insulation properties, excellent tensile strength, high toughness, and abrasion resistance. In addition, these fibers have recently been used as reinforcement in cementitious composites [83][84]. The sisal fiber length is between 1.0 and 1.5 m and the diameter is approximately 100-300 μm[84].

2.10.1. Sisal plant in Ethiopia and World Contribution

According to FAOSTAT data as shown in figure 2.10, 10 countries have a major contribution to the world total production of sisal fibers. As shown in the figure, the production of Agave sisalana in Ethiopia is quite minimal. Nevertheless, most parts of the country are semi-arid [85], accounting for about 71% of the entire 1.115km^2 land area. About 46% of this land can be used to produce Agave Americana [86]. Much of the dry land is fertile ground with a remarkable potential to produce Agavesisalana by individual farmers or on a large-scale mechanized level. Since the harvest of sisal is quite labor-intensive, it could offer good job opportunities for the many rural inhabitants [86].

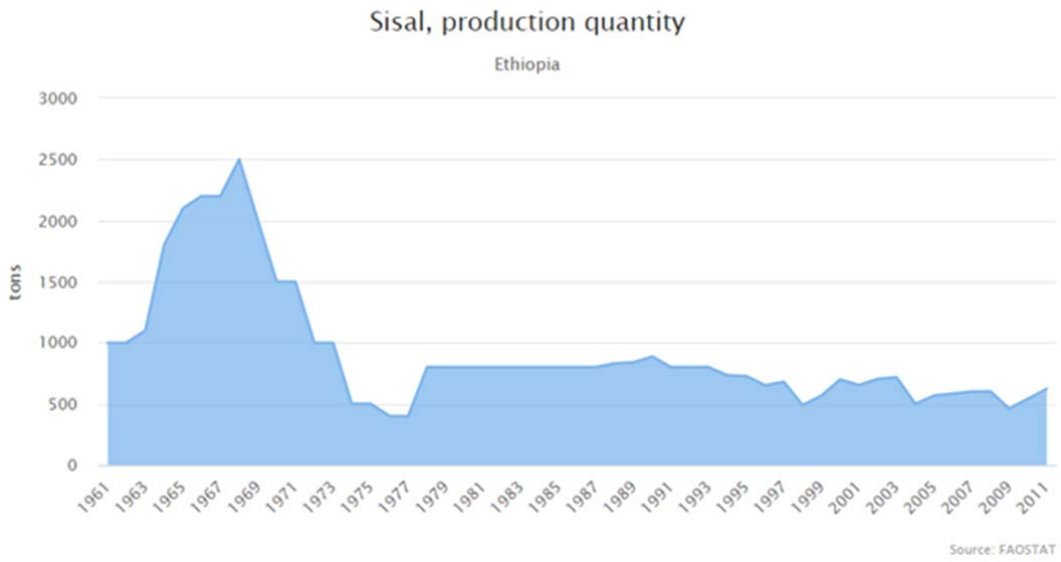

Figure 2-10 Sisal production quantity in Ethiopia 1961-2011

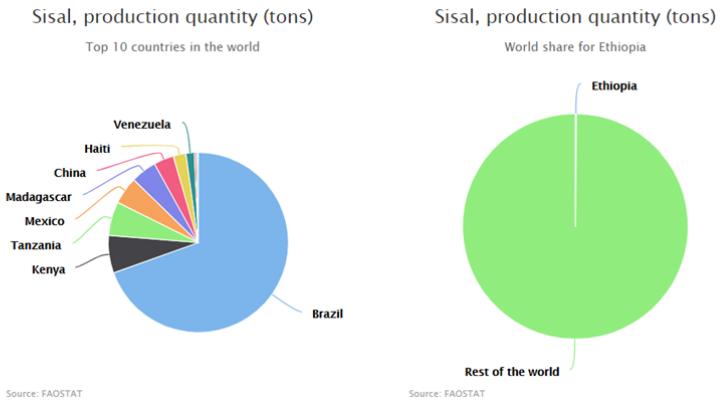

Figure 2-11 Top Sisal Production Countries in the World and Ethiopia's Share for the World Market

The Awasa State Farm accounts for 54 percent of all production of sisal. In the Metekel region (western Gojam), there is a wild variety of sisal growing abundantly, but it is not completely exploited due to collecting problems. Also, there is a great potential in Tigray regional state but it's mostly wild.[87].

2.11. Application of Natural Fiber Composites in the Automotive Industry

The application of composites is growing in different engineering fields. The automotive industry sector is among the manufacturers that are producing engineering components using natural fiber-reinforced polymers. Natural fibers such as sisal, jute, hemp, kenaf, oil palm, and bamboo reinforced polymer composites have grown in importance in the automotive, structural components, packaging, and construction industries [67] [88].

Natural based fibres provide a number of benefits over synthetic fibres, including low density, high specific strength, and low embodied energy. Furthermore, automotive applications are driving designers to transition away from oil-derived polymers and synthetic fibers and toward natural materials, concentrating on sustainability and green products that are either biodegradable or recyclable[89]. Table2.4,Figure 2.12,and Figure 2:13. The Application Of Natural Fiber Reinforced Polymer Composites In The Automotive Industry [90][91]–[93].

Table 2-4 application of natural fibre in different automotive parts

Manufacturer	Model	Application
Rover	2000 and other	Rear storage shelf/ panel, and insulations
Opel	Vectra, Astra, Zafira	Door panels, pillar cover panel, head linear panel, and instrumental panel
Volkswagen	Passat Variant, golf, A4, Bora	Seat Back, door panel boot lid finish panel, and boot liner
Audi	A2,A3,A4,A4 Avant,A6,A8,Roadstar,coupe	Boot-liner, spare tire-linin, side and back door panel, seatbacks, and hat rack
BMW	3,5 and 7 series and another pilot	Seatback, headliner panel, boot – lining, door panels, noise insulation panels, and molded footwell linings
Fiat	Puto,Brava, Marea, Alfa Romeo,146,156,159	Door panel
Peugeot	406	Front and rear door panels,

		seatbacks, and parcel shelf
General Motor	Cadillac De Ville, Chevrolet TrailBlazer	Seat backs, cargo area floor mat
Toyota	ES3, Raum, Brevis Harrier, celsior	Pillar garnish and other interior parts, floor mat, spare tire cover, door panels, and seatback
Volvo	V70, C70	Seat padding, natural foams, and cargo floor tray
Ford	Mondeo CD 162, Focus	Floor trays, door inserts, door panels, and seatback
Renault	Clio, Twingo	Rear parcel shelf
Mitsubishi		Cargo area floor, door panels, and instrumental panel
Mercedes Benz	C,S,E and A classes trucks	Door panels, glove box, instrument panel support, molding rod, seat backrest panel, trunk panel, seat backrest, engine cover, sun visor, interior insulation, bumper, wheel box, and roof cover
Citroen	C5	Interior door panel
Saturn	L300	Package trays and door panel

Automobile manufacturers are looking for greener materials to use in their products. As a result, there is a growing need for lightweight cars to decrease costs and environmental concerns. Furthermore, as compared to glass fibres in their respective composite constructions, natural fibres offer superior acoustic and thermal insulation, as well as higher energy efficiency and vibration damping[94].

Figure 2-12 Different parts of Automotive made of Natural Fiber

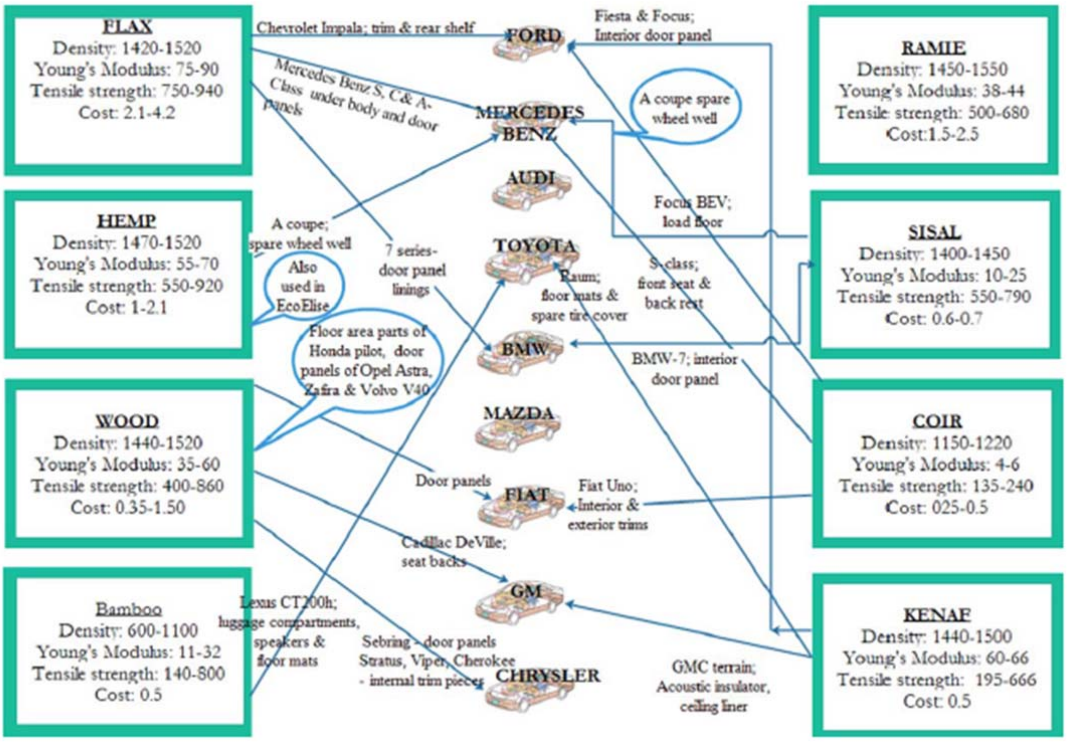

Figure 2-13 M. F. Ashby, material and Environment 2013

2.12. Research gap

Natural fiber reinforced composites have a number of benefits, but their usage in non-structural applications like car interior components has been limited. One reason for this is a lack of test data on how these composites perform in various load-bearing conditions, such as mechanical properties, thermal properties, dynamic properties, and fracture toughness modes. Despite this, natural fibre composites have progressively been extended to structural applications because of issues such as delamination and cracking, leading to the production of flaw-free goods. Figure 2.14 shows the research outputs of natural fiber reinforced polymer composites in 2016-2018

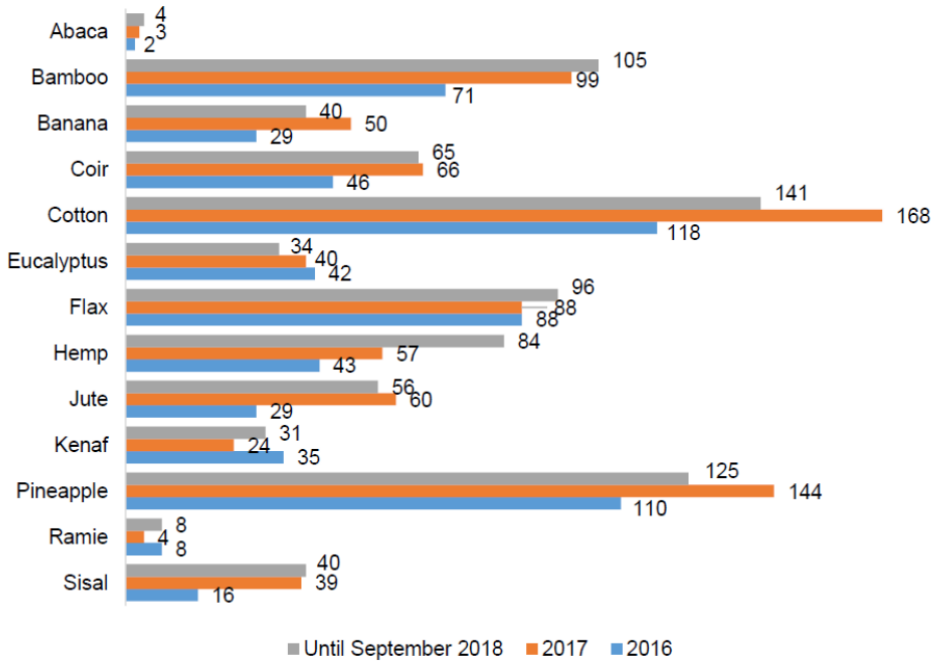

Figure 2-14 Number of research articles about natural fibres on composites.

CHAPTER 3:

Materials and Experimental methods

3.1. Materials

This chapter is focused on the experimental materials used, and the procedures followed to realize the research objective mentioned in chapter one section 1.3. The raw sisal fiber used in this study is obtained from Metekel Zuria Woreda, Akaki Woreda, and Harer Mountains in Ethiopia. For ease of processing and characterization, the outer part of the fiber is decorticated manually and the resulting raw fibers are subsequently cleaned using tap water to remove the lignin and waxy substances and other impurities on the fiber surfaces. After cleaning, is the fibers are dried in open air for 5 consecutive days. Figure 3.1 shows the sisal fiber before and after cleaning and decortication.

Figure 3-2-15 Prepared Natural Fibers: as Extracted (a), as Washed (b) and as Treated and Dried (c)

The physical and mechanical properties of the fiber must be taken into consideration in the fiber selection process, since this can influence the overall structural strength of the composite. Thermal properties, ply thickness, tow scale, ply versatility, component curvature, sizing, surface treatments for matrix bonding and wetting, cost, lead time, and availability are other fiber selection considerations[95].

A thermosetting matrix type epoxy resin is used as a matrix for this study. It is supplied from the local market in Addis Ababa, World Fiber Glass PL and from Composite Canada in Toronto. Sisal fiber has good compatibility with various types of thermoset and thermoplastic matrices as seen from various research works over the years. Epoxy is selected as the matrix material due to its ready availability, and ease of processing at room temperature. The general flow chart used to prepare the composite is shown in Figure 3.2

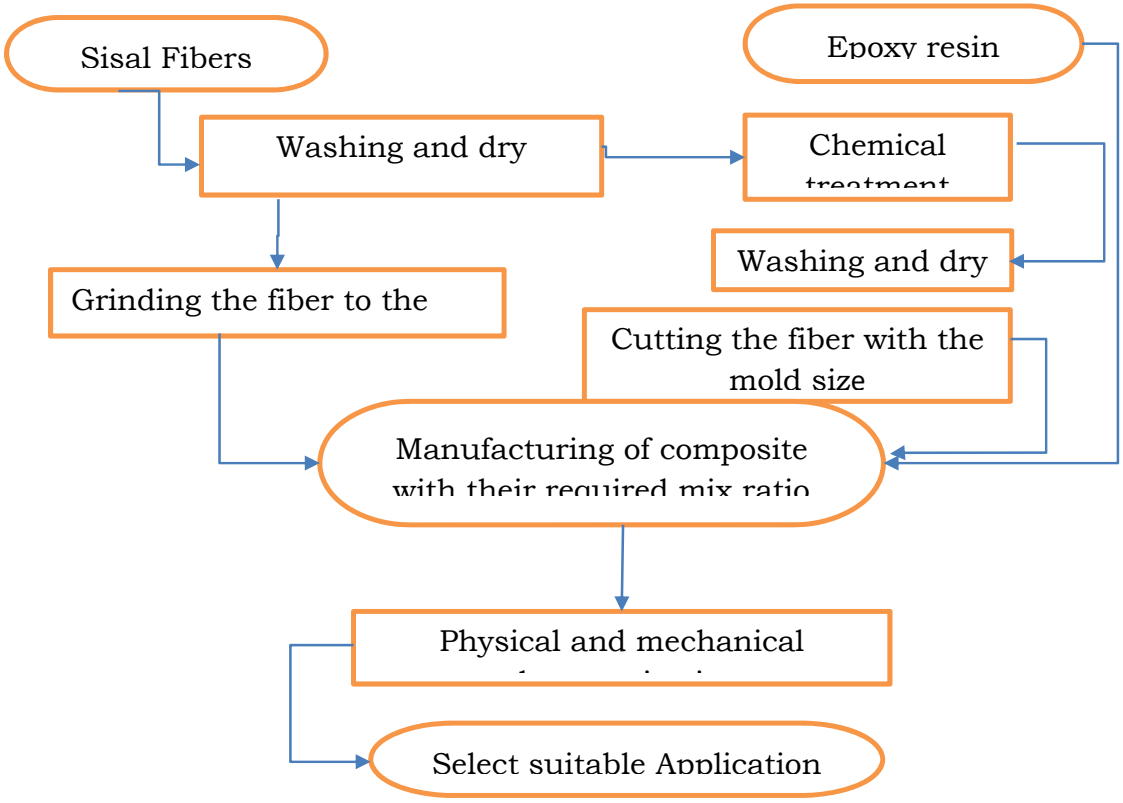

Figure 3-2-16 Flow Chart for Sisal Fiber Processing, Treatment, And Characterization

3.2. Characterization of Sisal fibers

To fully understand the behavior of sisal fibers, different physical, thermal, chemical, and mechanical tests are carried out. These include diameter measurement, thermal analysis, tensile test, and water absorption measurements.

3.2.1 Fiber Diameter

The diameter of the fiber is measured using single fibers to determine the average diameter. The diameter of the selected fiber is then measured using a biological microscope scanner with magnification power 10X0.22. Ten fibers with 50mm length at four different locations are measured as shown in figure 3.3.

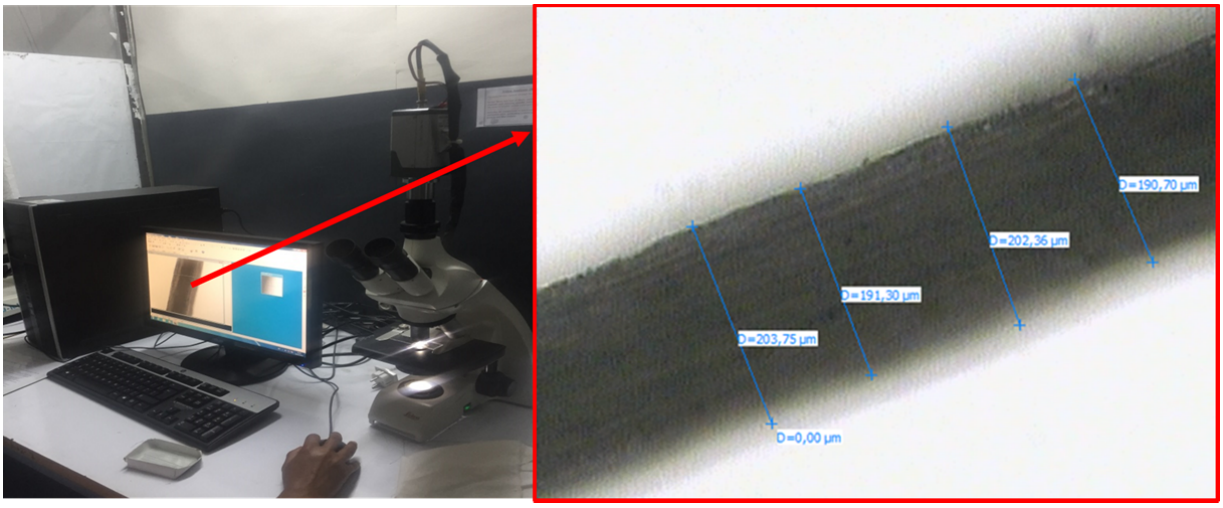

Figure 3-2-17 Diameter of Sisal Fiber Measurement

3.2.2 Tensile test

The tensile properties of the cleaned fibers are determined according to ASTM D 3822-14 standard using a 5 kN capacity Instron universal testing machine (model 3366) at a crosshead speed of 2mm/min and using fiber length of 45mm. The tensile test is conducted at an ambient temperature of 23^{0}C and relative humidity of 25%. The diameter and cross-sectional area of each fiber used in the test are measured and recorded. The single fibers are mounted individually into the grips of the tensile testing machine with brown tissue paper to prevent slippage and fracture of the fiber in the grips. The fiber lengths are measured from one end of the tensile grip to the other as shown in figure 3.4

Figure 3-2-18 Picture Showing A Schematic Drawing Of A Single Sisal Fiber Prepared For Tensile Test.

To study the effect of fiber length on the tensile properties of sisal fiber, two different fiber lengths (45, 70 mm) are used. Five sisal fibers are tested at each length. The effect of fiber length on the percent elongation is also investigated. In this test, a fixed gauge length of 50 mm is used while the fiber length is varied. Five fibers are tested at each length. A crosshead speed of 2 mm/minute is used.

3.2.3 Water Absorption of Sisal fiber

The objective of the test is to determine the water absorption capability of dry sisal fiber when it is immersed in water. The apparatus and the material used in this test included an oven and a weighing balance. Five samples of approximately 1g each are used in this experiment. The fiber is dried for 48 hours in an oven at 60_0C. After drying and final weight is noted, the fibers are immersed in distilled water at room temperature. The fibers are removed from the water bath after various amounts of time, the surface water is removed, and the fibers are weighed immediately. The weight mass recorded as a function of time until saturation is reached. The water content of the fiber (in wt.%) is computed using the equation below

$$M_t(\text{wt.}\%) = \frac{(W_t - W_0)\,x\,100}{W_0} \quad \text{----------3.1}$$

Where Wo and W_t denote the dry weight of sisal fibers and weight of the fibers after a specific time t immersed in the water, respectively.

3.3 Chemical Treatment of Sisal Fiber

Good sisal fiber-matrix adhesion is necessary for the transfer of load from the matrix to the reinforcing fibers at their interface. To improve sisal matrix adhesion, chemical treatment is carried out on the fibers to modify their surface chemistry: alkaline (NaOH) treatment. Three solutions of NaOH with different concentrations (5%, 10% and 18 % by weight) are prepared by dissolving sodium hydroxide pallets in diluted water.

After immersion, all the fibers are initially washed in distilled water and finally washed using tap water to ensure that no NaOH is left until the Ph. value of the water is close to seven. Subsequently, the fibers are dried at 60_oC in an oven for 48 hours. The process is shown in figure 3.5.

Figure 3-2-19 Images of Sodium Hydroxide Solution before Use For Treatment And After Treatment

3.4 Manufacture of Sisal Fiber Reinforced Epoxy Composites

Figure 3.6 shows the flow chart for sisal fiber-reinforced epoxy processing and characterization. Before manufacturing, sisal fibers are dried at 60_0C for 48 h to eliminate moisture. After drying, 15%, 25%, 30%, 35%, and 40% by weight untreated and alkaline treated fiber are mixed with epoxy.

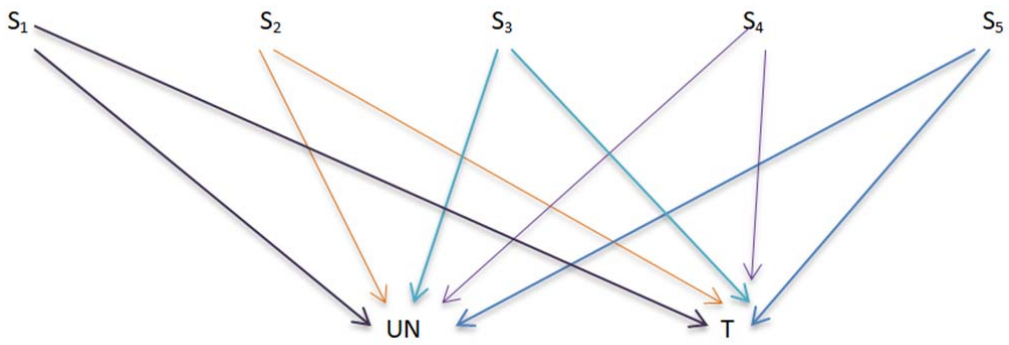

Figure 3-2-20 Processing chart showing the mixing of untreated and treated sisal fiber

Figure 3.6:- Processing chart showing the mixing of untreated and alkaline treated sisal fiber with epoxy resin to make sisal fiber reinforced epoxy composite. S_1= 15wt.%, S_2=25 wt.%, S_3=30 wt.%, S_4=35 wt.%, S_5=40wt.% of fiber and UN= untreated sisal fiber , T= treated with 10% w/v aqueous NaOH solution at ambient temperature for 3 hours.

3.4.1 Compression Molding Equipment and Process

The compression molding technique is used in formatting the sample plate composite with a predetermined thickness. The mold is coated with a mold release agent for easy removal of the composite plate from the mold.

Figure 3-2-21 Mold Release Agent Mold Plate And Compression Molding Machine Used For the Preparation of Sample Plates.

Composite plates of dimensions 200mmx250mmx3mm are prepared for pressing in the mold for 3 hours at room temperature under 5MPa to ensure

the pressing helps to release air voids and excess material. Test specimens are made for tensile, flexural, impact, fracture toughness, low-velocity impact test, mechanical dynamic analysis (DMA), and thermography analysis (TGA).

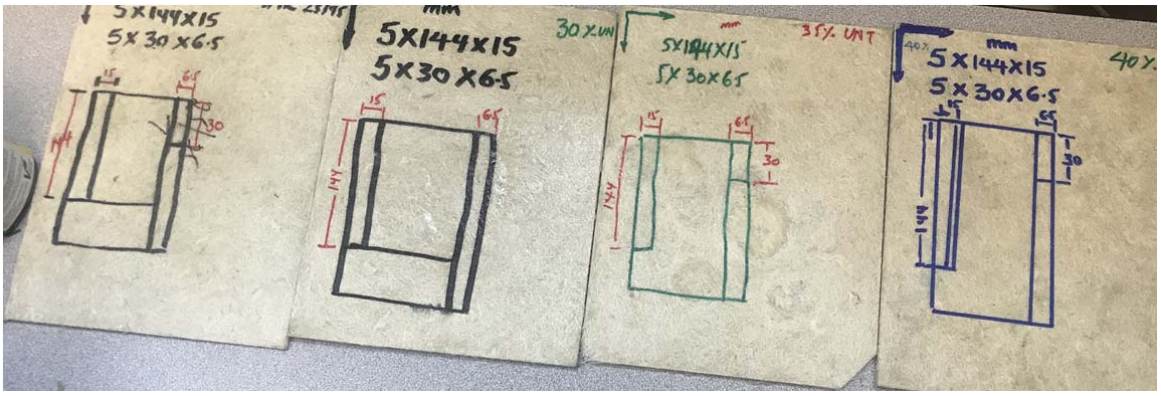

Figure 3-2-22 Image of Composite Plates Made Using Hand Layup and Compression Molding

3.5 Characterization Sisal Fiber Reinforced Epoxy Composites

The mechanical and physical properties of sisal reinforced epoxy matrix composites developed in this study are determined by experimental tests. The microstructures of the fractured surface of the specimens after mechanical testing are examined using a scanning electron microscope (SEM).

3.5.1 Tensile Test of Composites

Tensile test is conducted using an Instron™ (model 5500R) machine according to ASTM 638 standard [89]. The test is conducted at ambient temperature (23^0C). The test specimen is cut into a dog bone shape of dimensions 150mmx20mm x 3.mm using a water jet cutter. A typical specimen is shown in the figure3.9. Five specimens are tested for each composite formulation using a load cell of 5kN capacity and crosshead speed of 10mm/min. No extensometer is used for the determination of Young's modulus. Instead, crosshead displacement is recorded, and the modulus is calculated while adjusting for machine compliance.

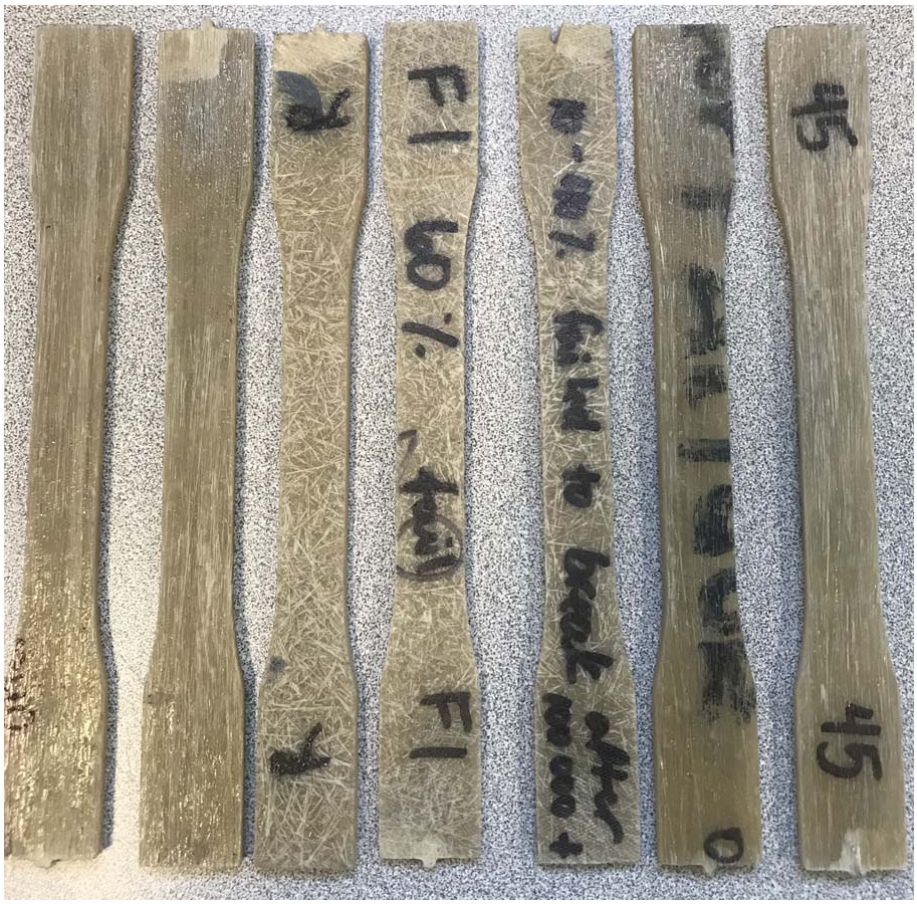

Figure 3-2-23 Dog Bone shaped specimens for tensile test

Figure 3-2-24 InstronTM Tensile Testing Machine for Determining Young's Modulus and Strength of the Test Specimen

3. 5.2. Flexural Test of Composites

Flexural tests are performed using an Instron load frame model 8511 universal testing machine according to [96] ASTM D 7264/ 7264 M – 07 standard test methods. Flexural tests are used to determine flexural stress at peak load, strain at peak load, and chord modulus. Procedure A is followed. In procedure A, the specimen is supported by two cylindrical support noses while a third cylindrical loading nose applies a force to the centre of the specimen, causing it to bend. Specimens are tested using a 32:1 span to thickness ratio, where "span" is the distance between specimen support noses; a support span of 50.8mm is chosen for all specimens.

The loading nose is lowered between the two support noses at a rate of 2 mm/min. After the peak load is reached, the load needed to bend the specimen is reduced. Break sensitivity on the machine is set for 75%, which stops the test when the load decreases to 25% of the peak load value.

The following procedures are used to find stress, strain, and chord modulus:

$$Flexural\ Stress = \frac{3PL}{2bh^2}$$ ----------eqn 3.2

Where P is the peak load, L is the distance between loading noses, b is test specimen width and h is thickness.

$$Strain = \frac{6hx}{L^2}$$ ----------eqn3.3

Where h is test specimen thickness, and x is the maximum specimen deflection.

Chord modulus is found by dividing the change in stress over a strain range of 0.002. SEM images are taken at the locations of specimen failure.

3.5. 3. Impact Test of Composites

The toughness of the material can be determined by measuring the impact properties. The higher the impact energy of the material, the higher the toughness. The impact test is performed using an Instron impact tester on sisal reinforced epoxy composites. The tests are carried out according to ASTM D256 standard[97][98][99].

The test specimen has dimensions 55mm (length) x 3mm (thickness) x 10mm (width), and is notched using a broaching machine as shown in figure 3.12. The depth, radius, and angle of the specimen are 1.75mm, 0.25 mm, and 22.5^0 respectively; see Figure 3.13. For each sample type, five specimens are tested. The energy absorbed per unit area (E_i) is calculated using equation 3.3 [92], and the reported energy absorbed per unit area (E_i) is the average value for the 5 specimens.

$$E_i=\frac{E_a}{bxd}\text{----------eqn 3.4}$$

Where E_i, b, and d are the energy absorbed, the width and thickness of each sample, respectively. All parameter values are recorded.

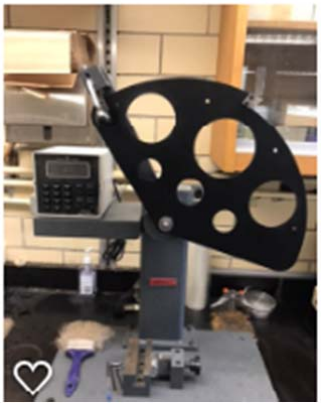

Figure 3-2-25 impact-testing machine used for this study

Figure 3-2-26 Notch making machine used for this study

Figure 3-2-27 Impact Test Samples

3.5.4 Water absorption

The water absorption behavior of the composites is determined by immersing samples measuring 30mm (length) x 3mm (thickness) x10 mm (width) in distilled water at room temperature. Five specimens per composite are used. The samples are measured before immersion in distilled water at room temperature following ASTM D570-98 standard[100]–[102]. Each test is done in 24-hour intervals followed by the moisture from the surface. The process is repeated until the samples reach their saturation limit. The percentage of water absorbed is determined using equation 3.1

$$Water\ Absorption\ (\%) = \frac{W_2 - W_1}{w_1} x100 \text{---------- eqn 3.6}$$

3.5 .5 Thermal Analysis

The thermal analysis of sisal reinforced epoxy composites is carried out using the TGA instrument Q500 V20.13 (Figure 3.13). Each scan is performed in a platinum Pan under nitrogen gas from room temperature up to 800^0C at a heating rate of 10^0C/min. Composite samples of mass 15mg are used for each test.

Figure 3-2-28 TGA Testing Machine Used To Test The Thermal Effect Analysis

3.5. 6 Microscope Inspection of Composites

Microstructural evaluation of fractured test samples is conducted using a Hitachi TM 3000 scanning electron microscope, with an accelerating voltage of 15000 V at varying magnification levels.

3.5 .7. Dynamic Mechanical Analysis

In a Dynamic Mechanical Analysis (DMA) test a stress or strain is applied to a sample at controlled frequencies, and the response is analyzed to obtain phase angle δ and deformation data (Figure 3.15). This data allows the calculation of the material damping or tan δ, as well as the storage modulus (E') and loss modulus (E").

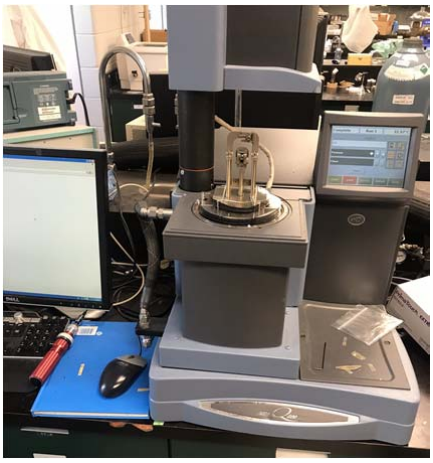

Figure 3-2-29 DMA Testing Tool

3.5. 8 Fracture Toughness Test

Fracture toughness was measured for the sisal reinforced epoxy composites using ASTM Standard D 5045, 1999 ASTM E 399-90 test standard method for plane strain fracture toughness and strain energy release rate for plastic and composite material [93]. These tests are designed to characterize the toughness of composite materials with regard to the critical stress intensity factor, $K_{IC,}$ and the energy per unit area of crack surface or critical strain energy release rate, G_{IC}, at fracture initiation and propagation.

(a) (b)

Figure 3-2-30(a) Typical CT specimen under compact tension test using UTM machine in AAIT lab, (b) sisal fiber reinforced epoxy composites after compact tension test.

3.5.9 Fatigue test

This test is used to determine the response of sisal reinforced epoxy composite materials under fluctuating loading conditions. Fatigue testing is performed on the Instron 8511 hydraulic fatigue machine on 30:70 – Random and 30:70 [0,90] samples at the University of Toronto Mechanical Engineering Department. A sine waveform and frequency of 10Hz were used. Two randomly oriented samples were used as dummies to find a range over which to test samples. They were tested at roughly 80% and 40% of the peak load sustained by 30:70 – Rand samples in the tensile test. at the mechanical and industrial engineering department , university of Toronto , Canada at room temperature. An extensometer is not used to determine the limit of deflection. The frequency used for this test is 10 Hz with a crosshead speed of 2mm/min. The specimens are dog bone shaped and have the same dimensions as used in the tensile test.

3.6. Low velocity Impact Testing Machine designed and prototyped

Since the proto type and the design procedure all done by our Msc student we simply pass to experimental investigation. In these parts, the test method for drop weight impact using drop weight impactor is discussed. In particular, this means each different type of impact is identified, and the impactor mass and drop height configuration used are described. The typical results from an impact are presented, showing what information can be garnered from the data.

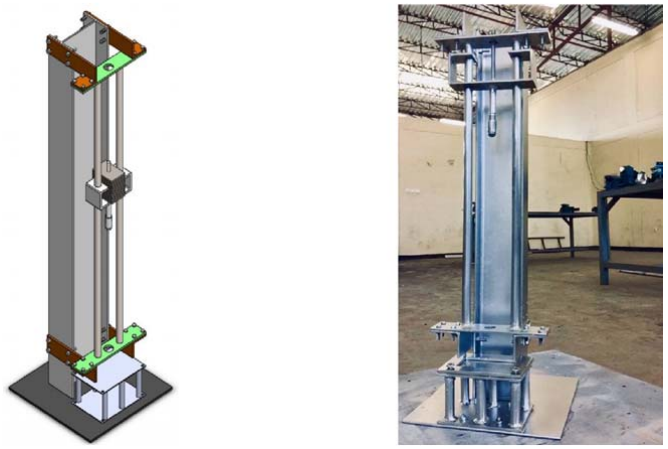

Figure 2-31 Designed and manufactured Low velocity impact machine

3.6.1 Test Specimen

The test specimen for low velocity impact test machine is designed as per ASTM Standard Test Specimen D7136/D7136M-05 [103] as it is shown in the figure 3.17

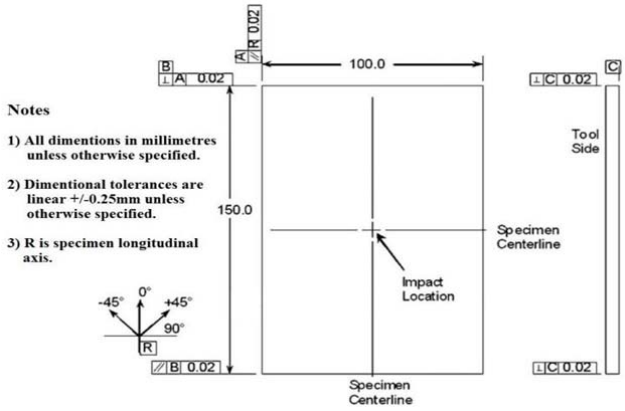

Figure 3-2-32 ASTM D 7136 Standard specimen for drop weight impact testing

3.6.2 Impact Testing

It is known that in the low velocity impact of isotropic solids the softer body is permanently deformed. Although the softer body will always deform largely, the behavior of composite structures under impact is very much material dependent.

The main objective of the current research is to investigate the response of fiber reinforced composite laminates at perpendicular impacts. The design facilitated impact energies up to 33.5 Joules and impact velocities in the range 0 to 3.49 m/s. A 5.5 kg mass, with a 16 mm hemispherical impactor, was raised to specified level, released and caught manually at its maximum rebound height. The incident an Rebound kinetic energies were evaluated, by accurately monitoring the striking and rebound velocities of the indenting mass.

The measurement system, which described section 3.6.3 in details, consisted of piezoelectric accelerometer connected to the drop weight. The output of the sensor fed to Model 485B39 digital ICP signal conditioner.

3.6.3 Impact Instrumentation

To fully characterize the impact behavior of the material under test and to determine the energy dissipated by the specimen, the following parameters should be measured at least: crushing force, specimen defection under compressive load, initial and final linear impact velocity or initial impact energy (immediately before the impact) and energy dissipated by the specimen during the impact.

In addition, other important properties (i.e., fracture/damage propagation, extent of plastic strain, formation of plastic hinges, etc.) can be determined by a careful examination of the specimen after the test, which will not be covered in this work.

This paper presents the design of an instrumented tester, using an accelerometer as the sole instrumentation, in which a PC computer is used for data acquisition, computations, and the reporting of results.

3.6.4. Sensor selection

In order to record relevant impact data such as the load/time history etc., some sensors selection needs to be necessary. The following sensors are widely used in impact assessment of composite materials, which are also reviewed in literature.

1. Load cell: have been widely used in the past either mounted on the tup or in the sample support. This measured the loads experienced by the tup or those transmitted to the support. Several researchers took this type of instrumentation approach, as it provides a reliable method of analyzing the dynamic response of structures[104][105] [106][107]

2. Laser Doppler Velocity meter (LDV): originally developed to measure the velocity of fluids. Rayes.G.etl. [108] record velocity of the tup using LDV during impact.

3. Accelerometer: the device can be mounted on the tup, the support or even the test specimen itself [109]. Compared to the other types

of sensors, piezoelectric accelerometers have important advantages[110]

- Extremely wide dynamic range, low output noise - suitable for shock measurement as well as for almost imperceptible vibration.
- Excellent linearity over their dynamic range
- Wide frequency range
- Compact yet highly sensitive
- No moving parts - no wear
- Self-generating - no external power required
- Great variety of models available for nearly any purpose
- Acceleration signal can be integrated to provide velocity and displacement - no need of additional velocity, displacement sensors.

Selection: Cessna et al [111]. Seem to have been the first to realize that it is possible to obtain both kinematic information (deflections, velocities) and dynamic information (forces, energies) from a single accelerometer attached to the falling weight in falling weight-plaque geometry. This minimizes the cost for force, velocity and deflection measurements independently. According to Newton's law, acceleration in the impact direction (measured by the accelerometer) immediately yields the total force on the striker in the impact direction. Since only the use of an accelerometer in situations in which all forces on the striker not related to its interaction with the sample are known is being proposed, the force between striker and sample can be obtained by subtraction. In addition, as long as the force between sample and striker is different from zero the sample and striker are in contact which means that the velocity of the sample at the contact point is equal to the velocity of the striker, and the deflection of the sample at the contact point is equal to the displacement of the striker (assuming the striker to be rigid in comparison with the sample). The velocity and displacement of the striker, in turn, may be obtained from the acceleration by successive integration[112].

3.6.5. Sensor Mounting

The mounting of sensors are as shown in figure 3.19. When choosing a mounting method, consideration both on advantages and disadvantages of each techniques. Characteristics like location, ruggedness, amplitude range, accessibility, temperature and portability are extremely critical. However, the most important and often overlooked consideration is the effect the mounting technique has on the high frequency performance of the accelerometer [113].

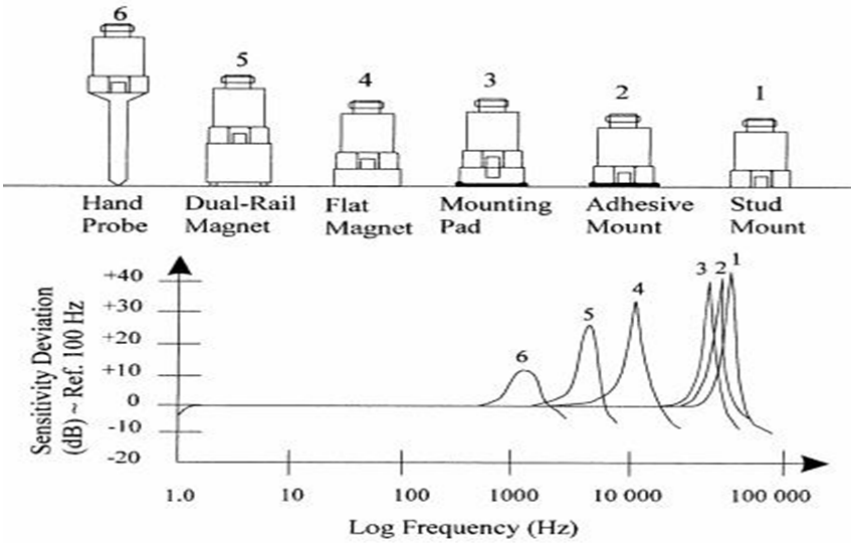

Figure 2-33 Assorted mounting configurations and their effects on high frequency

The accelerometer is positioned directly on the impactor mass, which needs permanent mounting technique in order to avoid misalignment of the accelerometer from the mass. Also hand probe, dual-rail magnet and at magnet mounting are highly sensitive above 10,000 Hz, but the others sensitivity rise above 10,000 Hz. For these reasons stud mount is selected for long-term measurement.

3.6.6 Data Acquisition and Manipulation

For simple drop-weight impact testing, no data acquisition equipment is required. According to ASTM D7136, if such equipment utilized, it shall be in accordance with Annex E, Minimum Instrumentation Requirements, of Test Method D3763. The natural frequency of the transducer-impactor assembly shall be greater than 6 kHz, the analog-to-digital converter shall be 8-bit or greater, the minimum sampling rate shall be 100 kHz, and the data storage capacity shall be 1000 points or larger.

The accelerometer puts out a voltage proportional to acceleration. The signal is recorded using the ICP signal conditioner. The 485B39 is a 2-channel ICP (IEPE) sensor signal conditioner featuring 2 BNC inputs and a USB digital signal out-put. Play & plug connectivity is achieved via USB without any cumbersome setup or driver installation. The 485B39 powers ICP sensors while digitizing their signals: simply plug the unit into a USB port of Lenovo E51 laptop computer to view, record, or process signal from the accelerometer. The data then plotted using Spectral PLUS-SC software as shown in the Figure

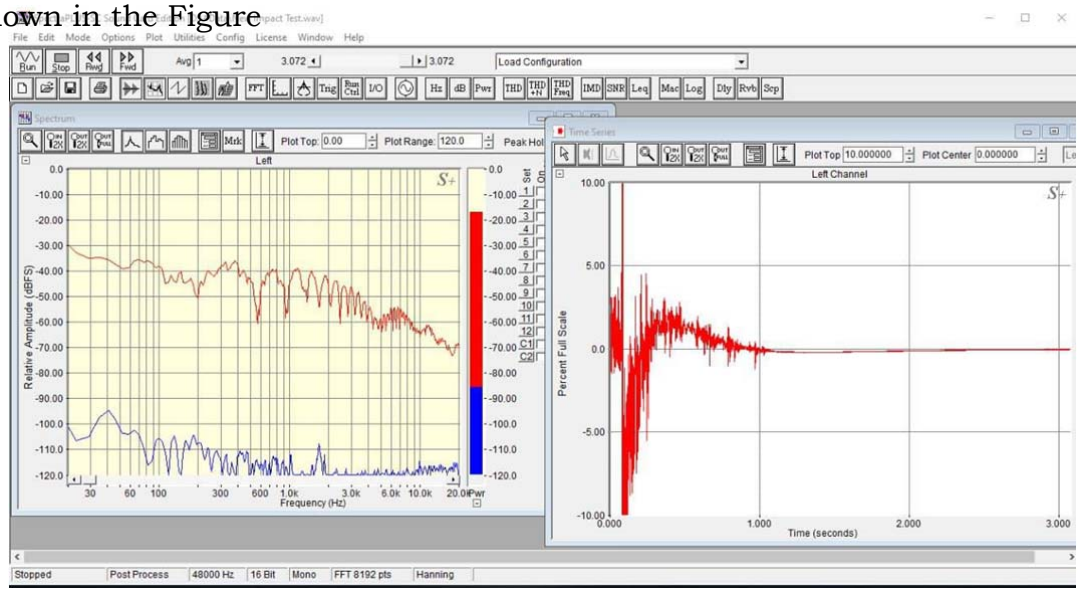

Figure 2-34 Spectral data from 352B accelerometer

Using Mat lab the result from spectral data plotted into force-time graph, energy-time graph, displacement-time graph, velocity-time graph, acceleration-time graph using free undamped vibration analysis. For

conversion of spectral data from the accelerometer data acquisition system to the required velocity and acceleration, we used the following procedure.

Spectra are defined by the maximum response of a simple oscillator subjected to Base acceleration a (t). The equation of motion of the oscillator is given as [114].

$$X^{||} + 2\beta\omega X^{|} + \omega^2 X = -a(t) \text{----------eqn 3.7}$$

In which β=the fraction of critical damping and ω= the natural frequency of vibrations of oscillator. Assuming that a(t) may be approximated by segmentally linear function, therefore equation 3.6 may be written as

$$X^{||} + 2\beta\omega X^{|} + \omega^2 X = -a_i - \frac{\Delta a_i}{\Delta t_i}(t - t_i) \dots\dots t_i \leq t \leq t_{i+1} \text{----------eqn 3.8}$$

$$\Delta t_i = \Delta t_{i+1} - \Delta t_i, \Delta a_i = \Delta a_{i+1} - \Delta a_i$$

CHAPTER 4

4.1. RESULTS & DISCUSSION

From the experiments described in chapter three, results are presented and discussed in this chapter. The results contain two main sections, the first which is focused on characterization of sisal fiber and its treatment. The second section contains results of characterization of the sisal fiber reinforced epoxy composites.

4.1.1 Characterization of Sisal Fiber (SF)

Chemical composition, mechanical and thermal properties, crystallinity, water and moisture absorption characteristics and behavior are the main findings of characterization of the sisal fiber. Chemical composition of SF was performed both before and after chemical treatments. The results of computational analysis are obtained by varying the concentration of NaOH, and are presented in Table 4.1. Table 4.2 shows the results of chemical composition measurements of sisal fiber on a "dry matter" basis, which excludes the presence of moisture. The dry matter basis (DMB) chemical composition is calculated using equation 4.1

$$DMB(\%) = \left[\frac{\text{As-recived content (\%)}}{100\% - \%\text{moisture}}\right] x100 \text{---------- eqn 4.1}$$

Table 4-1 Estimate of Cellulose Hemicellulos And Lignin For Both NaOH treated and untreated sisal fiber

Cellulose (%)	Hemicellulose (%)	Pectin (%)	Wax (%)	Lignin (%)	Ash (%)	Reference	Remark
77.1	18.8			1.8		Current work	NaOH treated 10%
73.6	21			2.4		Current work	NaOH treated 18%

68.5	24.6			3.3		Current work	NaOH treated 5%
64.2	31.5			3.9		Current work	Untreated fiber
72	10.1			7.6	3.1	Sydenstricker et al[115]	
78	10			8	1	Jacob et al [116]	
85-88	4			4.5		Joseph et al [117]	
65-75	10-14			9.9	2	Bismarck[118]	
67-78	10-14.2			8-11		Li-et al [47]	

An increase of 20% in the cellulose content is recorded after NaOH treatment. A decrease of 35% in the hemi-cellulose content in relation to untreated sisal fiber is also recorded. The cellulose content of the fiber is very important because it provides good bond strength and stability for composites. Mechanical properties of natural fiber depend on the NaOH treatment; it was observed that the fibers treated with 10 % NaOH solution at 60^0C for 5 h and dried for 48 hours inside an oven exhibit the highest cellulose content [119].

4.1.2 Mechanical Properties

The stress-strain curve found for treated sisal fiber (crosshead speed =2mm/min, gauge length of 25mm) is shown in figure 4.1. The fiber deformed elastically until the maximum stress was reached. A similar result was reported for sisal in the literature [120].

For five treated and untreated fiber specimens, the average fracture strength was 538 MPa. Table 4.2 illustrates the relationship between fiber strength and fiber gage length. The likelihood of having flaws on the fiber rose as the fiber length increased, resulting in failure in the tested fiber and a reduction in tensile strength.

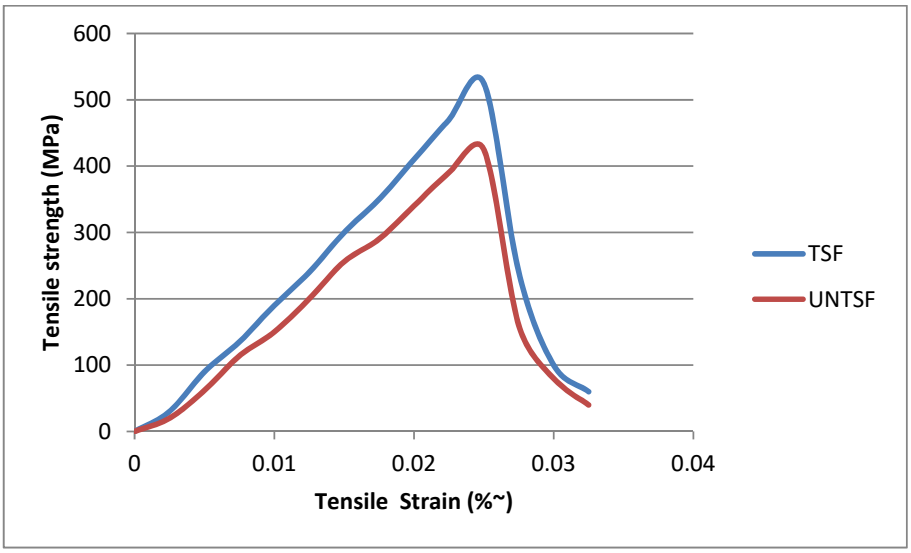

Figure 4-0-1 Tensile Strength vs. Tensile Strain of Sisal Fiber both treated (TSF) and Untreated (UNSF)

A comparison of these results with published data is tabulated in table 4.2.The literature generally agrees with our findings; therefore the average tensile strength of sisal fiber generally lies between 250-700MPa for both treated and untreated sisal fiber.

Table 4-2 presents the average Mechanical Properties of Sisal Fiber for untreated and alkaline treated current work and literature results

Gage Length (mm)	Tensile strength (MPa)	Young's Modulus (GPa)	Strain to Failure (%)	Reference
50	440	12.5	2.5	Untreated
50	578	14.8	4.2	5%NaOH treated
50	538	7.8	2.5	10%NaOH treated
50	369	11.6	2.1	18%NaOH treated
10	375	9.1	-	[120]
20	567	10.4	5.5	[121]
30	487	14.8	3.4	[120]
40	577	15.7	3.4	[120]
50	526	8.4	3.2	[122]
65	481	19	3	[123]

The greatest and lowest tensile strength values for treated samples ranged from 369 to 578, with the maximum tensile strength reported in 5 percent NaOH treated fiber. The tensile characteristics of the material diminish as the concentration of NaOH increases. Khan *et al* [124] studied the mechanical characteristics of untreated and treated sisal fibers and obtained similar results to ours. Chemical treatments have been reported to reduce fiber strength by breaking the binding structure and causing non-cellulosic materials to disintegrate[125].

Figure 4.2 shows the FTIR spectrum of untreated and treated sisal fiber. The peak at 1733.8 cm-1 is selected to C=O unconjugated stretching of carboxylic acid or ester of the hemicelluloses and the peak at 1239.1 cm-1 is allotted to C–O stretching vibration of acyl group present in the lignin. The broad peak in the range of 3300–3500 cm-1 and a peak at 1630 cm-1 are due to the characteristic axial vibration of hydroxyl group of cellulose. The peak at around 1080 cm-1 is due to the associated hydrogen group [126]. For the evaluation of all spectra is possible to verify that there was no disappearance of any of the major peaks. This indicates that the treatment applied does not alter the chemical structure of the fibers and sisal residues[127].

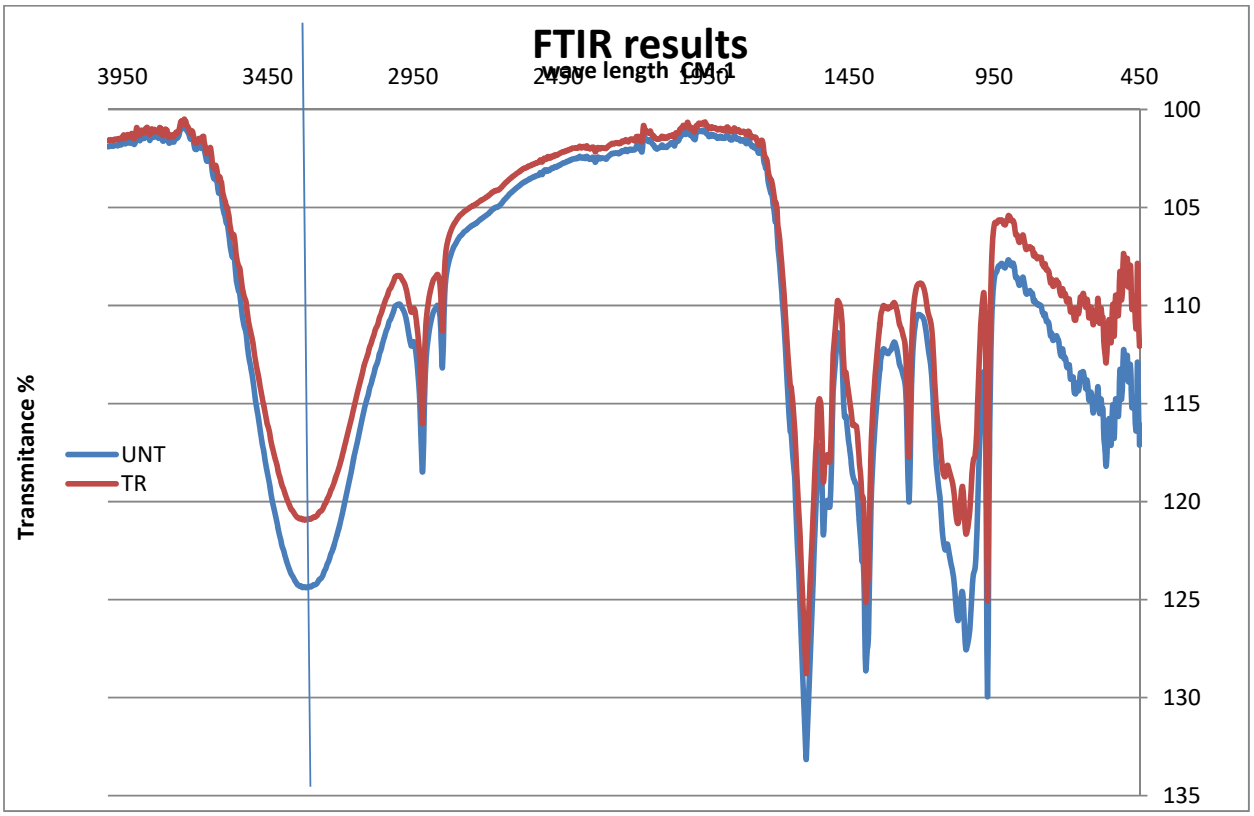

Figure 4-0-2 FTIR spectrum of untreated and treated sisal fiber

4.2. Tensile test results and discussion for SREC

Figure 4.3 shows average stress strain curves of test specimens cut from sample plates R15: 85, R 25:75, R 30:70, R 35:65, R 40:60 Average calculated peak tensile strength, modulus of elasticity and percent elongation at break for all samples are shown in Table4.4. A comparison between treated and untreated sisal fibre reinforced epoxy composite tensile strength is shown in Figure 4.4. SEM images of the fracture surfaces morphologies are studied using a TM3000 microscope, with accelerating voltage of 15 kV, at various magnifications. All specimens are mounted onto aluminum stubs and spatter coated with platinum and palladium to make them conductive prior to observation. SEM images for each tensile specimen are shown in Figure4.5 to illustrate the morphologies of the composite surfaces; they show evidence of fibre fracture and pull-out, plus resultant

voids left in the matrix from fibre pull-out, which depends on the fibre content inside the composites.

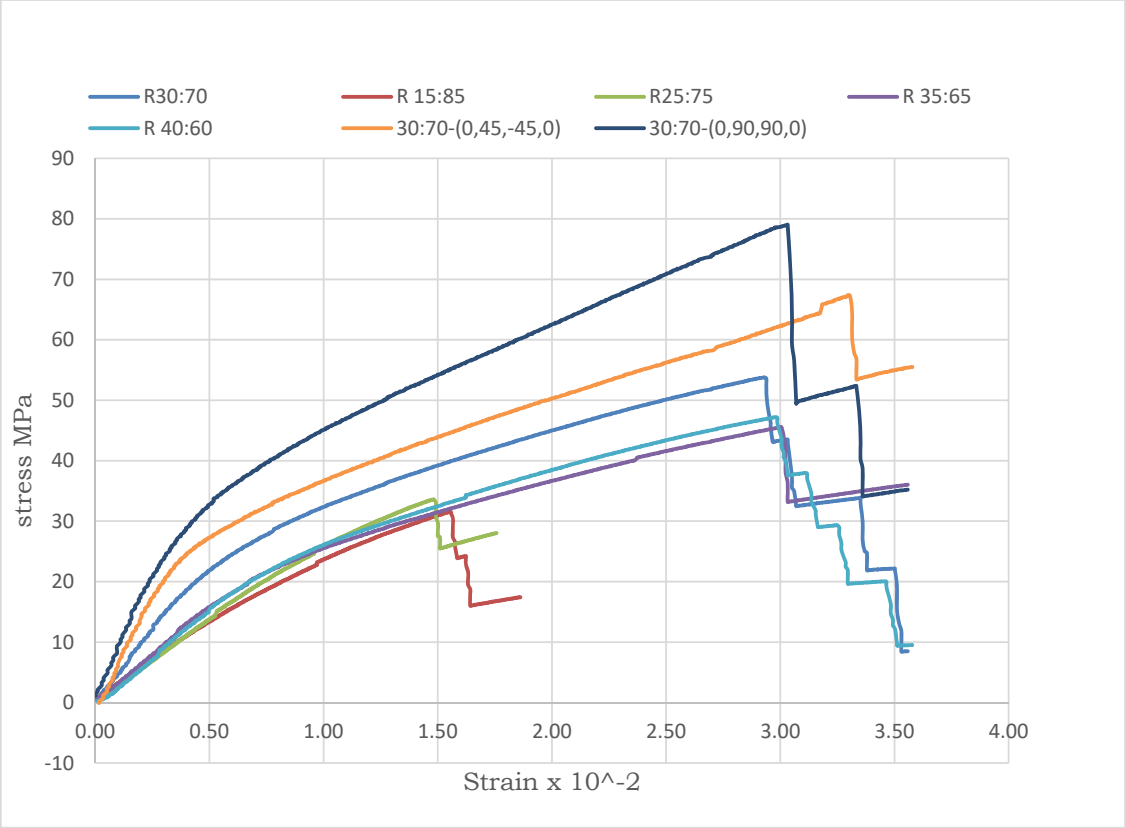

Figure 4-0-3 Average Stress-Strain Curves, Tensile Test Case For Treated Sisal Fibre Reinforced Epoxy Composites

Table 4-3 Average Tensile Properties Of Tested Specimens For Random Fibre Orientation For Different Fibre Loading Condition.

sample	average modulus (GPa)	average peak strength (MPa)	average yield stress (MPa)	average % elongation %	Peak Strength Coefficient of variation %

RSNT 15:85	1.18	26.59	23.93	1.27	
RSNT25:75	1.66	29.3	26.37	1.34	
RSNT30:70	1.55	30.5	27.45	1.81	
RSNT 35:65	1.56	37.1	33.39	1.82	
RSNT40:60	1.81	40.6	36.54	1.76	
R ST15:85	1.95	35.6	33.5	2.85	13.8
RST25:75	2.35	40.4	38.8	2.77	5.9
RST30:70	2.53	58	56.6	6.32	12
RST 35:65	2.49	54.6	50.4	5.64	8.6
RST40:60	2.39	50.1	49.1	4.85	5.7

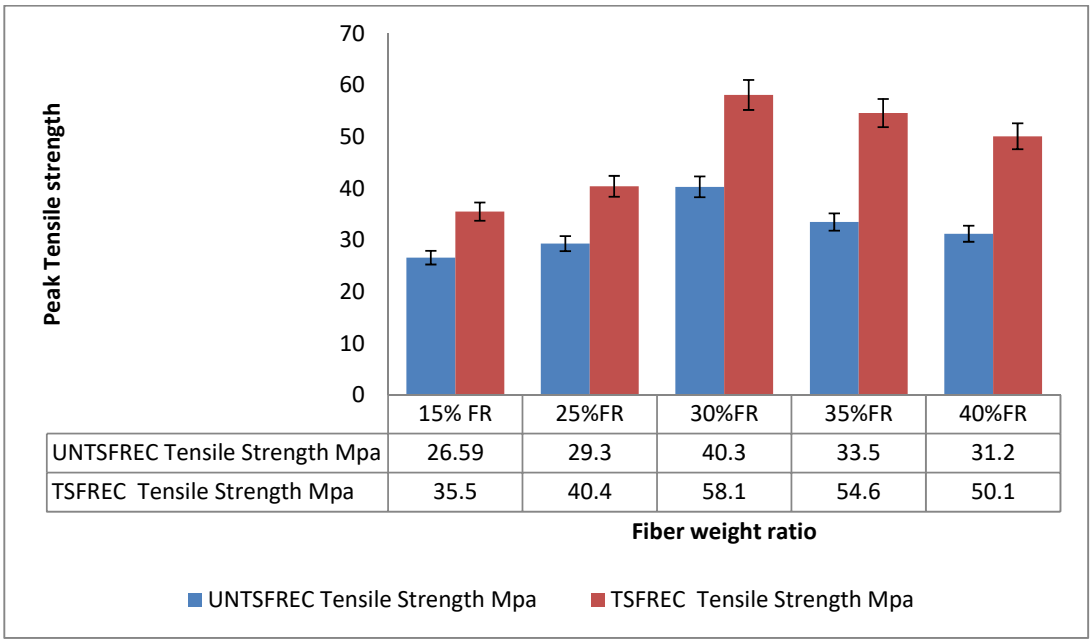

Figure 4-0-4 Comparison Of The Average Peak Tensile Strength (MPa) For Different Wt.%. Of Fiber Content

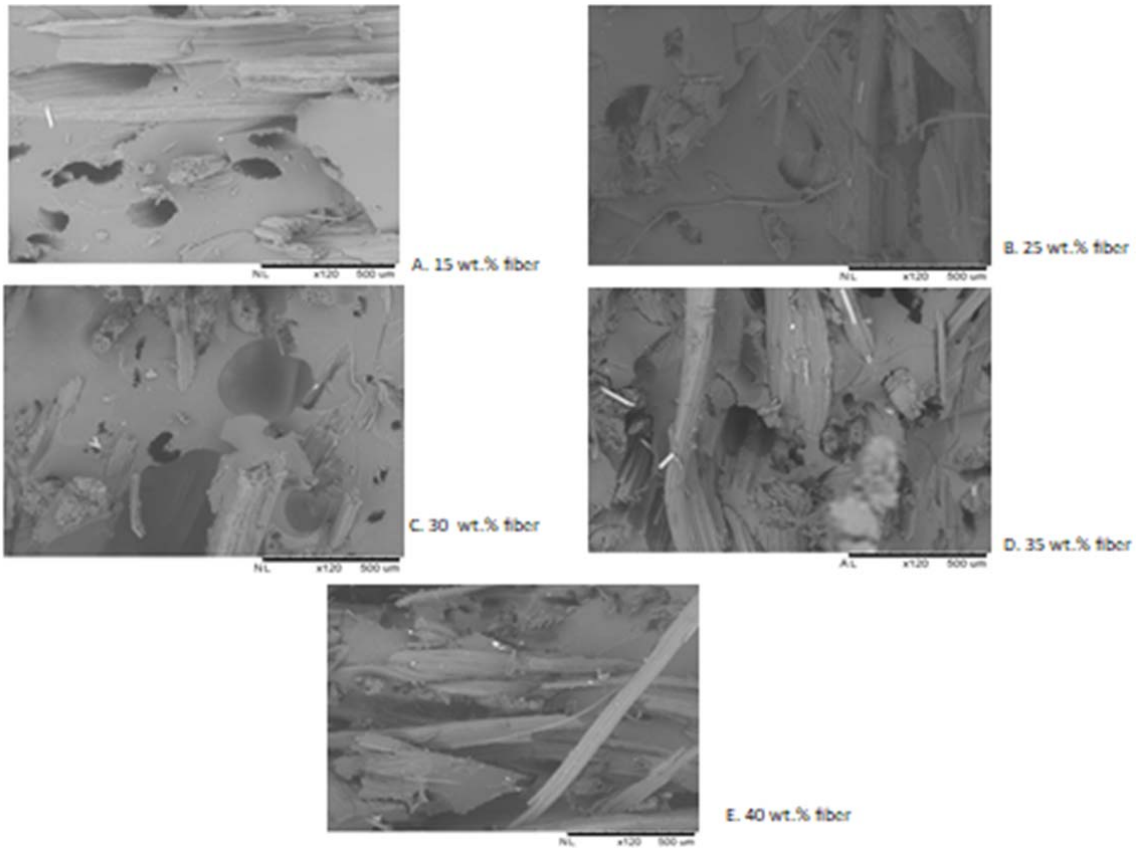

Figure 4-0-5 SEM Image For SFREC For Several Fibre Loading Levels

As shown in the results for tensile strength, the fibre volume fraction has an important role in the mechanical properties of reinforced composites. The tensile strength increases with increasing fibre fraction up to 30 wt% sisal fibre, but then decreases for 35 wt.%. and 40 wt.%. This is because low fibre content creates flaws between the fibre and matrix due to inadequate reinforcement; this led to mechanical failure. At the higher fibre volume fractions, short fibres causes agglomeration of the fibres across the composite matrix; this leads to stress concentrations and failure. Lopez *et al*[72] studied the effect of fibre loading on mechanical properties of composites reinforced with newspaper fibre. They found the tensile strength increased significantly by 150% for fibre content of 15wt%, compared with pure TPS resin. For our research, the tensile strength corresponding to 30wt% fiber samples increased by 51.5% and 63.3 % for treated and untreated sisal fibre reinforced epoxy composites respectively, compared with 15wt% Sisal reinforced epoxy composites. Other researchers have reported similar results. Gupta and Srivastava [128] observed that the tensile strength of sisal reinforced epoxy composite increases significantly by 98% with the increase of fibre loading to 30 wt. % compared with 15wt% of sisal fibre.

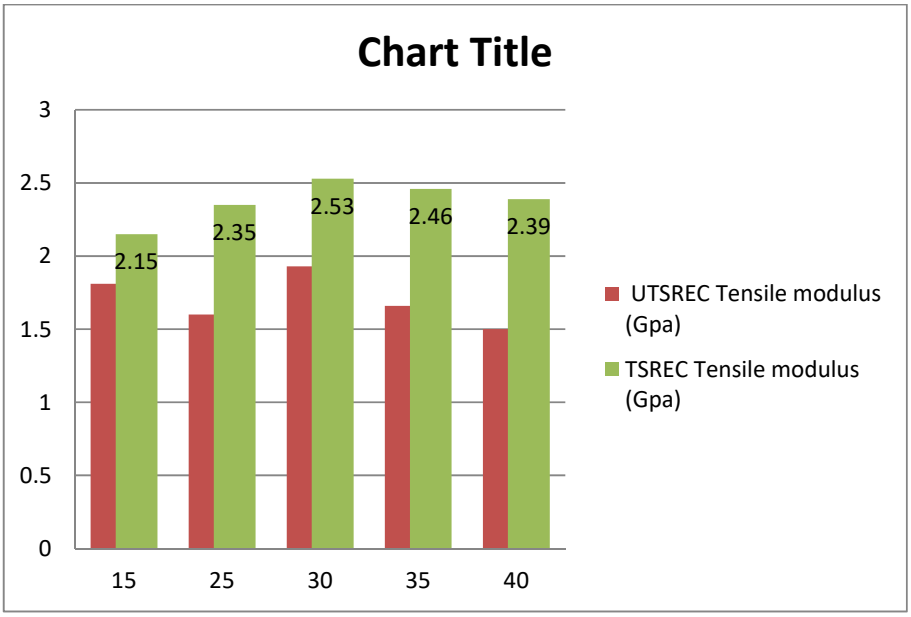

Figure 4-0-6 Fibre Loading Effect For Tensile Modulus For Both Treated And Untreated SFREC

Practically it is difficult to measure experimental values of Young's modulus of natural fibre reinforced polymer composites due to matrix fibre parameters such as aspect ratio of fibres, fibre orientation, surface morphology etc. Several mathematical models are used to estimate the theoretical values of tensile modulus of natural fibre reinforced polymer composites[127].

Tensile moduli of our specimens are shown in figure 4.7. The graph shows increasing modulus with increasing fiber content and shows maximum modulus of elasticity at 30wt% fiber. The tensile modulus increases significantly: more than 6.6 % and 17.6% for the untreated and alkaline treated sisal fibre reinforced composite, respectively, for the same fibre content (30wt%). This shows an improved interfacial adhesion between the sisal fibre and the epoxy matrix due to the effective removal of lignin and non-cellulosic materials from the surface of the fibres through the surface treatments; this led to improved tensile properties.

The cracked surface SEM micrographs reveal significant details on how the specimens fail in terms of fibre-matrix adhesion and the ensuing failure processes. Failure of fibre yarns with load direction, fibre pull-out, debonding, and brittle fracture of the matrix are the major elements of failure processes of sisal fiber reinforced epoxy composites, according to a SEM research shown in Figure 4.5.

Table 4-4 Tensile Properties Of Sisal Fibre Reinforced Epoxy Composite For Various Orientations Of Fiber

sample	average modulus	average peak strength	average yield stress	average % elongation	Peak Strength Coefficient of variation
Type	(GPa)	(MPa)	(MPa)	%	%

UNT30:70-[0,45,45,0]	2.4	48.4	44.2	5.6	10.5
UNT30:70-[0,90,90,0]	3.15	53.5	48.3	6.3	11.2
TR 30:70-[0,45,-45,0]	3.87	73.8	67.4	8.84	12.8
TR 30:70-[0,0,0,0]	4.43	85.5	80.7	7.78	10.9

By keeping the fibre loading or wt.% constant and changing the orientation of the fibres in a composite, the average tensile modulus and average peak strength for treated 30:70 [0, 0, 0, and 0] has 45% and 43.3 % increment respectively as compared with the composite of 30:70(0,45,45,0) orientation as shown in table 4.5. This is because of the good load transfer between the fibre and epoxy compared with other orientations.

On the other hand, calculating the tensile properties of the composites for various values of fibre length shows another trend in mechanical behaviour for SREC. Composite specimens are made of fibres of different length (3, 6, 9, 12and 15 mm) and weight ratio (15, 25, 30, 35, and 40). Figures4.7 and figure 4.9 show the effect of fibre length and weight ratios on tensile strength and modulus of the composite, respectively. An increase in fibre length or weight ratio increases the tensile strength and modulus, up to 9 mm fibre length and 30 % weight ratio (table 4.6). Further increases in fibre length and weight ratio cause the mechanical property values to decrease because of poorer fibre–matrix adhesion and due to the curling effect of the fiber. From figures4.7 and figure 4.8, the maximum tensile strength and modulus of the composite are 56.6MPa and 4.67 GPa, respectively for the fibre length of 9mm and 30 wt. % fibre ratio. Examples of fiber length and dispersion are shown in figure 4.10.

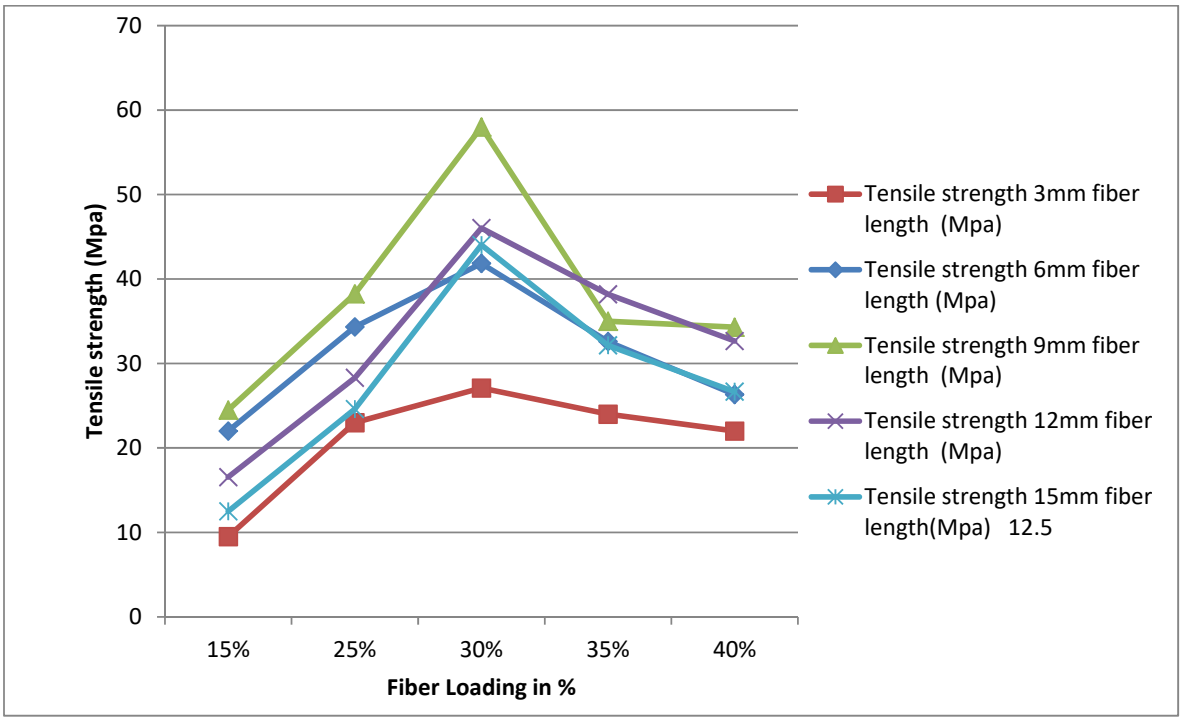

Figure 4-0-7 The Effect Of Fiber Length On The Tensile Strength Of SFREC

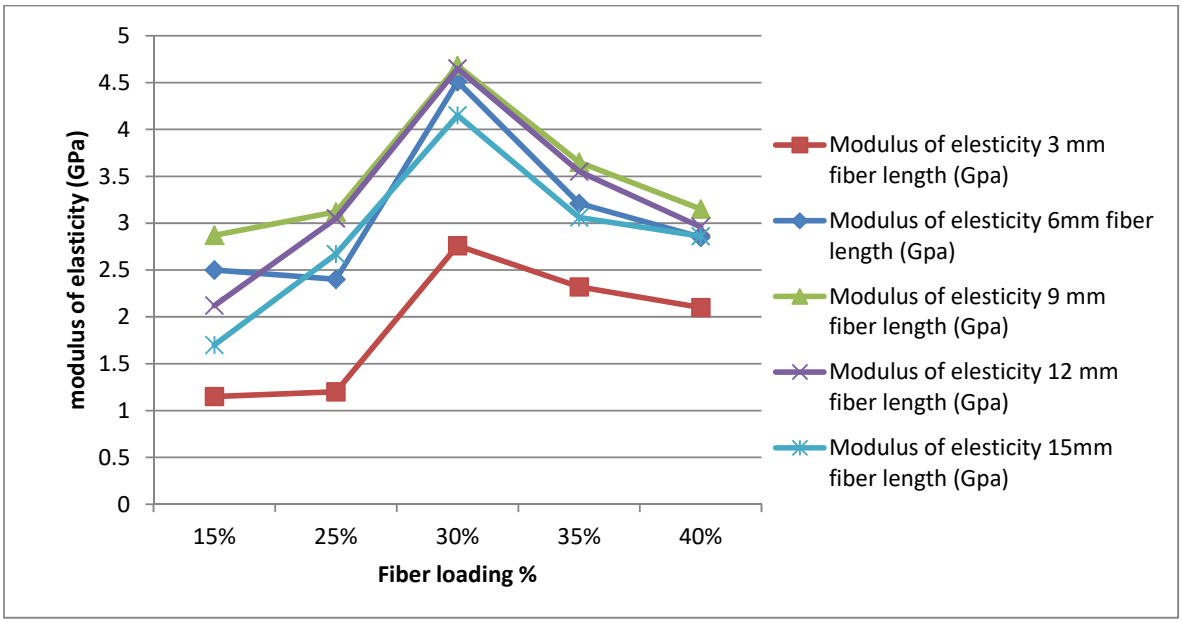

Figure 4-0-8 Effect Of Fibre Length On The Tensile Modulus Of SFREC

Table 4-5 Tensile Properties for Composites With Different Fibre Length And Different Fibre Dispersion

Fiber Length(mm)	Average Stress at max load (MPa)	Young's Modulus (GPa)	Max Displacement (mm)	Load at Max Disp (kN)
3	27.11	2.76	4.27	0.94
6	41.84	4.51	1.61	1.92
9	58	4.68	3.46	2.35
12	46.04	4.65	2.411	2.03
15	44.03	4.15	1.81	1.81

As it is shown in the table 4.6 the fibre length and its quality of dispersion affect the tensile properties of 30 wt.% SREC. The increase in fibre length increases its tensile property till the fibre length become 9mm then the property decrease. The increase of fibre length beyond the 9mm shows significant reduction in its tensile properties these happen due to the curling effect of the fibre, which makes a defect for stress transfer. The curling effect can easily seen from the photography shown in the figure 4.9.

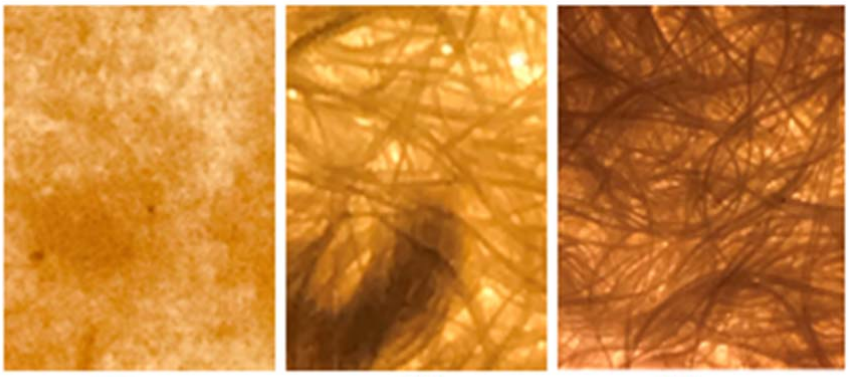

Figure 4-0-9 Randomly oriented fiber distribution for different fiber length

4.3. Flexural Test results and discussion

Figure 4.10 shows a typical stress strain curve of a specimen from each fiber-loading sample. In this comparison, peak stress is higher for

specimens with Fiber loading 30wt. % as compared with other sisal fiber loading.

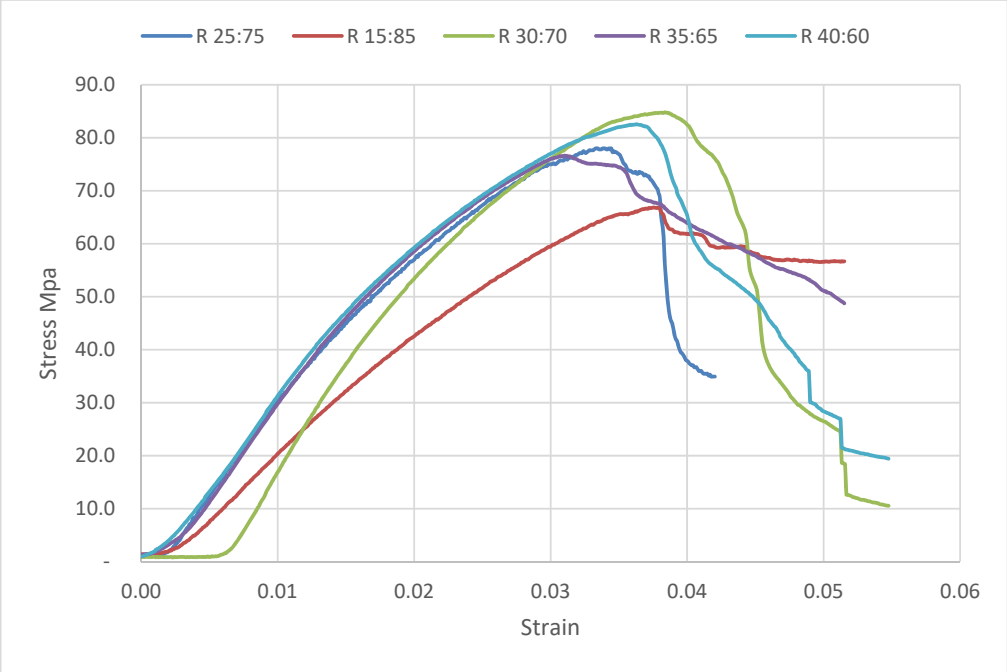

Figure 4-0-10 Average stress strain curves for flexural loading

Table 4-6 Flexural test result for both treated and untreated sisal fiber reinforced epoxy composite

sample type	max peak load (kg)	max flexural stress (MPa)	max strain	Δ strain	Δ stress	chord modulus (GPa)	Flexural Stress Coefficient of variation %
UNTR15:85	1.38	47.25				2.45	
UNTR25:75	2.25	44.89				1.45	
UNTR30:70			-			2.65	
UNTR35:65	2.34	26.18				1.88	
UNTR40:60	2.14	23.8				1.72	
TR15:85	3.67	66.63	.0705	0.00200	6.69	3.35	28
TR25:75	13.41	75.85	0.0378	0.00233	8.54	3.62	15.7
TR 30:70	26.41	84.79	0.0532	0.00198	7.20	3.64	6.9

TR 35:65	25.88	76.62	0.0529	0.00199	6.16	3.1	6.0
TR 40:60	26.21	82.52	0.0613	0.00199	6.44	3.23	2.6

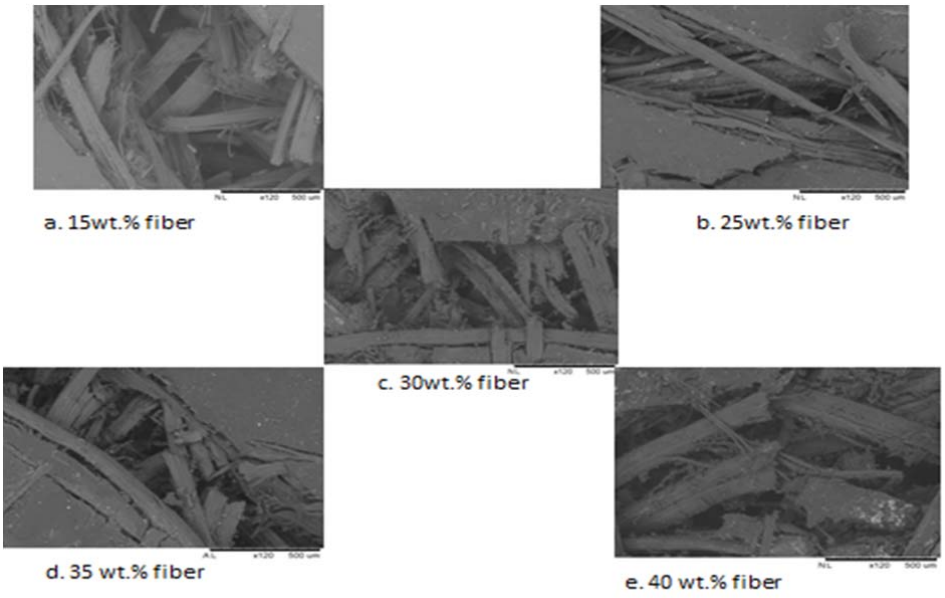

Figure 4-0-11 SEM Micrograph Of Fractured Surface Of Composite After Flexural Test With 120 X Magnification.

Peak flexural strength and cord modulus of sisal reinforced epoxy composite are presented in Table 4.7 Both the cord modulus and flexural strength are found to increase with increasing fiber content up to 30wt. %, where strong fiber-matrix adhesion is obtained. The flexural strength and flexural modulus of SFREC are 84.79 MPa and 3.64 GPa respectively for NaOH treated 30Wt. % samples. The superior results of the composites with 30 wt %. fiber is also seen in figure 4.11 Failure due to flexural loading for all tests occur due to tension at the loading nose, causing fiber fracture and matrix cracking as shown in the SEM results. In comparison to untreated samples, alkali-treated samples exhibited a significant increase in flexural strength and modulus. Because alkali treatment enhances fiber surface adhesion by eliminating natural and manufactured contaminants, a rough surface topography is produced[129].

4.4. Impact Test

Impact tests are performed with an Izod impact test machine. Specimens are prepared for the Izod impact test according to[130] ASTM D256, ISO 180, using test method "A, with a pendulum capacity of 2.74 Joules. The impact properties of the composites are studied by applying an indentation load normal to the specimen length. A notched specimen is secured with the notch facing the approaching pendulum. The pendulum breaks the specimen; the height of the pendulum swing is corrected for wind resistance, and the impact test machine calculates specimen breaking energy automatically. Results are shown in Table 4.8.

Table 4-7 Impact Properties Of Sisal Reinforced Epoxy Composites.

Sample type)	Impact energy(J)	Average impact strength (kJ/m^2)	Impact Strength Coefficient of variation %
R15:85	0.21	9.35	20.7
R25:75	0.36	11.89	11.8
R 30:70	0.60	13.28	21
R 35:65	0.71	16.39	18.1
R 40:60	1.11	24.49	10.3

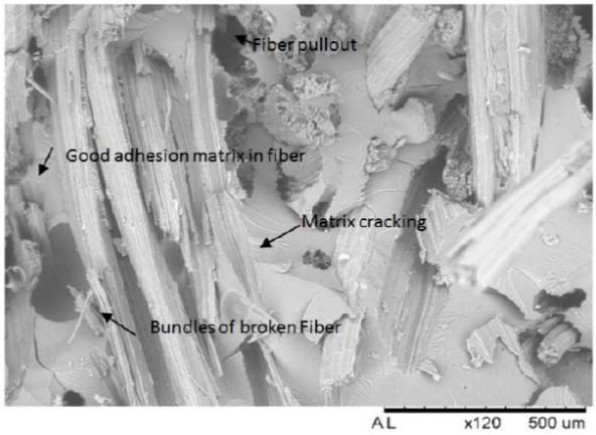

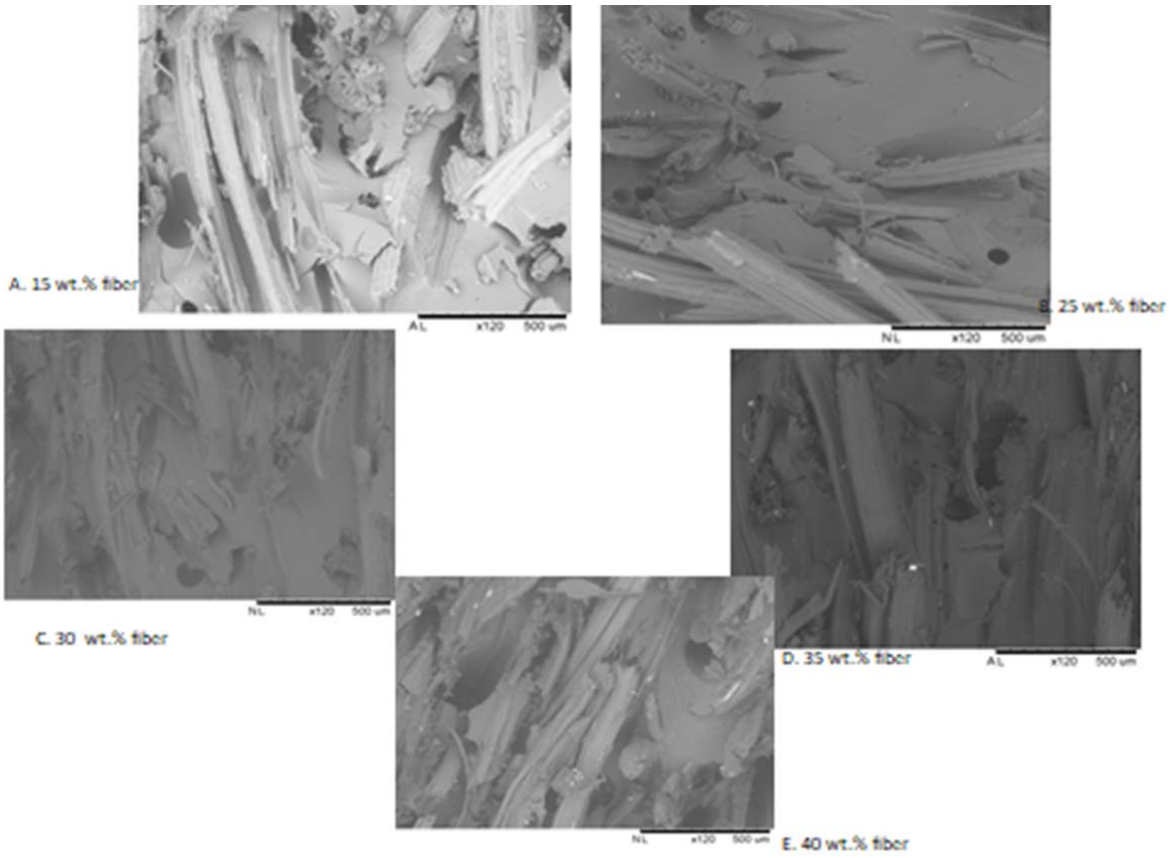

Figure 4-0-12 . SEM Micrograph Of Fractured Surface Of SFREC After Impact Test At 120 X Magnification

Figure 4.12 shows SEM micrographs of composite fracture surfaces following impact fracturing. In the fractography, fiber pull-out from the matrix is seen. Also, greater fiber pull-out was seen for specimens with larger fiber content. In the composites reinforced with alkali treated fiber, delamination and debonding of the fibers from the epoxy matrix were also detected.

Table 4.8 shows the impact strength and impact energy of sisal reinforced epoxy composites. Impact properties are found to increase with increasing percentage of sisal fiber content up to 40 wt. %. As seen in the SEM picture of Figure 4.12, crack formation in the matrix and broken fibers are associated with the impact damage. The portion of the specimen where the rupture occurred longitudinally via the fiber/matrix contact, on the other hand, indicates that the fiber surface accounts for the majority of the

fracture area. Because of the poor interfacial strength, fractures preferentially spread between the sisal fiber surface and the polymeric matrix[131].

Impact test results for 30 wt. % fiber, with fibers of various lengths ,are shown in Table 4.9.

Table 4-8 Fiber length effect on the impact resistance of SFREC

Type	impact energy (j)	Impact resistance (j/m)
30wt.% 3mm random Fiber	0.4	109.9
30wt.% 6mm random	0.44	160.98
30wt.% 9 mm random	0.62	194.35
30wt.%15mm random	0.53	169.97

The impact resistance for 9mm fiber length is 76% higher than the impact resistance of 3mm random fiber reinforced composite.

4.5. Comparison results with other researchers

Table 4-9 Comparative Mechanical Properties Of Some Natural Reinforced Polymer Composites

fiber	matrix	fiber Orientation	ratio fiber/matrix	method of fabrication	type of treatment	tensile strength (MPa)	tensile modulus (GPa)	impact Strength (KJ/m2)	flexural strength (Mpa)	flexural modulus (Gpa)	reference
Sisal	Epoxy	Random	30/70	Hand Layup	NaOH 10%	58	2.53	13.28	84.79	3.62	Current work
Sisal	Epoxy	0,90, 90,0	30/70	Hand Layup	NaOH 10%	85.5	4.43	----	----	----	Current work
Sisal	polyester	Random	30/70	Hand Layup	NaOH 18%	65.93	1.85	-----	115.62	4.83	20

Sisal	Epoxy	Random	30/70	Hand Layup	NaOH 10%	83.96	1.58	22.03	252.39	11.32	21
Sisal	Polypropylene	short	30/70	Hand Layup	Alkaline	34.4	0.94	-----	-----	-----	22
Sisal	polyester	long	30/70	Hand Layup	Alkaline	44.4	1.04	----	----	----	23
Sisal	Epoxy	mat form	30/70	Hand Layup	----	89.3	0.39	----	----	----	23
Sisal	Epoxy	long	39.6/60.4	RTM	-----	36.1	2.19	----	74.5	3.07	24
Hemp	polypropylene	random	50/50	Hand layup	Alkaline	50	6.5	53	85	4	26
Jute	Epoxy	random	30/70	Hand Layup	Alkaline	69.5	6.28	---	89.63	5.94	25

Table 4.10 shows measured mechanical properties of fiber-reinforced composites determined in various laboratories. Although some of those tests featured sisal fibers as the reinforcing agent, the properties of those sample plates can vary widely depending on the geographical area of sisal cultivation and method of manufacture. Our results feature materials and a manufacturing method that are viable for Ethiopia; mechanical properties vary for specimens characterized in various laboratories but are not inconsistent with each other.

As shown in Table4.10, our findings for sisal reinforced epoxy composites with a fiber ratio of 30 wt.% are consistent with published data. Mechanical properties for Ethiopian sisal reinforced epoxy composite were found to be good for engineering applications.

4.6. Water Absorption SFREC.

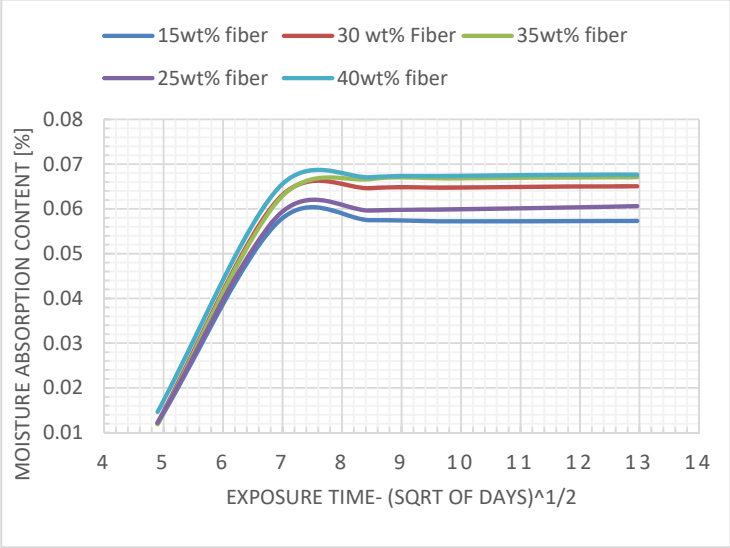

Figure 4-0-13 Water Absorption Behavior For Various Fiber Weight Ratios

Figure 4.13 shows the % water absorption of sisal fibre reinforced epoxy composites against the square root of time. The initial rate of water absorption and maximal water intake both increase as the fiber content increases up to 40% by weight. This might be owing to the existence of microvoids in the matrix, which allow water molecules to diffuse into them until they reach saturation. The water absorption of the composite TR 40 wt. % is 21, 14, 11, and 8% greater than that of the composites TR15 wt. %, TR 25 wt. %, TR 30 wt. %, and TR 35 wt. %, respectively. The hydrophilic nature of sisal fiber and the larger interface area between fiber and matrix account for the increased water absorption. Due to the presence of cellulose, sisal fiber has a hydrophilic character. The quantity of cellulose, micro voids, and interface surface area increase as the weight percentage of sisal fibers increases in the composites.

4.7 TGA result and analysis

The TGA curves shown in the figure 4.15 show the fiber content effect of alkali treated sisal fiber reinforced epoxy composites.

As it is Shown in the figure 4.15 The TGA curves of alkali treated sisal fibers reinforced epoxy composites shows three different region where the weight loss of specimen type are exhibited. The 5% weight loss region for

15wt%, 25wt%, 30wt%; 35wt% and 40 wt.% epoxy composites found that 196^{0}c,105^{0}c, 101^{0}c,116^{0}c and 204.16^{0}c respectively the primary weight loss of the weight for the composites are due to removal of solvents & evaporation of water as it is stated [132]. About 75% of the weight loss for all the composite specimens is obtained between 390^{0}C to 495^{0}C. The main weight loss is due to the degradation & volatilization of epoxy. In the third region, there is continuous degradation of the composite and residues are formed. As shown in figure 4.15, when the fiber content is increased in the composite specimen, the thermal stability improves until the wt. fraction reach 30wt%. Therefore the thermal stability of specimens with 30 wt.% weight ratio is much better than all the other sample types; this is due to the strong interface between fiber and matrix.

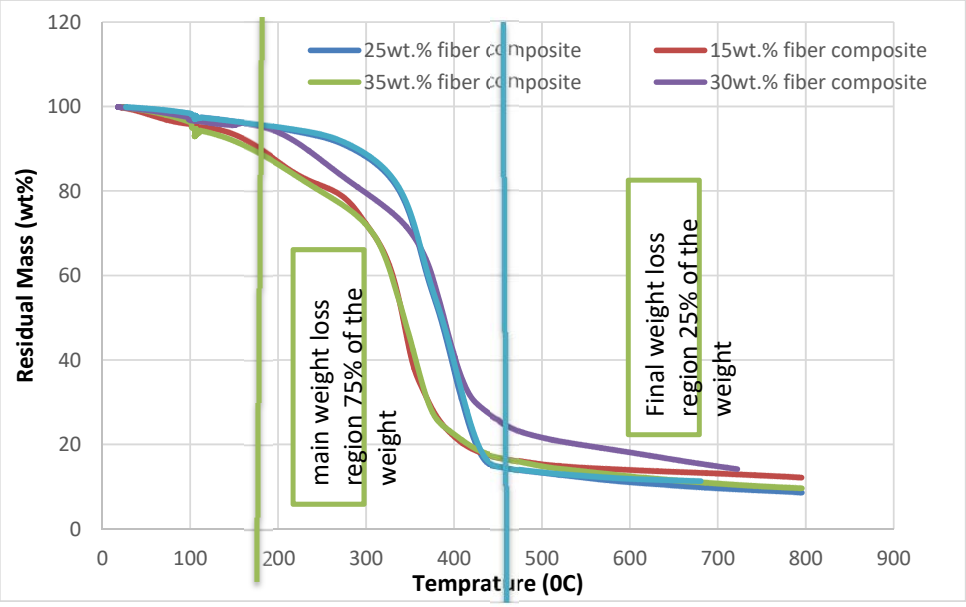

Figure 4-0-14 TGA Results For Different Fiber Loading Conditions Weight Loss Vs. Temperature Graph

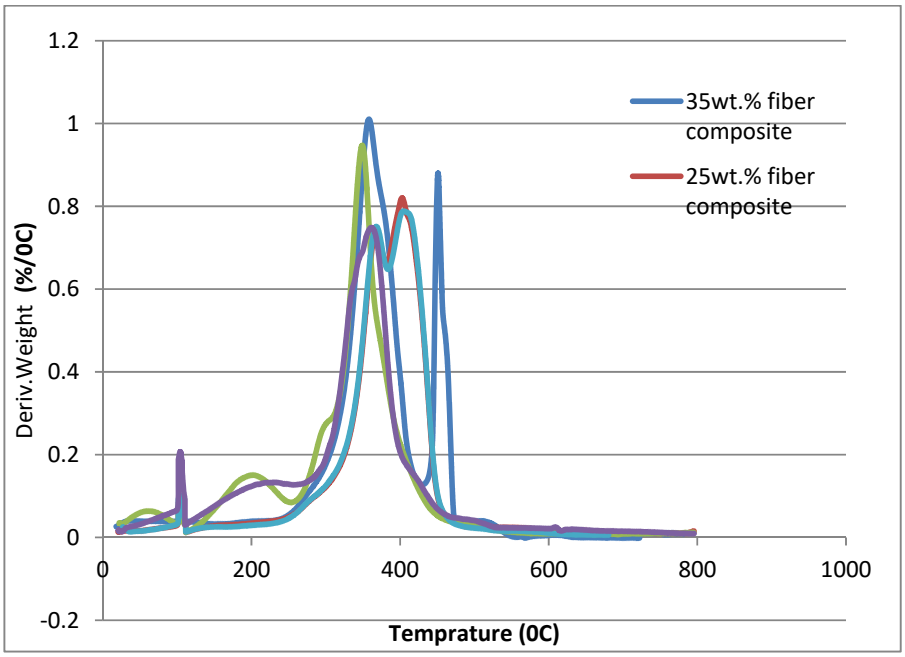

Figure 4-0-15 TGA Results for Different Fiber Loading Conditions Derive Weight vs. Temperature Graph

4.8. DMA Analysis

The DMA analysis is performed to study the viscoelastic properties of the composite, such as storage modulus (E^{I}), loss modulus (E^{II}) and tan delta (tan δ) of SFREC as a function of temperature at 1 Hz frequency. This study is important in determining the dynamic mechanical performance of composites at various temperatures and mechanical stresses [133].

4.8.1. Storage Modulus

The storage modulus is related to the energy stored by the composite during one cycle a. Values for SFREC are shown in figure 4.16 as a function of temperature at a frequency of 1Hz. With increasing fiber content up to 30%, the value of the storage modulus increases. It reaches a maximum value of 6.64 GPa for 15wt% fiber content, and 15.92 GPa for 30wt% fiber content. This shows that the stress transfer from epoxy to the fiber is better for 30wt% fiber loading. The storage modulus of SFREC decrease as the temperature increases due to the loss of fiber stiffness. Because the storage modulus of the fiber has a positive impact on the matrix, the storage modulus in composites falls slowly with rising temperature.[134]

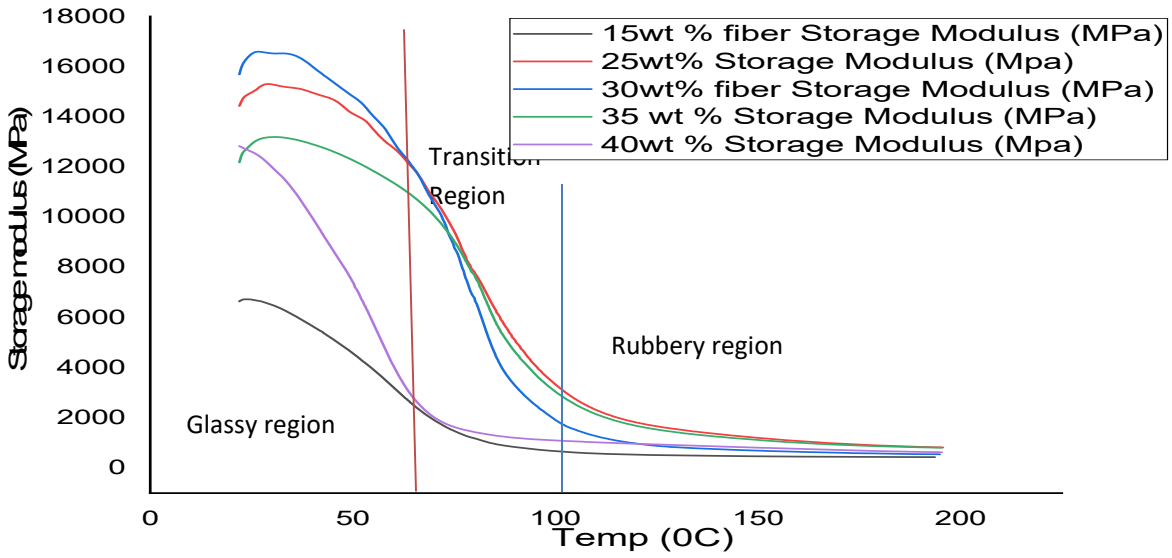

Figure 4-0-16 Storage Modulus Of SFREC For Different Fiber Loading Content

To determine the efficacy of reinforcement in the composite, we apply the following equations [134].

$$Efectiveness(E) = \frac{(\frac{E'_g}{E'_r})Composite}{\left(\frac{E'_g}{E'_r}\right)epoxy} \text{----------eqn 4.2}$$

Table 4-10 Effectiveness Constant Of Sisal Fiber Reinforced In Composite

Fiber loading in SFREC	E'_g Storage modulus at glass temperature For composite (GPa)	E'_r Storage modulus at rubbery temperature For composite (GPa)	E'g Storage modulus at glass temperature For epoxy (GPa)	E'r Storage modulus at rubbery temperature For epoxy (GPa)	E effectiveness
15Wt.%	1.18	0.66	0.56	0.015	0.047
25wt.%	3.63	1.88	0.56	0.015	0.051
30wt.%	3.76	3	0.56	0.015	0.033

35wt.%	3.21	1.79	0.56	0.015	0.048
40wt.%	3.09	1.09	0.56	0.015	0.075

As indicated in Table 4.11, the 30wt% fiber reinforcement has the lowest value of efficacy constant, while 40wt% SFREC has the greatest effectiveness constant. As a result, 30wt% reinforcement has the highest efficiency. From the above result, we have seen 30wt% SFREC has better interface bonding between the fiber and matrix compared with other fiber loading cases.

4.8.2 Loss Modulus (E")

It is defined the loss of energy in the form of heat from the composite per cycle.

The loss modulus properties of different fiber loading conditions as a function of temperature at 1 Hz frequency is shown in figure 4.17. The loss energy corresponding to 25wt% fiber content is much greater than for other types of fiber loading.

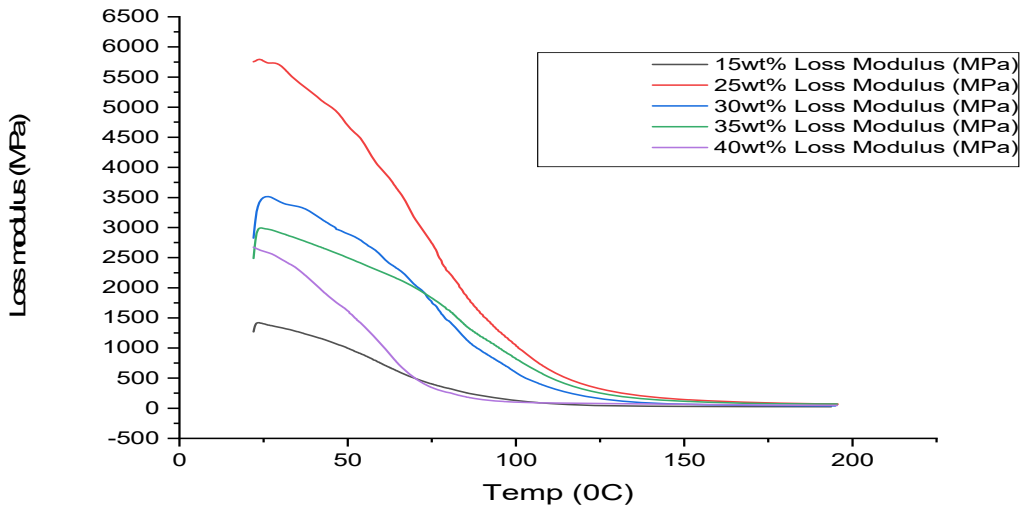

Figure 4-0-17 Loss Modulus of SFREC for different fiber loading conditions

4.8.3. Damping Parameter (tan δ)

Tan(δ) is the ratio of storage modulus to loss modulus, and is used to determine the composites' impact characteristics. The greater the tan δ value, the better the impact characteristics. The apex of the tan δ graph is the glass transition temperature Tg. Tg varies depending on the fiber loading situation, as illustrated in figure 4.18. Due to the simple mobility of molecules in the polymer, the transition from a rigid to a more elastic state occurs at the temperature T_g.

.

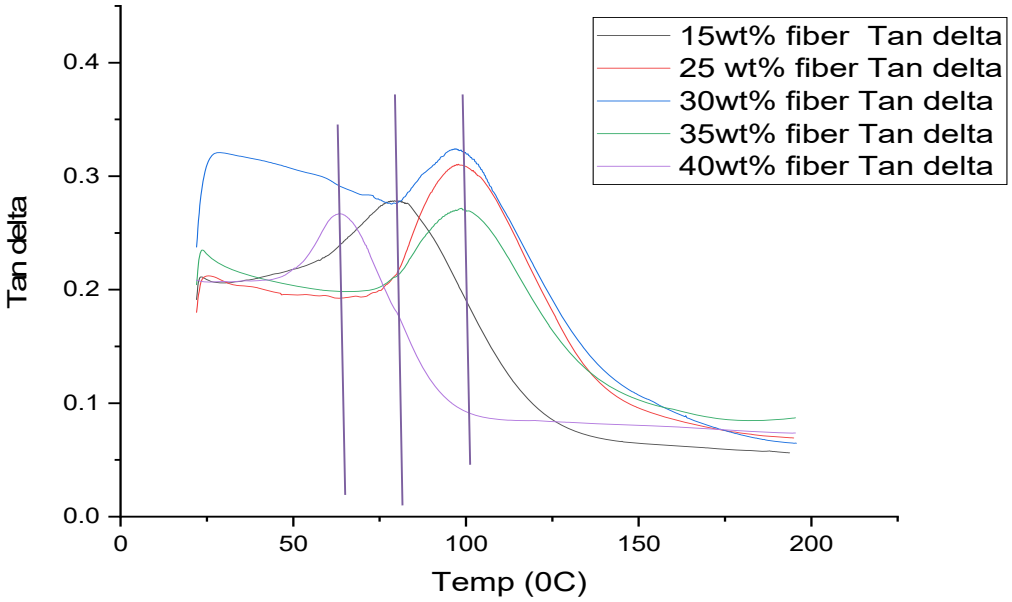

Figure 4-0-18 Tan δ of SFREC for Different Fiber Loading Conditions

4.9. Fracture toughness for SFREC for different fiber loading case.

The compact tension specimens were used to experiment the fracture toughness properties of epoxy and random sisal fiber reinforced epoxy composites as it's given in Table4.12.

Table 4-11 calculated fracture toughness of different fiber loading Critical stress intensity factor

Fiber Loading	Maximum Force at fracture KN	Critical stress intensity factor (KIC), MPa·m 1/2
R15:85	0.47	2.19
R25:75	0.88	3.96

R30:70	1.23	5.54
R35:65	0.78	3.52
R40:60	0.64	2.88

It is clearly observed from the experimental investigations, which are shown in table 4.12, the stress intensity factor is the main parameter to determine the fracture toughness. The fracture toughness increases with increasing sisal fiber content up to 30 wt.%. The maximum values of load and critical stress intensity factor (K_{IC}) for the composite R30:70 are 1.230 KN and 5.54 MPa·$m^{1/2}$. It is observed that the maximum values of load applied for the composite R30:70 is 62, 28, 37, and 48% more than those of composites R15:85, R25:75, R35:65 and R40:60 respectively. Critical stress intensity factor (KIC) for the composite R30 is 60, 29, 37, and 48% of other fiber loading composites R15:85, R25:75, R35:65 and R40:60 respectively. The critical strain energy release rate is calculated for all the composites and the maximum critical strain energy release rate for R30: 70 are 13.72 MPa·mm.

4.10. Fatigue Testing of SFREC

Table 4.13 shows how many cycles passed before a specimen broke from fatigue loading. The loads were determined roughly by using a percentage of the average peak load for a sample as determined by earlier tensile tests.

Table 4-12 Fatigue Test Result For Tensile Specimens

Sample	Fiber orientation	Min Load (N)	Max Load (N)	Cycle to break	Rough percentage of peak load	Remark
1	Random (30:70)	560	1700	217000	60%	no break -over 21700 cycles
2		560	1800	30160	65%	did not break in narrow section
3		560	2000	11395	70%	did not break in narrow section
4		560	2100	7857	75%	did not break in narrow section
5		560	2200	8910	80%	did not break in narrow section
	30:70					

1	[0,90]	965	2900	6233	60%	did not break in narrow section
2		965	3100	71204	65%	did not break in narrow section
3		965	3400	6350	70%	did not break in narrow section
4		965	3600	9309	75%	did not break in narrow section

SEM images were taken using a TM3000 microscope, with an accelerating voltage of 15 000 V, and at varying magnifications. Representative results are shown in Figure 4.19.

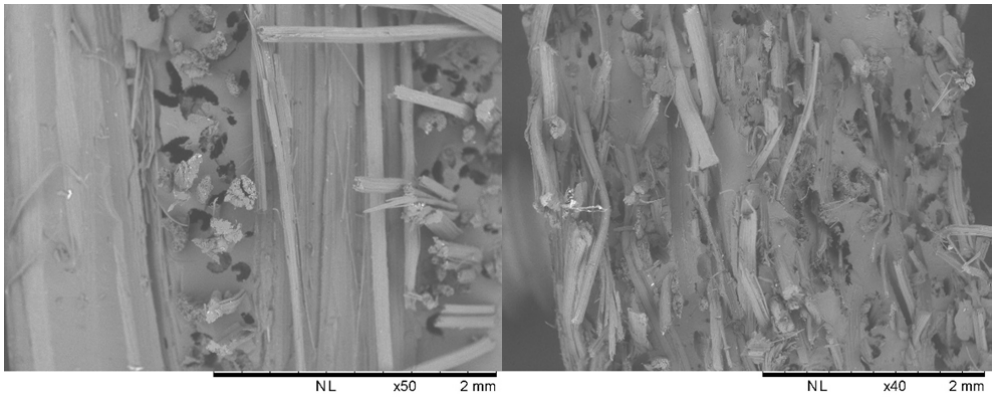

Figure 4-0-19 30:70 –0, 90 And Rand Fatigue Sample Shown At 50x Magnification And 40x Magnification.

The randomly oriented specimens had a shorter number of cycles to failure due to a greater load, as predicted. In the thin portion of the test specimen, however, two out of four specimens did not break even after substantial numbers of cycles. The specimens orientated in a [0,90], on the other hand, did not display this pattern. Table 4.12 shows that specimens one and three broke significantly sooner than predicted. Flaws in the specimens might cause this or minor twisting caused by the crossheads. A fracture was heard at the start of the test in all [0,90] specimens (after only a few cycles had passed). This indicates that one of the laminated layers, most likely the one with fibers running perpendicular to the pulling axis, broke first.

4.11. Low velocity impact test results using new DWITM

The experiment itself contains three stages; i) measurement taken during the impact event from the accelerometer with two programs (program 1 & 2). ii) Recording the result using Spectral PLUS software. iii) Conversion of spectral data using MATLAB software. Two test programs i.e. first program conducted from drop height of 600 mm and second program conducted from 500 mm, the results obtained from MATLAB software and shown in details below.

4.11.1 Data from Data acquisition and spectra plus

The results from the machine directly Indicates the impact amplitude which is proportional to acceleration. At 0.15 sec on program 1 and at 3.5 sec on program 2, considerable noise is suddenly seen on the signal. This noise is due to vibrations in the body of the falling weight caused by sudden changes in the force as the sample plate cracks.

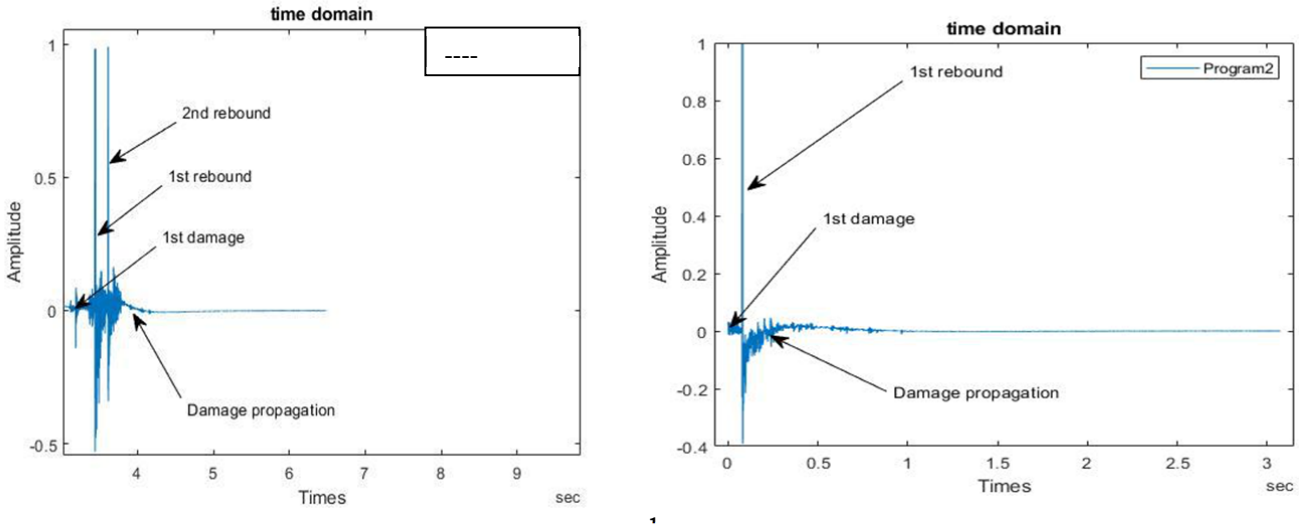

Figure 4-0-20 Spectral plus plot results a and b for both program 1 and 2

4.11.2. Force-time curve

The signal measured by accelerometers during impact can be recorded as the sum of several terms [109].

- The actual specimen reaction;
- The inertial load on the tup caused by the acceleration of the specimen;
- Ringing of impactor and specimen

To highlight the relative influence of the various components of the load signal, a first step was to determine the natural frequencies of the impactor, the accelerometer signal, in fact, represents the local dynamics of a complex system. Many dynamic models of impact, for example, represent the system as an assemblage of mass and springs and the estimate of the tup-specimen contact force from accelerometer signals can therefore be affected by significant errors.

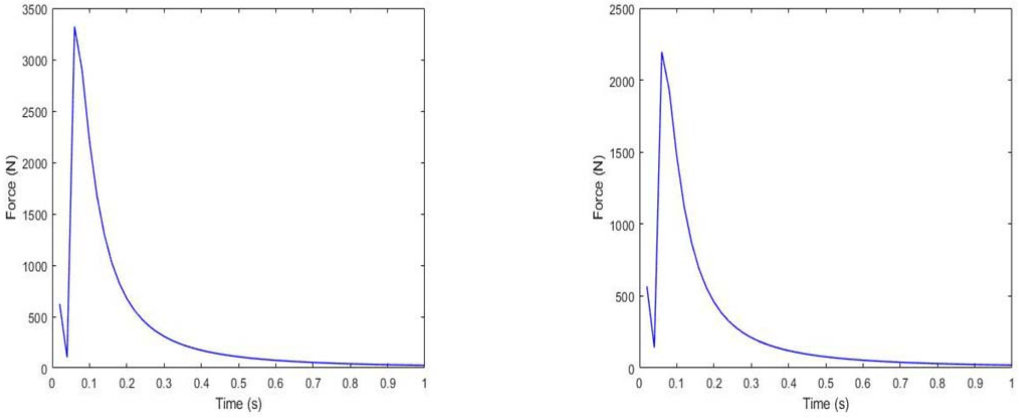

Figure 4-0-21 Force vs. time curve for both program 1 and 2

4.11.3 Energy-time curves

Figure 4.22 Shows a steadily increasing energy transfer up to the moment of cracking within 0.3 sec, and becoming essentially level during the free-fall interval of the falling weight. If the damage occurred on the specimen additional increase in energy could be noticed on the curve.

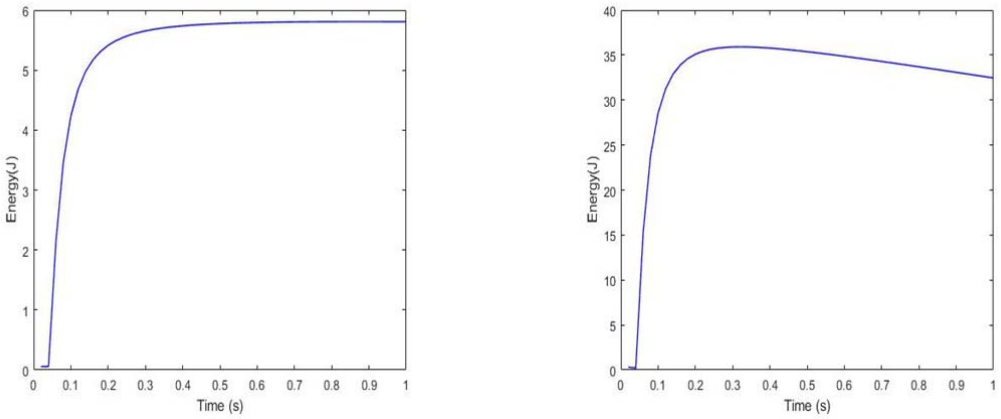

Figure 4-0-22 absorbed energy vs time curve for both program 1 and 2

4.11.4 Velocity-time curves

The velocity trace as shown in the figure 4.23 shows increases suddenly for about 0.1 sec in program 1 and 2 and reaches 3.3 m/s and 4.4 m/s respectively. Then decreases for 0.5 sec on both test programs which indicates the moment of cracking before becoming essentially constant relatively for about another 0.5 sec. The nearly constant velocity is due to the weight falling freely after damage on the specimen occurs.

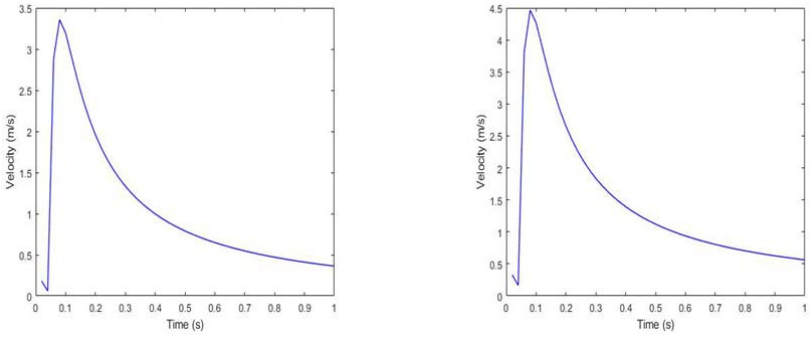

Figure 4-0-23 Velocity vs time curve for both program 1 and 2

The result found from the drop weight impactor designd showed an agreement with other experimental setup results for the same low velocity

impactor tests. To optimize our testing machine we will focus on the indenter geometry and automation of the droping mechanism.

4.12 Summary

In this study, SFREC are characterized and treated using alkaline treatment. The sisal fibers are mixed into an epoxy matrix with varying fiber content and orientation. A hand layup technique is used, and specimens are compressed using a cold molding compression machine. To see the characteristics of fiber dispersion, we use a back lighting technique. Different physical, mechanical and thermal properties of manufactured composites are measured. Some of the properties studied in these experiments are density of fiber, tensile strength, Young's modulus, flexural strength, flexural modulus, impact strength, tensile fatigue strength, and water absorption. From the result, we found we can easily understand the sisal reinforced epoxy composite can be one substitute for automotive parts. Since most of the properties found from the experiment shows an agreement with materials studied before for application of automotive parts

CHAPTER 5:

5. Conclusions and Recommendation's

In this research work, fiber reinforced polymer matrix composites are developed from sisal fibers and epoxy using a hand layup method and compression molding techniques. The mechanical and physical properties related to composites are investigated.

5.1. Conclusion

Different fiber to epoxy weight ratios and fiber orientations are used to make sisal fiber-reinforced composites for both treated and untreated fiber. The sample plates are made utilizing a hand layup compression molding method using a cold press procedure, and the specimen is cut using ASTM standards for each case. From the experimental study made on the composites, mechanical and physical properties are investigated, and the following conclusions are made.

1. The extracted sisal fiber from Ethiopian highlands was manually fabricated. The sisal fiber was treated using 10% NaOH solution for three hours and dried for 48 hours using an autoclave at 600C.
2. Chemical treatment of sisal fiber with NaOH changed morphological and chemical properties of the fiber. The surface of the treated fiber is much cleaner than untreated fiber; therefore most of the wax, oil and other impurities from the surface of the fibers are removed.
3. Tensile strength , Young's modulus, flexural strength, chord modulus and water absorption increase with an increase of fiber content i the composites, until the fiber wt.% reaches 30 %; the mechanical properties then start to decrease when fiber content is raised beyond 30%.
4. The maximum tensile strength and modulus are 85.5 MPa and 4.5 GPa respectively, observed for specimens with 30 wt. % fiber in a [0, 90, 90, 0] pattern. The maximum flexural strength and chord modulus are 84.8 MPa and 3.6GPa, respectively, observed in specimens with random fiber orientation and 30 wt. % fiber.
5. The maximum impact strength is 24.5 kJ/m^2, corresponding to specimens with random fiber orientation and 40% fiber content.

6. From the SEM results, evidence of fiber pullout, matrix cracks, and fiber fracture are observed for all specimens.
7. From the experimental results, composite materials with 30 wt. % fiber content have the best overall mechanical properties. It may be possible to use such sisal reinforced epoxy composites as substitute material for automotive parts, such as door panels, seat backs, bolsters, load floors and packaging trays.
8. From the TGA and DMA results, we found 30wt% fiber reinforced composite to be more stable with good viscoelastic behavior compared to the other specimens.
9. Our test results are generally consistent with those of other researchers who worked on a variety of natural fiber reinforced polymer composites for automotive applications.

5.2. Recommendations for future work

Although some new understanding has been acquired into how natural fiber reinforcements might improve the mechanical and physical characteristics of polymer composites, several experiments must be addressed before natural fiber–reinforced polymer composites can be considered commercially feasible for automotive applications. To that aim, the following are some recommendations for further research:

1. Different chemical treatments can be tried to modify the surface morphology of sisal fiber. We only used NaOH treatment, such that other researchers might try other treatments to improve the interfacial adhesion in the composite material.
2. The decortication of fiber and washing mechanisms can be further investigated and industrialized to use sisal fiber for industrial applications. The goals would be to decrease processing time and cost, while improving the uniformity of the final product.
3. Different orientations and fiber concentrations can be investigated, together with combinations of other natural and synthetic fibers.

4. Engineering analysis can be performed on various automotive parts using experimental results found here and composite theories.
5. The impacts of different processing methods on mechanical characteristics should be evaluated and compared.

5.3 Contribution of the Study to Science and Engineering

The primary goal of this study was to describe the mechanical and physical characteristics of sisal reinforced epoxy composites in order to utilize and replace automobile parts, which are made of conventional materials. The following are the key contributions made by this study:

1. Contributes to the scientific principles and data corresponding to the mechanical properties and physical properties of SFREC.
2. Helps to determine which automotive parts might be manufactured from SFREC.
3. Developed testing machine as per ASTM standard which is used for determining the low velocity impact effects. Which will help us to determine the damage mechanism of the parts.

REFERENCES

[1] P. Peças, H. Carvalho, H. Salman, and M. Leite, "Natural Fibre Composites and Their Applications: A Review," *J. Compos. Sci.*, vol. 2, no. 4, p. 66, 2018, doi: 10.3390/jcs2040066.

[2] K. Huang, L. Q. N. Tran, U. Kureemun, W. S. Teo, and H. P. Lee, "Vibroacoustic behavior and noise control of flax fiber-reinforced polypropylene composites," *J. Nat. Fibers*, vol. 16, no. 5, pp. 729–743, 2019, doi: 10.1080/15440478.2018.1433096.

[3] S. Goutianos, T. Peijs, B. Nystrom, and M. Skrifvars, "Development of flax fibre based textile reinforcements for composite applications," *Appl. Compos. Mater.*, vol. 13, no. 4, pp. 199–215, 2006, doi: 10.1007/s10443-006-9010-2.

[4] Y. S. Munde, R. B. Ingle, and I. Siva, "Vibration damping and acoustic characteristics of sisal fibre–reinforced polypropylene composite," *Noise Vib. Worldw.*, vol. 50, no. 1, pp. 13–21, 2019, doi: 10.1177/0957456518812784.

[5] D. K. Rajak, D. D. Pagar, P. L. Menezes, and E. Linul, "Fiber-Reinforced Polymer Composites :"

[6] J. Agarwal, S. Sahoo, S. Mohanty, and S. K. Nayak, "Progress of novel techniques for lightweight automobile applications through innovative eco-friendly composite materials: A review," *Journal of Thermoplastic Composite Materials*, vol. 33, no. 7. pp. 978–1013, 2020, doi: 10.1177/0892705718815530.

[7] A. T. Mayyas, A. R. Mayyas, and M. Omar, "Sustainable lightweight vehicle design," in *Lightweight Composite Structures in Transport*, 2016.

[8] A. T. Mayyas, A. Mayyas, A. Qattawi, and M. A. Omar, "Sustainable lightweight vehicle design: A case study of eco-material selection for body-in-white," *Int. J. Sustain. Manuf.*, vol. 2, no. 4, 2012, doi: 10.1504/IJSM.2012.048586.

[9] T. Submitted, R. Fulfillment, and R. For, "Manufacture and Characterization of Fiber Reinforced Epoxy for Application in Cowling Panels of Recreational Aircraft," no. April, 2014.

[10] P. S. Bains, S. S. Sidhu, and H. S. Payal, "Fabrication and Machining of Metal Matrix Composites: A Review," *Materials and Manufacturing Processes*, vol. 31, no. 5. pp. 553–573, 2016, doi: 10.1080/10426914.2015.1025976.

[11] M. Properties, A. R. Jour, I. D. Ibrahim, T. Jamiru, and R. E.

Sadiku, “The use of polypropylene in bamboo fibre composites and their mechanical properties – A review,” no. January, 2017, doi: 10.1177/0731684415591302.

[12] A. K. Sharma, R. Bhandari, A. Aherwar, and R. Rimašauskiene, “Matrix materials used in composites: A comprehensive study,” *Mater. Today Proc.*, vol. 21, pp. 1559–1562, 2020, doi: 10.1016/j.matpr.2019.11.086.

[13] F. Vilaseca, R. Del Rey, R. Serrat, J. Alba, P. Mutje, and F. X. Espinach, “Macro and micro-mechanics behavior of stifness in alkaline treated hemp core fibres polypropylene-based composites,” *Compos. Part B Eng.*, vol. 144, no. March, pp. 118–125, 2018, doi: 10.1016/j.compositesb.2018.02.029.

[14] A. . Bledzki and J. Gassan, “Composites reinforced with cellulose_Bledzki_1999.pdf,” *Prog. Polym. Sci*, vol. 24, pp. 221–274, 1999, [Online]. Available: http://ac.els-cdn.com/S0079670098000185/1-s2.0-S0079670098000185-main.pdf?_tid=af34542c-0260-11e7-a49c-00000aab0f27&acdnat=1488800173_c95596c7ddcc4673fe88c8ec84262bb9.

[15] S. K. Ramamoorthy, M. Skrifvars, and A. Persson, “A review of natural fibers used in biocomposites: Plant, animal and regenerated cellulose fibers,” *Polym. Rev.*, vol. 55, no. 1, pp. 107–162, 2015, doi: 10.1080/15583724.2014.971124.

[16] T. Uygunoglu, I. Gunes, and W. Brostow, “Physical and mechanical properties of polymer composites with high content of wastes incluDing boron,” *Mater. Res.*, vol. 18, no. 6, pp. 1188–1196, 2015, doi: 10.1590/1516-1439.009815.

[17] I. S. A. Review, “High-Strength Hybrid Textile Composites with Carbon , Kevlar , and E-Glass,” no. May 2018, 2017, doi: 10.1007/s11029-017-9696-2.

[18] O. Faruk, A. K. Bledzki, H. P. Fink, and M. Sain, “Biocomposites reinforced with natural fibers: 2000-2010,” *Prog. Polym. Sci.*, vol. 37, no. 11, pp. 1552–1596, 2012, doi: 10.1016/j.progpolymsci.2012.04.003.

[19] F. I. Mahir, K. N. Keya, B. Sarker, K. M. Nahiun, and R. A. Khan, “A brief review on natural fiber used as a replacement of synthetic fiber in polymer composites,” *Mater. Eng. Res.*, vol. 1, no. 2, pp. 88–99, 2019, doi: 10.25082/mer.2019.02.007.

[20] J. M. Tools, “No 主観的健康感を中心とした在宅高齢者における 健康関連指標に関する共分散構造分析Title,” vol. 7, no. 1, pp. 45–56, 2017.

[21] O. Faruk, A. K. Bledzki, H. P. Fink, and M. Sain, “Biocomposites reinforced with natural fibers: 2000-2010,” *Progress in Polymer Science*, vol. 37, no. 11. 2012, doi: 10.1016/j.progpolymsci.2012.04.003.

[22] M. E. Alves Fidelis, T. V. C. Pereira, O. D. F. M. Gomes, F. De Andrade Silva, and R. D. Toledo Filho, “The effect of fiber morphology on the tensile strength of natural fibers,” *J. Mater. Res. Technol.*, vol. 2, no. 2, pp. 149–157, 2013, doi: 10.1016/j.jmrt.2013.02.003.

[23] L. Y. Mwaikambo and M. P. Ansell, “The effect of chemical treatment on the properties of hemp, sisal, jute and kapok for composite reinforcement,” *Angew. Makromol. Chemie*, vol. 272, no. December 1999, pp. 108–116, 1999, doi: 10.1002/(sici)1522-9505(19991201)272:1<108::aid-apmc108>3.3.co;2-0.

[24] A. Barbulée and M. Gomina, “Variability of the mechanical properties among flax fiber bundles and strands,” *Procedia Eng.*, vol. 200, pp. 487–493, 2017, doi: 10.1016/j.proeng.2017.07.068.

[25] N. M. Barkoula, B. Alcock, N. O. Cabrera, and T. Peijs, “Flame-Retardancy Properties of Intumescent Ammonium

Poly(Phosphate) and Mineral Filler Magnesium Hydroxide in Combination with Graphene," *Polym. Polym. Compos.*, vol. 16, no. 2, pp. 101–113, 2008, doi: 10.1002/pc.

[26] R. Mahjoub, J. M. Yatim, A. R. Mohd Sam, and S. H. Hashemi, "Tensile properties of kenaf fiber due to various conditions of chemical fiber surface modifications," *Constr. Build. Mater.*, vol. 55, 2014, doi: 10.1016/j.conbuildmat.2014.01.036.

[27] S. Pujari, "Comparison of Jute and Banana Fiber Composites: A Review," *Int. J. Curr. Eng. Technol.*, vol. 2, no. 2, pp. 121–126, 2013, doi: 10.14741/ijcet/spl.2.2014.22.

[28] B. L. S. Sipiäo, R. L. M. Paiva, S. A. S. Goulart, and D. R. Mulinari, "Effect of chemical modification on mechanical behaviour of polypropylene reinforced pineapple crown fibers composites," *Procedia Eng.*, vol. 10, pp. 2028–2033, 2011, doi: 10.1016/j.proeng.2011.04.336.

[29] D. Nabi Saheb and J. P. Jog, "Natural fiber polymer composites: A review," *Adv. Polym. Technol.*, vol. 18, no. 4, pp. 351–363, 1999, doi: 10.1002/(SICI)1098-2329(199924)18:4<351::AID-ADV6>3.0.CO;2-X.

[30] A. Espert, F. Vilaplana, and S. Karlsson, "Comparison of water absorption in natural cellulosic fibres from wood and one-year crops in polypropylene composites and its influence on their mechanical properties," *Compos. Part A Appl. Sci. Manuf.*, vol. 35, no. 11, pp. 1267–1276, 2004, doi: 10.1016/j.compositesa.2004.04.004.

[31] G. W. Beckermann and K. L. Pickering, "Engineering and evaluation of hemp fibre reinforced polypropylene composites: Fibre treatment and matrix modification," *Compos. Part A Appl. Sci. Manuf.*, vol. 39, no. 6, 2008, doi: 10.1016/j.compositesa.2008.03.010.

[32] X. Li, L. G. Tabil, I. N. Oguocha, and S. Panigrahi, “Thermal diffusivity, thermal conductivity, and specific heat of flax fiber-HDPE biocomposites at processing temperatures,” *Compos. Sci. Technol.*, vol. 68, no. 7–8, pp. 1753–1758, 2008, doi: 10.1016/j.compscitech.2008.02.016.

[33] M. Ferrandez-Villena, C. E. Ferrandez-Garcia, T. Garcia-Ortuño, A. Ferrandez-Garcia, and M. T. Ferrandez-Garcia, “Analysis of the thermal insulation and fire-resistance capacity of particleboards made from vine (Vitis vinifera L.) prunings,” *Polymers (Basel).*, vol. 12, no. 5, 2020, doi: 10.3390/POLYM12051147.

[34] P. V. C. R. K. Santosha, A. S. Shiva Shankare Gowda, and V. Manikanth, “Effect of fiber loading on thermal properties of banana and pineapple leaf fiber reinforced polyester composites,” in *Materials Today: Proceedings*, 2018, vol. 5, no. 2, doi: 10.1016/j.matpr.2017.12.155.

[35] A. R. Mohamed, S. M. Sapuan, and A. Khalina, “Mechanical and thermal properties of josapine pineapple leaf fiber (PALF) and PALF-reinforced vinyl ester composites,” *Fibers Polym.*, vol. 15, no. 5, 2014, doi: 10.1007/s12221-014-1035-9.

[36] R. Siakeng, M. Jawaid, H. Ariffin, and S. M. Sapuan, “Mechanical, dynamic, and thermomechanical properties of coir/pineapple leaf fiber reinforced polylactic acid hybrid biocomposites,” *Polym. Compos.*, vol. 40, no. 5, 2019, doi: 10.1002/pc.24978.

[37] J. C. Damfeu, P. Meukam, and Y. Jannot, “Modeling and measuring of the thermal properties of insulating vegetable fibers by the asymmetrical hot plate method and the radial flux method: Kapok, coconut, groundnut shell fiber and rattan,” *Thermochim. Acta*, vol. 630, pp. 64–77, 2016, doi: 10.1016/j.tca.2016.02.007.

[38] S. Rwawiire and B. Tomkova, “Morphological, Thermal, and Mechanical Characterization of Sansevieria trifasciata Fibers,” *J. Nat. Fibers*, vol. 12, no. 3, pp. 201–210, 2015, doi: 10.1080/15440478.2014.914006.

[39] B. Deepa *et al.*, “Structure, morphology and thermal characteristics of banana nano fibers obtained by steam explosion,” *Bioresour. Technol.*, vol. 102, no. 2, pp. 1988–1997, 2011, doi: 10.1016/j.biortech.2010.09.030.

[40] J. Cruz and R. Fangueiro, “Surface Modification of Natural Fibers: A Review,” in *Procedia Engineering*, 2016, vol. 155, doi: 10.1016/j.proeng.2016.08.030.

[41] N. Venkatachalam, P. Navaneethakrishnan, R. Rajsekar, and S. Shankar, “Effect of pretreatment methods on properties of natural fiber composites: A review,” *Polym. Polym. Compos.*, vol. 24, no. 7, 2016, doi: 10.1177/096739111602400715.

[42] A. Oushabi, S. Sair, F. Oudrhiri Hassani, Y. Abboud, O. Tanane, and A. El Bouari, “The effect of alkali treatment on mechanical, morphological and thermal properties of date palm fibers (DPFs): Study of the interface of DPF–Polyurethane composite,” *South African J. Chem. Eng.*, vol. 23, 2017, doi: 10.1016/j.sajce.2017.04.005.

[43] M. Jacob, K. T. Varughese, and S. Thomas, “Water sorption studies of hybrid biofiber-reinforced natural rubber biocomposites,” *Biomacromolecules*, vol. 6, no. 6, 2005, doi: 10.1021/bm050278p.

[44] M. Rokbi, H. Osmani, A. Imad, and N. Benseddiq, “Effect of chemical treatment on flexure properties of natural fiber-reinforced polyester composite,” *Procedia Eng.*, vol. 10, pp. 2092–2097, 2011, doi: 10.1016/j.proeng.2011.04.346.

[45] M. A. Sawpan, K. L. Pickering, and A. Fernyhough, “Effect of

various chemical treatments on the fibre structure and tensile properties of industrial hemp fibres," *Compos. Part A Appl. Sci. Manuf.*, vol. 42, no. 8, 2011, doi: 10.1016/j.compositesa.2011.03.008.

[46] J. Gassan and A. K. Bledzki, "Alkali Treatment of Jute Fibers: Relationship between Structure and Mechanical Properties," *J. Appl. Polym. Sci.*, vol. 71, no. 4, 1999, doi: 10.1002/(sici)1097-4628(19990124)71:4<623::aid-app14>3.0.co;2-k.

[47] X. Li, L. G. Tabil, and S. Panigrahi, "Chemical treatments of natural fiber for use in natural fiber-reinforced composites: A review," *J. Polym. Environ.*, vol. 15, no. 1, pp. 25–33, 2007, doi: 10.1007/s10924-006-0042-3.

[48] L. Y. Mwaikambo and M. P. Ansell, "Chemical modification of hemp, sisal, jute, and kapok fibers by alkalization," *J. Appl. Polym. Sci.*, vol. 84, no. 12, 2002, doi: 10.1002/app.10460.

[49] A. P. Johari, S. Mohanty, S. K. Kurmvanshi, and S. K. Nayak, "Influence of Different Treated Cellulose Fibers on the Mechanical and Thermal Properties of Poly(lactic acid)," *ACS Sustain. Chem. Eng.*, vol. 4, no. 3, 2016, doi: 10.1021/acssuschemeng.5b01563.

[50] M. Z. Rong, M. Q. Zhang, Y. Liu, G. C. Yang, and H. M. Zeng, "The effect of fiber treatment on the mechanical properties of unidirectional sisal-reinforced epoxy composites," *Compos. Sci. Technol.*, vol. 61, no. 10, 2001, doi: 10.1016/S0266-3538(01)00046-X.

[51] M. M. Mughal, M. W. Akhtar, M. M. Baloch, M. A. Memon, J. A. Syed, and J. S. Kim, "Effect of silanized sisal fiber on thermo-mechanical properties of reinforced epoxy composites," *J. Compos. Mater.*, vol. 54, no. 15, pp. 2037–2050, 2020, doi: 10.1177/0021998319890660.

[52] W. Chen, H. Yu, and Y. Liu, "Preparation of millimeter-long

cellulose i nanofibers with diameters of 30-80 nm from bamboo fibers," *Carbohydr. Polym.*, vol. 86, no. 2, 2011, doi: 10.1016/j.carbpol.2011.04.061.

[53] S. Wang and Q. Cheng, "A novel process to isolate fibrils from cellulose fibers by high-intensity ultrasonication, part 1: Process optimization," *J. Appl. Polym. Sci.*, vol. 113, no. 2, 2009, doi: 10.1002/app.30072.

[54] H. Fu *et al.*, "Overview of Injection Molding Technology for Processing Polymers and Their Composites," *ES Mater. Manuf.*, pp. 3–23, 2020, doi: 10.30919/esmm5f713.

[55] S. Torres-Giner, N. Montanes, V. Fombuena, T. Boronat, and L. Sanchez-Nacher, "Preparation and characterization of compression-molded green composite sheets made of poly(3-hydroxybutyrate) reinforced with long pita fibers," *Adv. Polym. Technol.*, vol. 37, no. 5, 2018, doi: 10.1002/adv.21789.

[56] T. B. Yallew, S. Aregawi, P. Kumar, and I. Singh, "Response of natural fiber reinforced polymer composites when subjected to various environments," *Int. J. Plast. Technol.*, vol. 22, no. 1, 2018, doi: 10.1007/s12588-018-9202-2.

[57] J. Andersons, E. Sparniņš, and R. Joffe, "Stiffness and strength of flax fiber/polymer matrix composites," *Polym. Compos.*, vol. 27, no. 2, 2006, doi: 10.1002/pc.20184.

[58] Y. A. El-Shekeil, S. M. Sapuan, M. Jawaid, and O. M. Al-Shuja'a, "Influence of fiber content on mechanical, morphological and thermal properties of kenaf fibers reinforced poly(vinyl chloride)/thermoplastic polyurethane poly-blend composites," *Mater. Des.*, vol. 58, 2014, doi: 10.1016/j.matdes.2014.01.047.

[59] ASTM D638-14, "Standard Practice for Preparation of Metallographic Specimens," *ASTM Int.*, vol. 82, no. C, pp. 1–15, 2016, doi: 10.1520/D0638-14.1.

[60] ASTM INTERNATIONAL, “Standard Test Methods for Flexural Properties of Unreinforced and Reinforced Plastics and Electrical Insulating Materials. D790,” *Annu. B. ASTM Stand.*, pp. 1–12, 2002.

[61] X Li, L G Tabil, S Panigrahi, and W J Crerar, “The Influence of Fiber Content on Properties of Injection Molded Flax Fiber-HDPE Biocomposites,” 2013, doi: 10.13031/2013.22101.

[62] M. Tajvidi and A. Takemura, “Thermal degradation of natural fiber-reinforced polypropylene composites,” *J. Thermoplast. Compos. Mater.*, vol. 23, no. 3, 2010, doi: 10.1177/0892705709347063.

[63] G. Bujjibabu, V. C. Das, M. Ramakrishna, and K. Nagarjuna, “Mechanical and Water Absorption Behavior of Natural Fibers Reinforced Polypropylene Hybrid Composites,” in *Materials Today: Proceedings*, 2018, vol. 5, no. 5, doi: 10.1016/j.matpr.2018.02.202.

[64] M. Jacob, S. Thomas, and K. T. Varughese, “Mechanical properties of sisal/oil palm hybrid fiber reinforced natural rubber composites,” *Compos. Sci. Technol.*, vol. 64, no. 7–8, 2004, doi: 10.1016/S0266-3538(03)00261-6.

[65] M. R. Sanjay, G. R. Arpitha, L. L. Naik, K. Gopalakrishna, and B. Yogesha, “Applications of Natural Fibers and Its Composites: An Overview,” *Nat. Resour.*, vol. 07, no. 03, 2016, doi: 10.4236/nr.2016.73011.

[66] A. ElayaPerumal and N. Venkateshwaran, “Natural Fiber-Reinforced Polymer Composites in Automotive Applications- A Review,” *IJAEA*, vol. 1, no. 6, 2008.

[67] B. Ravishankar, S. K. Nayak, and M. A. Kader, “Hybrid composites for automotive applications – A review,” *J. Reinf. Plast. Compos.*, vol. 38, no. 18, 2019, doi:

10.1177/0731684419849708.

[68] F. M. Al-Oqla and S. M. Sapuan, “Natural fiber reinforced polymer composites in industrial applications: Feasibility of date palm fibers for sustainable automotive industry,” *J. Clean. Prod.*, vol. 66, 2014, doi: 10.1016/j.jclepro.2013.10.050.

[69] L. P. Composites, “Theoretical Modelling of Tensile Properties of Short Sisal Fibre-reinforced MODIFICATIONS ON THE TENSILE P OF INTIMATELY MIXED SHORT SISAL / GLASS,” no. August, 1997, doi: 10.1023/A.

[70] D. Zhang, M. He, S. Qin, and J. Yu, “Effect of fiber length and dispersion on properties of long glass fiber reinforced thermoplastic composites based on poly(butylene terephthalate),” *RSC Adv.*, vol. 7, no. 25, pp. 15439–15454, 2017, doi: 10.1039/c7ra00686a.

[71] A. Ashori and A. Nourbakhsh, “Reinforced polypropylene composites: Effects of chemical compositions and particle size,” *Bioresour. Technol.*, vol. 101, no. 7, 2010, doi: 10.1016/j.biortech.2009.11.022.

[72] J. P. López, P. Mutjé, A. J. F. Carvalho, A. A. S. Curvelo, and J. Gironès, “Newspaper fiber-reinforced thermoplastic starch biocomposites obtained by melt processing: Evaluation of the mechanical, thermal and water sorption properties,” *Ind. Crops Prod.*, vol. 44, 2013, doi: 10.1016/j.indcrop.2012.11.020.

[73] J. Sahari and S. M. Sapuan, “Natural fibre reinforced biodegradable polymer composites,” *Reviews on Advanced Materials Science*, vol. 30, no. 2. 2012.

[74] M. Asim *et al.*, “A review on pineapple leaves fibre and its composites,” *International Journal of Polymer Science*, vol. 2015. 2015, doi: 10.1155/2015/950567.

[75] A. L. Pereira, M. D. Banea, J. S. S. Neto, and D. K. K. Cavalcanti,

"Mechanical and thermal characterization of natural intralaminar hybrid composites based on sisal," *Polymers (Basel).*, vol. 12, no. 4, 2020, doi: 10.3390/POLYM12040866.

[76] B. C. Barkakaty, "Some structural aspects of sisal fibers," *J. Appl. Polym. Sci.*, vol. 20, no. 11, pp. 2921–2940, 1976, doi: 10.1002/app.1976.070201101.

[77] B. J. Snyder, J. Bussard, J. Dolak, and T. Weiser, "A Portable Sisal Decorticator for Kenyan Farmers," *Int. J. Serv. Learn. Eng. Humanit. Eng. Soc. Entrep.*, vol. 1, no. 2, pp. 92–116, 2006, doi: 10.24908/ijsle.v1i2.2087.

[78] Y. Li, Y. Mai, and L. Ye, "Sisal fibre and its composites : a review of recent developments IM PA US AS DO ME US EX ON AS," *Compos. Sci. Technol.*, vol. 60, no. 2000, 2000.

[79] K. Joseph *et al.*, "Influence of interfacial adhesion on the mechanical properties and fracture behaviour of short sisal fibre reinforced polymer composites," *Eur. Polym. J.*, vol. 32, no. 10, 1996, doi: 10.1016/S0014-3057(96)00051-1.

[80] P. V. Joseph *et al.*, "The thermal and crystallisation studies of short sisal fibre reinforced polypropylene composites," *Compos. Part A Appl. Sci. Manuf.*, vol. 34, no. 3, 2003, doi: 10.1016/S1359-835X(02)00185-9.

[81] M. Z. Rong, M. Q. Zhang, Y. Liu, H. M. Yan, G. C. Yang, and H. M. Zeng, "Interfacial interaction in sisal/epoxy composites and its influence on impact performance," *Polym. Compos.*, vol. 23, no. 2, 2002, doi: 10.1002/pc.10424.

[82] J. Müssig, *Industrial Applications of Natural Fibres: Structure, Properties and Technical Applications*. 2010.

[83] F. de A. Silva, R. D. T. Filho, J. de A. M. Filho, and E. de M. R. Fairbairn, "Physical and mechanical properties of durable sisal fiber-cement composites," *Constr. Build. Mater.*, vol. 24, no. 5,

2010, doi: 10.1016/j.conbuildmat.2009.10.030.

[84] A. Saez, “Industrial Applications of Natural Gas,” in *Natural Gas*, 2010.

[85] T.Swanson, “Consensus-as-a-service: a brief report on the emergence of permissioned, distributed ledger systems. Work,” *World Agric.*, vol. 1, no. May, 2015.

[86] S. Some and S. S. During, “School Studies,” no. July, 2005.

[87] K. G. Asfaw and F. Itanna, “Response of the Vegetative Growth of tef [Eragrostis tef (Zucc .) Trotter] Accessions and Varieties to Soil Salinity Response of the Vegetative Growth of tef [Eragrostis tef (Zucc .) Trotter] Accessions and Varieties to Soil Salinity,” no. July 2011, 2014.

[88] E. Sassoni, S. Manzi, A. Motori, M. Montecchi, and M. Canti, “Novel sustainable hemp-based composites for application in the building industry: Physical, thermal and mechanical characterization,” *Energy Build.*, vol. 77, 2014, doi: 10.1016/j.enbuild.2014.03.033.

[89] C. Alves *et al.*, “Ecodesign of automotive components making use of natural jute fiber composites,” *J. Clean. Prod.*, vol. 18, no. 4, 2010, doi: 10.1016/j.jclepro.2009.10.022.

[90] C. Goudenhooft, A. Bourmaud, and C. Baley, “Flax (Linum usitatissimum L.) fibers for composite reinforcement: Exploring the link between plant growth, cell walls development, and fiber properties,” *Frontiers in Plant Science*, vol. 10. 2019, doi: 10.3389/fpls.2019.00411.

[91] J. Holbery and D. Houston, “Natural-fiber-reinforced polymer composites in automotive applications,” *JOM*, vol. 58, no. 11. 2006, doi: 10.1007/s11837-006-0234-2.

[92] M. H. Norhidayah, A. A. Hambali, Y. M. Yuhazri, M. Zolkarnain, Taufik, and H. Y. Saifuddin, “A review of current development in

natural fiber composites in automotive applications," in *Applied Mechanics and Materials*, 2014, vol. 564, doi: 10.4028/www.scientific.net/AMM.564.3.

[93] N. Saba, M. Jawaid, M. T. H. Sultan, and O. Y. Alothman, "Green biocomposites for structural applications," *Green Energy Technol.*, no. 9783319493817, 2017, doi: 10.1007/978-3-319-49382-4_1.

[94] M. Miao and N. Finn, "Conversion of natural fibres into structural composites," *Journal of Textile Engineering*, vol. 54, no. 6. 2008, doi: 10.4188/jte.54.165.

[95] G. Kalaprasad, P. Pradeep, G. Mathew, C. Pavithran, and S. Thomas, "Thermal conductivity and thermal diffusivity analyses of low-density polyethylene composites reinforced with sisal, glass and intimately mixed sisal/glass fibres," *Compos. Sci. Technol.*, vol. 60, no. 16, pp. 2967–2977, 2000, doi: 10.1016/S0266-3538(00)00162-7.

[96] ASTM D7264/D7264M-07, "Standard Test Method for Flexural Properties of Polymer Matrix Composite Materials," *Annu. B. ASTM Stand.*, vol. i, pp. 1–11, 2007, doi: 10.1520/D7264.

[97] T. Molding and E. Materials, "Standard Test Methods for Determining the Izod Pendulum Impact Resistance of," *Methods*, no. January, 2004.

[98] ASTM D256-10, "Standard test methods for determining the Izod pendulum impact resistance of plastics," *ASTM Int.*, vol. 10, no. Reapproved 2018, 2018.

[99] ASTM International, "ASTM D7582-15 - Standard Test Methods for Determining the Izod Pendulum Impact Resistance of Plastics," *Annu. B. ASTM Stand.*, vol. 09, no. 1995, 2010.

[100] ASTM, "D570-98 Standard Test Method for Water Absorption of Plastics," *ASTM Stand.*, vol. 98, no. Reapproved 2010, 2010.

[101]ASTM International, “Standard Test Method for Water Absorption of Plastics,” *ASTM Standards*, no. Reapproved 2018. 2018.

[102]ASTM D570, *Standard Test Method for Water Absorption of Plastics*, vol. 98, no. Reapproved 2010. 2014.

[103]D7136/D7136M-05e1, “Standard Test Method for Measuring the Damage Resistance of a Fiber-Reinforced Polymer Matrix Composite to a Drop-Weight Impact Event,” *ASTM B. Stand.*, vol. i, pp. 1–16, 2005.

[104]S. I. Thorsson, S. P. Sringeri, A. M. Waas, B. P. Justusson, and M. Rassaian, “Experimental investigation of composite laminates subject to low-velocity edge-on impact and compression after impact,” *Compos. Struct.*, vol. 186, 2018, doi: 10.1016/j.compstruct.2017.11.084.

[105]M. S. Rajput, M. Burman, A. Segalini, and S. Hallström, “Design and evaluation of a novel instrumented drop-weight rig for controlled impact testing of polymer composites,” *Polym. Test.*, vol. 68, 2018, doi: 10.1016/j.polymertesting.2018.04.022.

[106]L. Gunawan, T. Dirgantara, and I. S. Putra, “Development of a Dropped Weight Impact Testing Machine,” *Int. J. Eng. Technol.*, vol. 11, 2011.

[107]J. L. Ruiz-Herrero, M. A. Rodríguez-Pérez, and J. A. De Saja, “Design and construction of an instrumented falling weight impact tester to characterise polymer-based foams,” *Polym. Test.*, vol. 24, no. 5, 2005, doi: 10.1016/j.polymertesting.2005.03.011.

[108]G. Reyes, B. P. Kumar, and T. Wehner, “Low velocity impact behaviorof composite sandwich panels,” in *International SAMPE Technical Conference*, 2015, vol. 2015-January.

[109]F. Aymerich, P. Marcialis, S. Meili, and P. Priolo, “Instrumented drop-weight machine for low-velocity impact testing,” 1996.

[110]Y. Liu, B. Hu, Y. Cai, W. Liu, A. Tovstopyat, and C. Sun, “A novel

tri-axial piezoelectric MEMS accelerometer with folded beams," *Sensors (Switzerland)*, vol. 21, no. 2. 2021, doi: 10.3390/s21020453.

[111]L. C. Cessna, J. P. Lehane, R. H. Ralston, and T. Prindle, "The development of an instrumented projectile impact test: Data glass-reinforced and impact-modified polypropylene," *Polym. Eng. Sci.*, vol. 16, no. 6, 1976, doi: 10.1002/pen.760160607.

[112]P. Zoller, "Instrumentation for impact testing of plastics," *Polym. Test.*, vol. 3, no. 3, 1983, doi: 10.1016/0142-9418(83)90005-3.

[113]J. Lally, "Accelerometer selection considerations Charge and ICP® Integrated Circuit Piezoelectric," *PCB Piezotronics Tech. Notes*, 2005.

[114]NIGAM NC and JENNINGS PC, "CALCULATION OF RESPONSE SPECTRA FROM STRONG-MOTION EARTHQUAKE RECORDS," *Bull. Seismol. Soc. Am.*, vol. 59, no. 2, 1969.

[115]T. H. D. Sydenstricker, S. Mochnaz, and S. C. Amico, "Pull-out and other evaluations in sisal-reinforced polyester biocomposites," *Polym. Test.*, vol. 22, no. 4, 2003, doi: 10.1016/S0142-9418(02)00116-2.

[116]M. Jacob, K. T. Varughese, and S. Thomas, "Dielectric characteristics of sisal-oil palm hybrid biofibre reinforced natural rubber biocomposites," *J. Mater. Sci.*, vol. 41, no. 17, 2006, doi: 10.1007/s10853-006-0298-y.

[117]K. Joseph, S. Thomas, and C. Pavithran, "Effect of chemical treatment on the tensile properties of short sisal fibre-reinforced polyethylene composites," *Polymer (Guildf).*, vol. 37, no. 23, 1996, doi: 10.1016/0032-3861(96)00144-9.

[118]A. Bismarck *et al.*, "Surface characterization of natural fibers; surface properties and the water up-take behavior of modified sisal and coir fibers," *Green Chem.*, vol. 3, no. 2, 2001, doi:

10.1039/b100365h.

[119]K. Senthilkumar *et al.*, "Mechanical properties evaluation of sisal fibre reinforced polymer composites: A review," *Constr. Build. Mater.*, vol. 174, pp. 713–729, 2018, doi: 10.1016/j.conbuildmat.2018.04.143.

[120]F. de A. Silva, N. Chawla, and R. D. de T. Filho, "Tensile behavior of high performance natural (sisal) fibers," *Compos. Sci. Technol.*, vol. 68, no. 15–16, pp. 3438–3443, 2008, doi: 10.1016/j.compscitech.2008.10.001.

[121]K. Rohit and S. Dixit, "A Review - Future Aspect of Natural Fiber Reinforced Composite," vol. 7, no. 2, pp. 43–59, 2016, doi: 10.1177/2041247916007002O2.

[122]K. M. M. Rao and K. M. Rao, "Extraction and tensile properties of natural fibers: Vakka, date and bamboo," *Compos. Struct.*, vol. 77, no. 3, pp. 288–295, 2007, doi: 10.1016/j.compstruct.2005.07.023.

[123]R. D. Tolêdo Filho, K. Joseph, K. Ghavami, and G. L. England, "the Use of Sisal Fibre As Reinforcement in Cement Based Composites," *Rev. Bras. Eng. Agrícola e Ambient.*, vol. 3, no. 2, pp. 245–256, 1999, doi: 10.1590/1807-1929/agriambi.v3n2p245-256.

[124]M. Akram Khan, S. Guru, P. Padmakaran, D. Mishra, M. Mudgal, and S. Dhakad, "Characterisation studies and impact of chemical treatment on mechanical properties of sisal fiber," *Compos. Interfaces*, vol. 18, no. 6, pp. 527–541, 2011, doi: 10.1163/156855411X610250.

[125]X. Wu, Y. Wang, J. Liu, S. He, L. Zhang, and F. Polymers, "Improved Crack Growth Resistance and Its Molecular Origin of Natural Rubber / Carbon Black by Nanodispersed Clay," *Polym. Eng. Sci.*, pp. 1–10, 2011, doi: 10.1002/pen.

[126]T. P. Mohan and K. Kanny, “Chemical treatment of sisal fiber using alkali and clay method,” *Compos. Part A Appl. Sci. Manuf.*, vol. 43, no. 11, 2012, doi: 10.1016/j.compositesa.2012.07.012.

[127]P. R. L. Lima, R. J. Santos, S. R. Ferreira, and R. D. Toledo Filho, “Characterization and treatment of sisal fiber residues for cement-based composite application,” *Eng. Agric.*, vol. 34, no. 5, 2014, doi: 10.1590/S0100-69162014000500002.

[128]M. K. Gupta and R. K. Srivastava, “Tensile and Flexural Properties of Sisal Fibre Reinforced Epoxy Composite: A Comparison between Unidirectional and Mat form of Fibres,” *Procedia Mater. Sci.*, vol. 5, no. December, pp. 2434–2439, 2014, doi: 10.1016/j.mspro.2014.07.489.

[129]E. T. N. Bisanda and M. P. Ansell, “The effect of silane treatment on the mechanical and physical properties of sisal-epoxy composites,” *Compos. Sci. Technol.*, vol. 41, no. 2, 1991, doi: 10.1016/0266-3538(91)90026-L.

[130]American Society for Testing & Mater, “Standard test methods for felt,” vol. 10, no. Reapproved 2018, pp. 1–20, 1987, doi: 10.1520/D0256-10R18.N.

[131]C. Y. Yue, H. C. Looi, and M. Y. Quek, “Assessment of fibre-matrix adhesion and interfacial properties using the pull-out test,” *Int. J. Adhes. Adhes.*, vol. 15, no. 2, 1995, doi: 10.1016/0143-7496(95)98740-D.

[132]A. Orue, A. Jauregi, U. Unsuain, J. Labidi, A. Eceiza, and A. Arbelaiz, “The effect of alkaline and silane treatments on mechanical properties and breakage of sisal fibers and poly(lactic acid)/sisal fiber composites,” *Compos. Part A Appl. Sci. Manuf.*, vol. 84, pp. 186–195, 2016, doi: 10.1016/j.compositesa.2016.01.021.

[133]N. Saba, M. Jawaid, O. Y. Alothman, and M. T. Paridah, “A review

on dynamic mechanical properties of natural fibre reinforced polymer composites," *Construction and Building Materials*, vol. 106. 2016, doi: 10.1016/j.conbuildmat.2015.12.075.

[134]D. Shanmugam and M. Thiruchitrambalam, "Static and dynamic mechanical properties of alkali treated unidirectional continuous Palmyra Palm Leaf Stalk Fiber/jute fiber reinforced hybrid polyester composites," *Mater. Des.*, vol. 50, pp. 533–542, Sep. 2013, doi: 10.1016/J.MATDES.2013.03.048.

APPENDIX

Appendix A: Tensile Data for All specimens

The following excel file, "Tensile_Adjusted_Curve_Data", contains all adjusted load-displacement and adjusted stress strain curves. The adjustments were made to account for machine compliance. Stress and strain are calculated as follows:

$$\varepsilon = \frac{\text{True Displ.}}{\text{Gage length}}$$

$$\sigma = \frac{\text{Load (N)}}{\text{x-sectional area}}$$

The following excel file, "All_Tensile_Calculations", contains all tensile strength, modulus, and elongation data for all specimens. Modulus was found byfitting a straight line to the roughly linear portion of the curve. The line was not forced to go through the origin to compensate for the toe region. Strength and % elongation are calculated as follows:

$$\text{Strength} = \frac{\text{Load (N)at yield or break}}{\text{x} - \text{sectional area}}$$

$$\%\ \text{elongation} = \frac{\text{True Displ. at break}}{\text{Gage length}}$$

Appendix B

The following file "Flexural_LD_Curves" contains load-extension data (data from machine) and stress-strain data (calculated).

The following calculations taken from ASTM D7264 are used to find maximum normal stress and strain values along all points in the flexural tests:

$$\epsilon = \frac{6\delta h}{L^2} \qquad (3)$$

where:
ϵ = maximum strain at the outer surface, mm/mm [in./in.],
δ = mid-span deflection, mm [in.],
L = support span, mm [in.], and
h = thickness of beam, mm [in.].

$$\sigma = \frac{3PL}{2bh^2}$$

where:
σ = stress at the outer surface at mid-span, MPa [psi],
P = applied force, N [lbf],
L = support span, mm [in.],
b = width of beam, mm [in.], and
h = thickness of beam, mm [in.].

The file "Flexural Calculations" contains all calculations required by ASTM D7264.

Appendix C

System 2000 Epoxy Resin and System 2060 hardener

Product Specifications of 2060 hardener

	2000	2020	2060	2120	ASTM Method
Color	Lt. Amber	Amber	Amber	Amber	Visual
Viscosity, @ 77° F, centipoise	1,650 cps	150-175 cps	190-200 cps	200-250 cps	D2393
Specific Gravity, gms./cc	1.15	0.96	0.96	0.95	D1475
Mix Ratio, By Wt		100 : 23 By Weight, or 4 to 1 By Volume	100 : 27 By Weight, or 3 to 1 By Volume		D2471
Pot Life, 4 fl. Oz. Mass @ 77° F		20 minutes	1 hour	2 hour	PTM&W

[Source: Fiber Glast Development Corporation, 385 Carr Drive-Brookville, Ohio 45309, USA]

Typical Mechanical Properties of system 200 Epoxy Resin with its hardener

Appendix D

Matlab code for conversion of machine response to required graphs

```
% Zfunction[u,v]=function2(xi,m,k,P1,dt,wn,t)
wd=wn*sqrt(1-xi^2);
sq=sqrt(1-xi^2);
ep=exp(-xi*wn*dt);
si=sin(wd*dt);
co=cos(wd*dt);
```

```
A=ep*(xi/sq*si+co);
B=ep*(1/wd*si);
C=1/k*(2*xi)/(wn*dt)+ep*(((1-2*xi^2)/(wd*dt)-xi/sq)*si-(1+2*xi/
(wn*dt))*co);
D=1/k*(1-2*xi/(wn*dt))+ep*((2*xi^2-1)/(wd*dt)*si+(2*xi/(wn*dt)*co));
Ap=-ep*(wn/sq*si);
Bp=ep*(co-xi/sq*si);
Cp=1/k*(-1/dt+ep*((wn/sq+xi/(dt*sq)))*si+1/dt*co);
Dp=1/(k*dt)*(1-ep*(xi/sq*si+co));
u=zeros(length(P1),1);
v=zeros(length(P1),1);
%initial conditions
u0=0;v0=0;
u(1)=u0;
v(1)=v0;
for i=1;length(P1)-1;
u(i+1)=A*u(i)+B*v(i)+C*(-m*P1(i))+D*(-m*P1(i+1));
v(i+1)=Ap*u(i)+Bp*v(i)+Cp*(-m*P1(i))+Dp*(-m*P1(i+1));
end
end
Not enough input arguments.
Error in function2 (line 2)
wd=wn*sqrt(1-xi^2);

Matlab code to convert The Spectral plus wave to required plots

clc;
close all;
[y,fs]=audioread('Second Test.wav'); % reading the second data
info=audioinfo('Second Test.wav');
%time domain
t=0:seconds(1/fs):seconds(info.Duration);
t=t(1:end-1);
figure;
plot(t,y); %plotting spectral response as a function of time
title('time domain')
xlabel('Times')
ylabel('Amplitude')
%fourier transform
Y=fft(y);
L=info.TotalSamples;
P2=abs(Y/L);
P1=P2(1:L/2+1);
P1(2:end-1)=2*P1(2:end-1);
f=fs*(0:(L/2))/L;
%frequency domain
sound(y,fs);
q=1; p=2;
[y1,af1]=resample(y,q,p); sound(y1,fs); keyboard %downsample
```

```
[y2,af2]=resample(y1,p,q); sound(y2,fs); keyboard %interpolate
%plot for showing the sampling information
figure(2)
t1=0:(1/fs):(info.Duration);
t1=t1(1:end-1);
t2=(0:(length(y1)-1))*p/(q*fs);
plot(t1(1:100),y(1:100,1),'-b*', t2(1:(100/p)+1),y1(1:100/p+1,1),'-
ro');
title('Sampling Info')
legend('origial', 'resampled', 'location', 'Northeast')
Time_history=(0:0.02:100);
t=Time_history;
%input data
xi=0.01;
dt=t(2)-t(1);
T=(0.02:0.02:1);
m=5.5;
h=0.62;
g=10;
omega_n=2.*pi./T;
K=m.*omega_n.*omega_n;
for j=1:length(T)
 wn=omega_n(j);
 k=K(j);
 [u,v]=function2(xi,m,k,P1,dt,wn,t);
 D(j)=max(abs(u))*10; %spectral displacement
end
V=omega_n.*D; % spectral velocity
A=omega_n.*omega_n.*D; % spectral acceleration
F=m.*A; % spectral force
e=((m.*g.*D)+(1/2.*k.*D.*D))*5; % spectral energy
%plot response
%f1=figure(1)
figure(1)
plot(T,D,'color','b','linewidth',1.0);
xlabel('Time(ms)');
ylabel('Displacement (m)');
%f2=figure(2)
figure(2)
plot(D,F,'color','b','linewidth',1.0);
xlabel('Displacement(m)');
ylabel('Force(kN)');
%f3=figure(3)
figure(3)
plot(T,e,'color','b','linewidth',1.0);
xlabel('Time(ms)');
ylabel('Energy(J)');
%f4=figure(4)
figure(4)
```

```
plot(T,F,'color','b','linewidth',1.0);
xlabel('Time(ms)');
ylabel('Force(kN)');
%f5=figure(5)
figure(5)
plot(T,V,'color','b','linewidth',1.0);
xlabel('Time(ms)');
ylabel('Velocity (m/s)');
%f6=figure(6)
figure(6)
plot(D,e,'color','b','linewidth',1.0);
xlabel('displacement(ms)');
ylabel('energy');
```

Aippdix E

CEAST 9350 Strain Gauge (Type 1) Tups

Catalog Number	Capacity		Minimum Insert Diameter (For Puncturing Test)	
	kN	lbs	mm	in
7529.301	22	5,000	10	0.394
7529.302	45	10,000	20	0.787
7529.303	90	20,000	20	0.787
7529.304	222	50,000	20	0.787

CEAST 9340 Strain Gauge (Type 1) Tups

Catalog Number	Capacity		Minimum Insert Diameter (For Puncturing Test)	
	kN	lbs	mm	in
7519.301	22	5,000	10	0.394
7519.302	45	10,000	20	0.787
7519.303	90	20,000	20	0.787

Tup Inserts for Strain Gauge (Type 1) Tups

Catalog Number	Description	Testing Standards	Tup Compatibility
7529.310	10 mm (0.394 in) Ø Hemispherical	ISO 6603-1,-2, ISO 7765-1,-2	7529.301
7519.310			7519.301
7529.311	12.7 mm (1/2 in) Ø Hemispherical	ASTM D3763, ASTM D7192, ASTM D5628 Method FD	7529.301
7519.311			7519.301
7529.313	20 mm (0.787 in) Ø Hemispherical	ISO 6603-1,-2, ISO 7765-1,-2 ASTM D5628 Method FE	All Strain Gauge (Type 1) Tups
7529.320	10 mm (0.394 in) Ø Hemispherical (For Non-Puncturing Test)	ISO 6603-1,-2, ISO 7765-1,-2	
7529.321	12.7 mm (1/2 in) Ø Hemispherical (For Non-Puncturing Test)	ASTM D3763, ASTM D7192, ASTM D5628 Method FD	
7529.322	16 mm (5/8 in) Ø Hemispherical (For Non-Puncturing Test)	ASTM D7136/7136M, Airbus AITM 1.0010, PR-EN 6038, ISO 18352, Boeing BSS 7260, SACMA 2R-94	
7529.324	25.4 mm (1 in) Ø Hemispherical	-	
7529.325	38.1 mm (1 1/2 in) Ø Hemispherical	ASTM D5628 Method FC	
7529.329	6.35 mm (1/4 in) Radius Conical, 25.4 mm Ø (1 in) Base	ASTM D5628 Method FB	
7529.330	Plastics Charpy Insert	ISO 179-2	
7529.331	Plastics Charpy Insert	ASTM D6110	
7529.332	Plastics Charpy Insert	ISO 180, ASTM D256	
7529.335	Metals Charpy Insert, 8 mm Tip Radius	ASTM E23, ISO 148	
7529.336	Metals Charpy Insert, 2 mm Tip Radius	ISO 148, DIN 50115, EN 10045	
7529.337	Metals IZOD Insert	ASTM E23	
7529.340	Metals DWTT Insert	ASTM E208	
7529.350	50 mm Ø Flat Faced	-	
7529.360	12.7 mm (1/2 in) Radius Conical, 50.8 mm Ø (2 in) Base	ASTM D2444 - Type A	
7529.361	50.8 mm (2 in) Radius Conical, 50.8 mm Ø (2 in) Base	ASTM D2444 - Type B	
7529.362	12.7 mm (1/4 in) Radius Conical, 50.8 mm Ø (2 in) Base	ASTM D2444 - Type C	

Model Number 485B39	DIGITAL ICP® - USB SIGNAL CONDITIONER	Revision: A ECN #:

	ENGLISH	SI
PERFORMANCE		
Channel Count	2	2
Voltage Range (nominal[1])	± 10 V pk	± 10 V pk
ADC Resolution	24-bit[2]	24-bit[2]
Frequency Range (± 5 %)	0.8 Hz to 20.7 kHz	0.8 Hz to 20.7 kHz
Sample Rate	48, 44.1, 32, 22.05, 16, 11.025, 8 kHz	48, 44.1, 32, 22.05, 16, 11.025, 8 kHz
Antialiasing Lowpass Filter (-3dB) at 48 kHz	22.9 kHz[3]	22.9 kHz[3]
AC High Pass Filter (-3dB)	1 Hz to 0.5 Hz[4]	1 Hz to 0.5 Hz[4]
Digital Output Interface	USB class 1 audio	USB class 1 audio
ENVIRONMENTAL		
Temperature Range (Operating)	14 °F to +176 °F	-10 °C to +80 °C
Temperature Range (Storage)	-40 °F to +176 °F	-40 °C to +80 °C
ELECTRICAL		
Excitation Voltage (to sensor: ± 5 %)	24 V DC	24 V DC
Constant Current Excitation (± 5 %)	4 mA	4 mA
DC Power (USB)	< 500 mW (5 V at 100 mA)	< 500 mW (5 V at 100 mA)
Settling Time	1.5 seconds	1.5 seconds
Electrical Isolation (case)	Grounded	Grounded
MECHANICAL		
Housing Material	Stainless steel	Stainless steel
Size (length x width x height)	2.36 in x 1.54 in x 0.75 in	60 mm x 39 mm x 19 mm
Weight	4.4 oz	125 gram
Sensor Inputs	2 BNC jacks	2 BNC jacks
Digital Output	9 in integral USB cable	23 cm integral USB cable
USB Connector	Type A	Type A

NOTES:
[1] ± 8 V pk, guaranteed
[2] 16-bit selectable by software
[3] Proportional to sample rate
[4] Sample rate dependent (48 kHz to 8 kHz)

OPTIONAL ACCESSORIES:
MD821AM/A USB A to Lightning camera adaptor
USB A to USB OTG adaptor

PRODUCT DRAWING

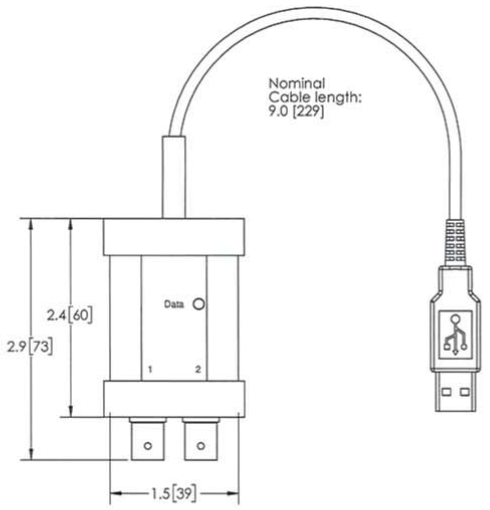

Dimensions in inches [mm]

In the interest of constant product improvement, specifications may change without notice.

All specifications are at room temperature unless otherwise specified.

CE

Project Engineer:	Product Manager:	Mkt Team Leader:	Spec Number:
tel	MAP		PS-0149
Date: 6/28/18	Date: 6/28/18	Date: 6/29/18	

THE MODAL SHOP
MTS SYSTEMS CORPORATION
3149 East Kemper Road
Cincinnati, OH 45241
800-860-4867 Fax (513) 458-2172
+1 513-351-9919
info@modalshop.com
SAM-F020 revNR 04/04/03

Appindix F

Low velocity impact test results from the machine corlated using matlab code

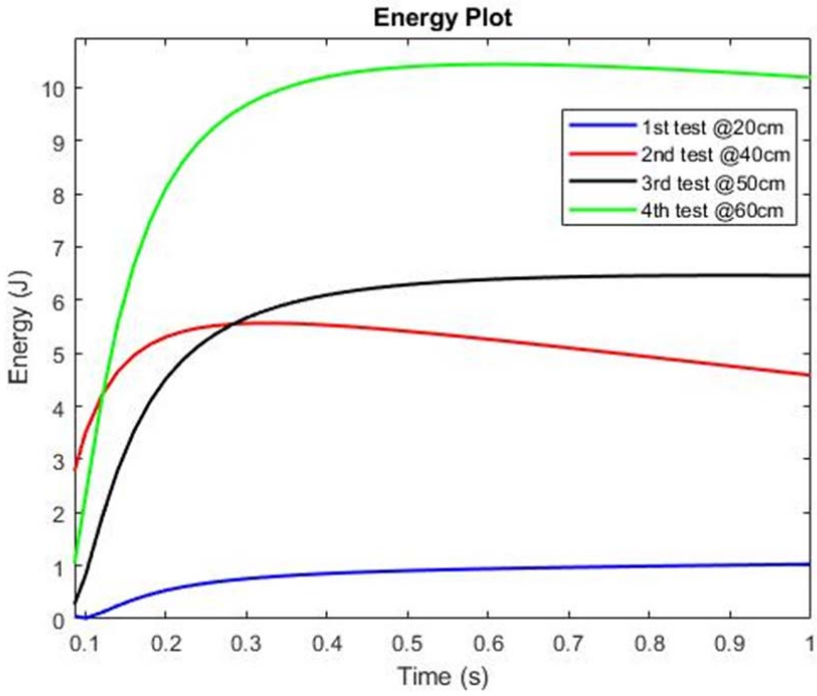

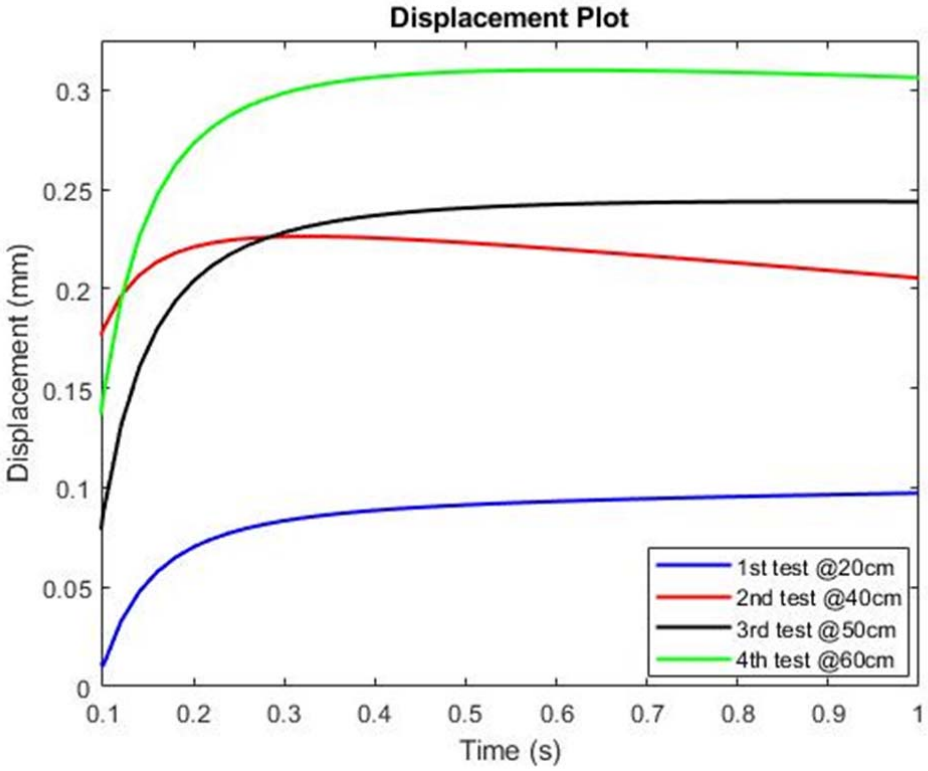

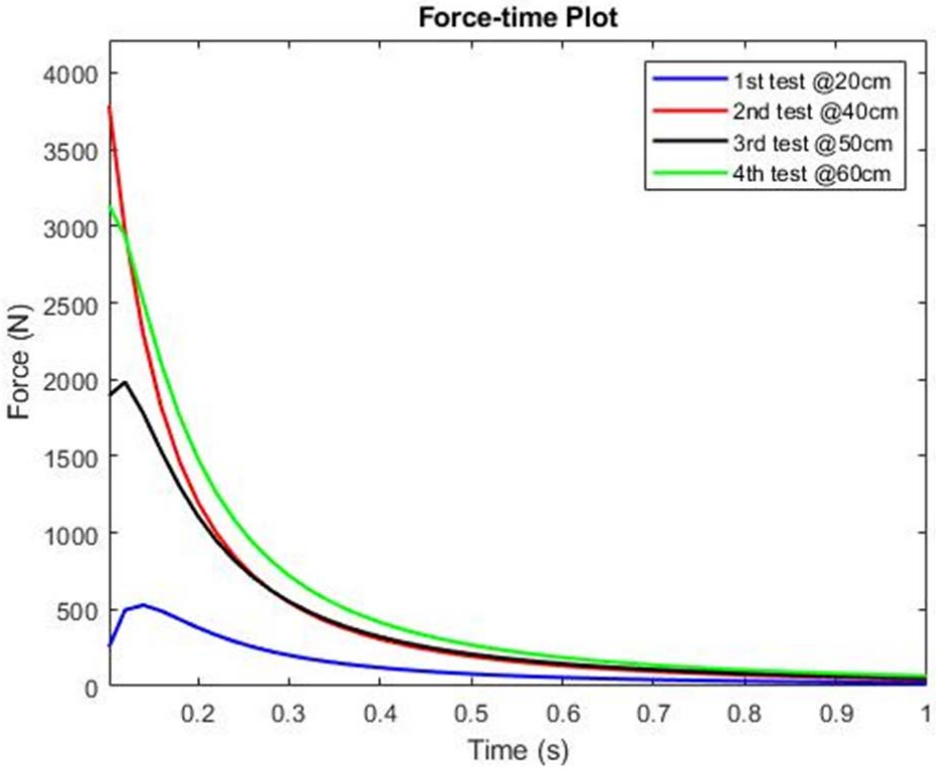
Force-time Plot
1st test @20cm
2nd test @40cm
3rd test @50cm
4th test @60cm
Force (N)
Time (s)
0
500
1000
1500
2000
2500
3000
3500
4000
0.2
0.3
0.4
0.5
0.6
0.7
0.8
0.9
1

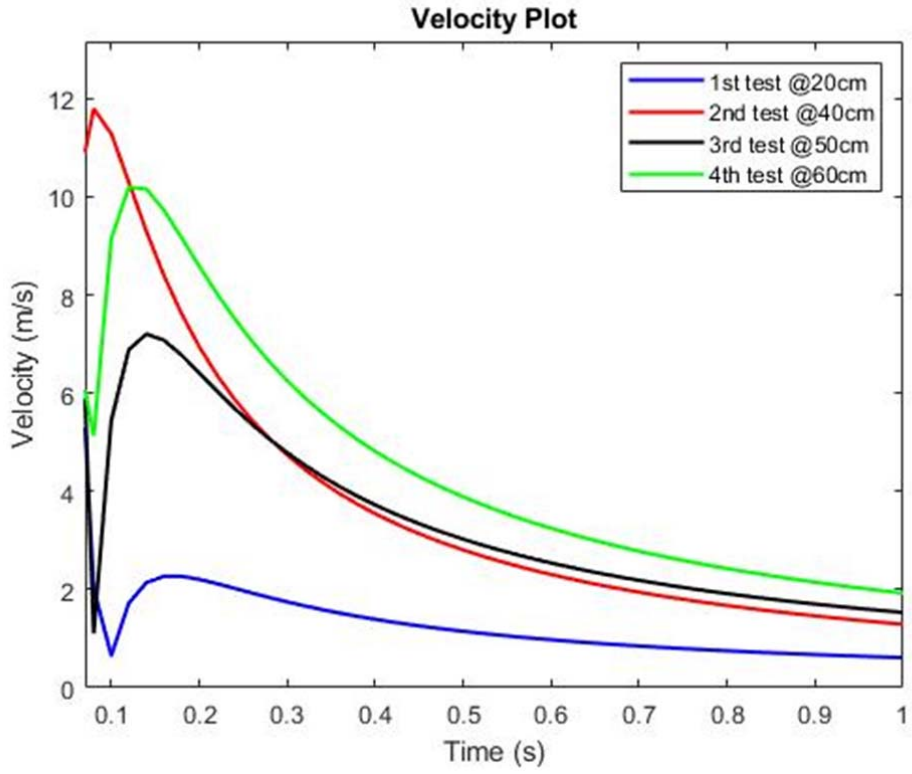
Velocity Plot
1st test @20cm
2nd test @40cm
3rd test @50cm
4th test @60cm
Velocity (m/s)
Time (s)
0
2
4
6
8
10
12
0.1
0.2
0.3
0.4
0.5
0.6
0.7
0.8
0.9
1

Advised MSC thesis

- Experimental Evaluation of Mode I and Mode II Fracture Behavior of Glass Fiber Reinforced Polymer Composite by Considering Different Environmental Aging
  Bekalu, Nebiy (Addis Ababa University, 2020-06)

  The influence of different environmental aging on mode I and mode II interlaminar fracture resistance of glass fiber reinforced polymer composite material is experimentally studied in this paper. Test specimens of ...

- Experimental Fatigue Behaviour Investigation of Sisal Reinforced Epoxy Composite
  Sitotaw, Mengistie (Addis Ababa University, 2019-07)

  Due to their environment friendliness, natural abundance of the fibers, lower weight and cheap production cost, natural fiber reinforced composites are being used in different application areas. Properties of this material ...

- Free Vibration Study on Edge Cracked Glass Fiber Reinforced Polymer Laminate
  Mulatu, Achenef (Addis Ababa University, 2019)

  The fiberglass-reinforced polymer is the most widely used composite because of its low cost and easy availability in the market. Fiberglass reinforced polymer is used for structural and semi-structural body parts of the ...

- Mechanical Characterization and Water Absorption Behavior of Woven Mat Glass Fiber / Epoxy Composite Materials
  Gulilat, Debebe (Addis Ababa University, 2020-07)

  In this research the Experimental study of glass fiber composite materials reinforced fiber types are presented. Composite materials have boundless engineering applications where the strength to weight ratio, low costs, ...

- Facture Toughness Investigation of Chopped Sisal Fiber Reinforced Epoxy Resin Composite
  Tsegaye, Yonas (Addis Ababa University, 2017-06)

- Design and prototyping of drop weight impact testing machine
  Dagmawe Tadesse (Addis Ababa University ,2021-05)
- Fracture Toughness and Water Absorption Behavior of Woven Sisal-Glass Composite

Oda Kerre (Addis Ababa University ,2021-05)

- Fabrication and Mechanical Property Characterization of Sisal fiber Reinforced Epoxy Resin Composite Material for Automotive body Application
  Kebede, Mesfin(Addis Ababa University ,2015-05)
- Structural Analysis of Bamboo and E-glass Fiber Reinforced Epoxy Composite for Wind Turbine Blade using Finite Element Method and CFD
  Netsnet, Berga (Addis Ababa University, 2020-10)
- Analytical and Numerical Analysis of Adhesive Joints for Vehicle Application
  Sura, Keneni (Addis Ababa University, 2018-12)
- Dynamic Analysis and Improving Crashworthiness of Side-Impact Beam for Saloon type Vehicles
  Amare, Bililign URI: http://localhost:80/xmlui/handle/123456789/5922